THE MINOR PLANET BULLETIN

BULLETIN OF THE MINOR PLANETS SECTION OF THE ASSOCIATION OF LUNAR AND PLANETARY OBSERVERS

VOLUME 50, NUMBER 3, A.D. 2023 JULY-SEPTEMBER 

# LIGHTCURVE ANALYSIS FOR SIXTEEN MAIN-BELT ASTEROIDS

Gonzalo Fornas, AVA – J57, CAAT
Centro Astronómico del Alto Turia, SPAIN
gon@iicv.es

Fernando Huet, AVA – Z93

Enrique Arce, AVA – J67
Vallbona Observatory

Alvaro Fornas, AVA – J57, CAAT
Centro Astronómico del Alto Turia, SPAIN

(Received: 2023 January 26)

Photometric observations of sixteen main-belt asteroids were obtained on the nights from 2022 August - December. We derived the following rotational periods: 1055 Tynca 11.893 ± 0.001 h, 1417 Walinskia, 1500 Jyvaskyla 8.827 ± 0.0002 h, 2003 Harding 4.453 ± 0.001 h, 2695 Christabel 5.623 ± 0.004 h, 3686 Antoku 6.744 ± 0.006 h, 4528 Berg 3.564 ± 0.001 h, 5501 1982 FF2 2.464 ± 0.002 h, 5643 Roques 7.490 ± 0.03 h, 7195 Danboice 8.689 ± 0.007 h, 7317 Cabot 2.345 ± 0.002 h, 12999 Torun 4.020 ± 0.002 h, 15476 Narendra, 19750 2000 CM62 6.518 ± 0.001 h, 23892 1998 SH49 3.722 ± 0.001 h, 33697 1999 KJ11 4.876 ± 0.003 h.

We report on the photometric analysis results for sixteen main-belt asteroids performed by Asociación Valenciana de Astronomía (AVA). This work has been done from the Astronomical Center Alto Turia (CAAT), with the MPC code J57, located in Aras de los Olmos, Valencia, and Observatorio Polop MPC Z93 (Alicante), both operated by members of the Valencian Astronomy Association (AVA) (*http://www.astroava.org*). This database shows graphic results of the data, mainly lightcurves, with the plot phased to a given period.

We have managed to obtain a number of accurate and complete lightcurves as well as some additional incomplete lightcurves to help analysis at future oppositions.

| Observatory | Telescope (meters) | CCD |
|---|---|---|
| C.A.A.T. J57 | 43 cm DK | SBIG STXL-11002 |
| C.A.A.T. J57 | 106 mm Refr | ZWO ASI 1600 |
| Z93 | SC 8” | SBIG ST8300 |
| J67 | SC 10” | SBIG ST7 |

Table I. List of instruments used for the observations.

We concentrated on asteroids with no reported period and those where the reported period was poorly established and needed confirmation. All the targets were selected from the Collaborative Asteroid Lightcurve (CALL) website at (*http://www.minorplanet.info/call.html)* and Minor Planet Center (*http://www.minorplanet.net*). The Asteroid Lightcurve Database (LCDB; Warner et al., 2009) was consulted to locate previously published results.

Images were measured using *MPO Canopus* (Bdw Publishing) with a differential photometry technique. The comparison stars were restricted to near solar-color to avoid introducing color dependencies, especially at larger air masses. The lightcurves give the synodic rotation period. The amplitude (peak-to-peak) that is shown is that for the Fourier model curve and not necessarily the true amplitude.

(1055) Tynka. This Main-Belt asteroid (inner) of the FLO category was discovered on 1925 Nov 17 by E. Buchar at the Algiers observatory, Argelia. We made observations on 2022 May 22 to Jun 04. In the ALCDEF we found data from Robert D. Stephens 2012/03/27 - 2012/05/09 and we have joined them to ours to improve the quality of the result. From this data we derive a rotation period of 11.893 ± 0.001 h and an amplitude of 0.07 mag. This is a bimodal period. We agree with Kryszczynska et al. (2012) and Higgins and Pilcher (2009), with a period of 11.893 h. Durech et al. (2020) and Behrend (2012web, 2021web) have interpreted it’s lightcurve as monomodal, with half period. Looking at halves of the period in the graphic, we think it is a bimodal asteroid since the halves are slightly different.

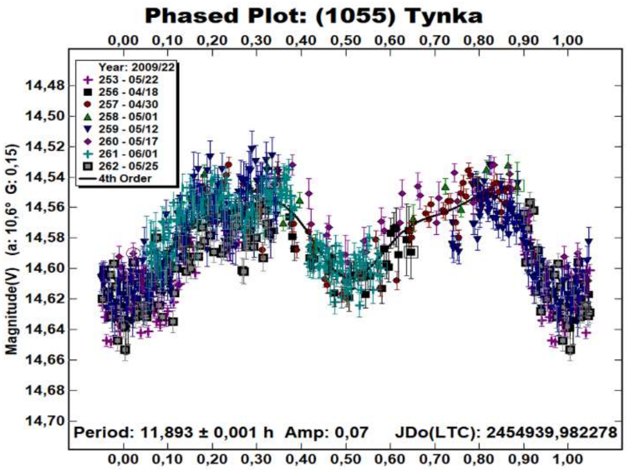


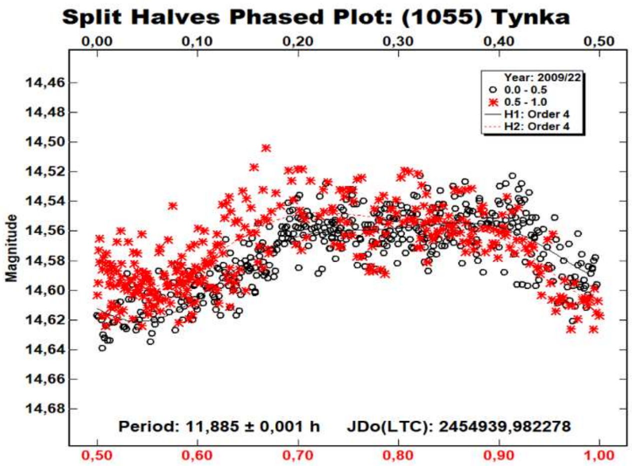


(1417) Walinskia. This Main-Belt asteroid (outer) was discovered on 1937 April 1 by K. Reinmuth at Heidelberg. We made observations on 2022 December 26. From our data we are not able to derive any rotation period. In ALCDEF a period of Behrend (2018web) appears, but when consulting the data we found that it is classified as uncertain by a curve provided by R. Roy. We can only confirm the uncertain character. Of course, we cannot confirm the period shown by ALCDEF with 2.93 h and with A=0.04. We do find some growth in luminosity, of 0.02 mag, that could indicate a longer period. We do not have better data at the moment.

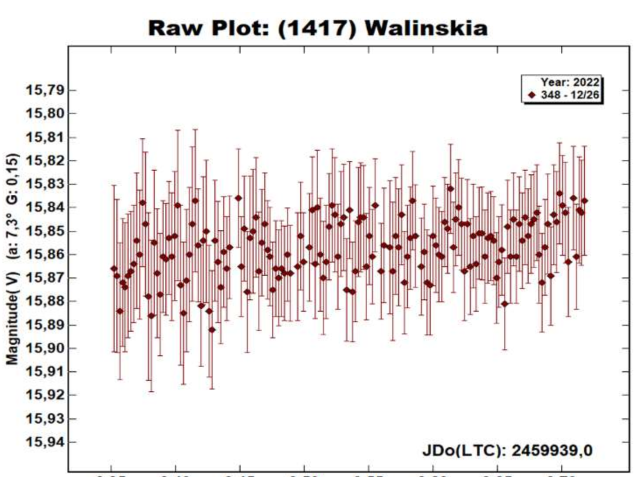


(1500) Jyvaskyla. This Main-Belt asteroid (inner) was discovered on 1938 Oct 16 by Y. Väisälä at the Turku observatory, Finland. We made observations on 2022 Nov 6 to 23. From our data we derive a rotation period of 8.8268 ± 0.0002 h and an amplitude of 0.95 mag. We assume a bimodal lightcurve, but it could be analyzed as monomodal asteroid. We show also the monomodal graphic and the halves. Durech et al. (2016) also found a period of 8.827 h. with incomplete data (U=2).

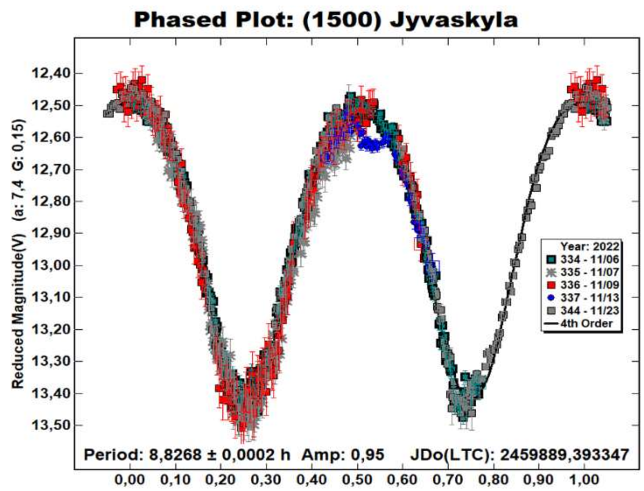


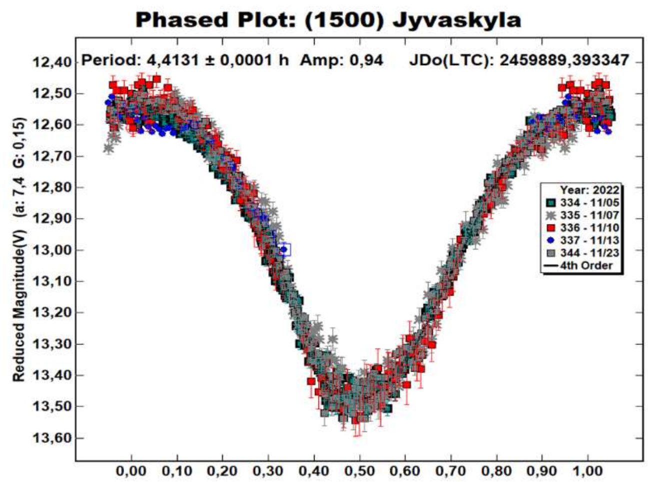


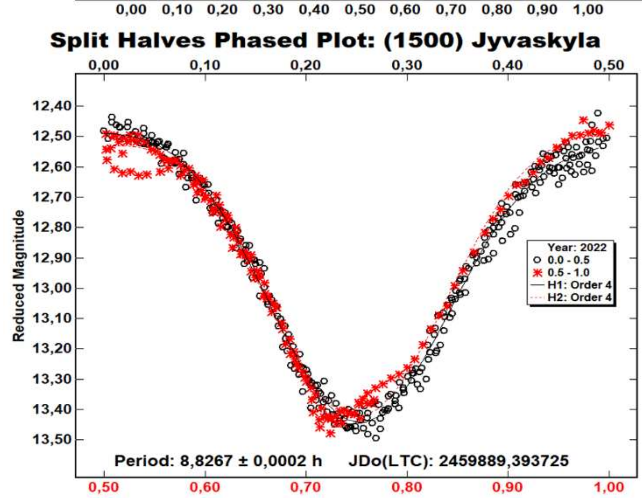

(2003) Harding. This Main-Belt asteroid (outer) was discovered on 1960 Sep 24 by the Palomar Leiden Survey. We made observations on 2022 Apr 4 to May 5. From our data we derive a rotation period of 4.453 ± 0.001 h and an amplitude of 0.08 mag. We assume it as bimodal, even with a very symmetrical drawing. Alvarez-Candal et al. (2004) found a period of 2.96 h. We have reviewed our data with the periodogram and confirm the period of 4.45 h.

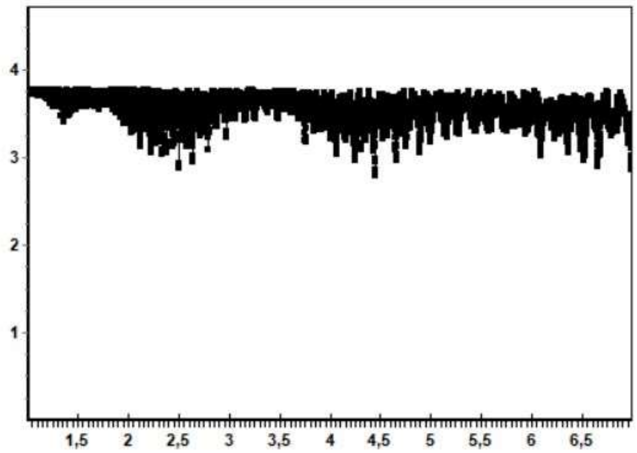

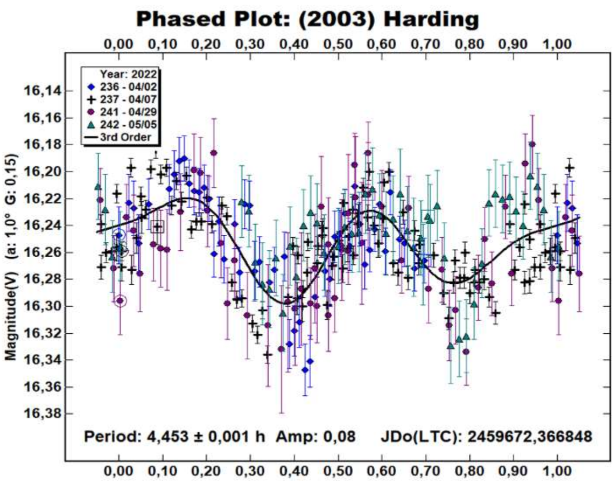


(2695) Christabel. This Main-Belt asteroid (middle) was discovered on 1979 Oct 17 by E. Bowell at Anderson Mesa Station, Arizona. We made observations on 2022 May 5-7. From our data we derive a rotation period of 5.623 ± 0.004 h and an amplitude of 0.73 mag. We assume it as bimodal, even with a very symmetrical drawing. Behrend (2018web) found a period of 6.009 h.

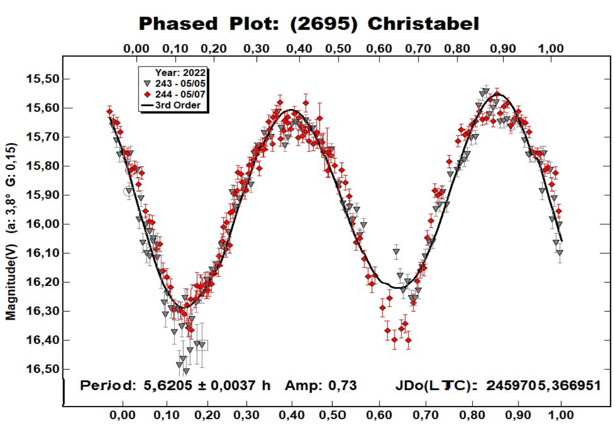


(3686) Antoku. This Main-Belt asteroid (middle) was discovered on 1987 March 3 by T. Niijima and, T. Urata at Ojima. We made observations on 2019 March 13-16. From our data we derive a rotation period of 6.744 ± 0.006 h and an amplitude of 0.3 mag. Waszczak et al. (2015) found 6.73 h and Behrend (2019web) found 6.374 h, which agrees with our observations.

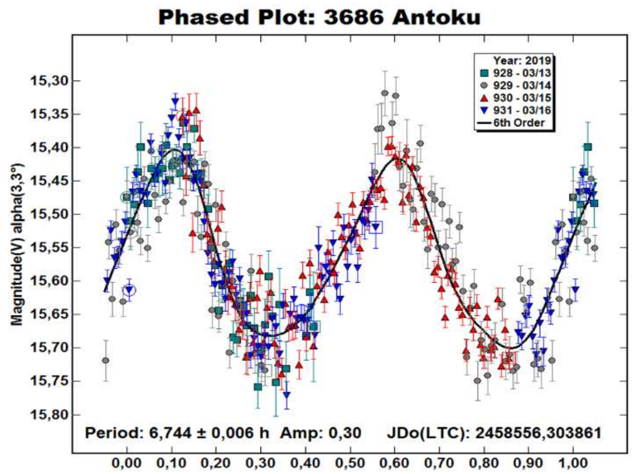


(4528) Berg. This Main-Belt asteroid (middle) was discovered on 1983 Aug 13 by E. Bowell at Anderson Mesa observatory. We made observations on 2022 May 16 -25. In the ALCDEF we found data from T.A. Polakis 2018/02/27 - 2018/03/12 and we have joined them to ours to improve the quality of the result. Data analysis found a rotation period of 3.564 ± 0.001 h and an amplitude of 0.28 mag. Behrend (2006web) found a period of 3.52 h, Setcher (2015) found 3.47 h and Polakis (2018) found 3.56 h.

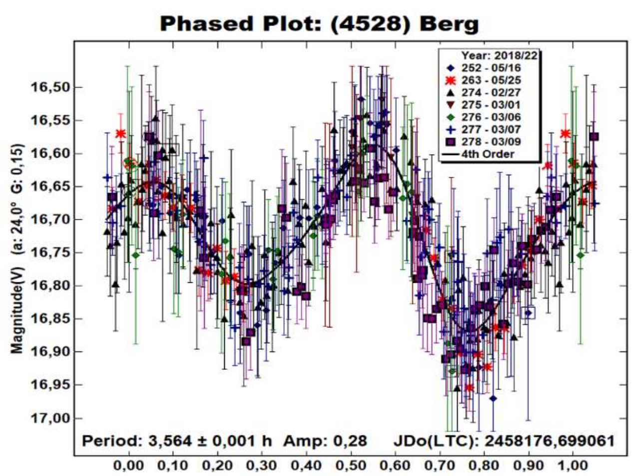


(5501) 1982 FF2. This Main-Belt asteroid (inner) was discovered on 1982 March 30 by L. G. Taff at SOCORRO, USA. We made observations on 2022 December 26-27. From our data we derive a rotation period of 2.464 ± 0.002 h and an amplitude of 0.16 mag. Chang et al. (2016) found a similar period of 2.46 h with U=1.

The asteroid could be perfectly monomodal since the lightcurve is completely symmetric. In any case we accept the bimodal form as good. This point is outside the accuracy of our team at this time. We attach the graph with helves.

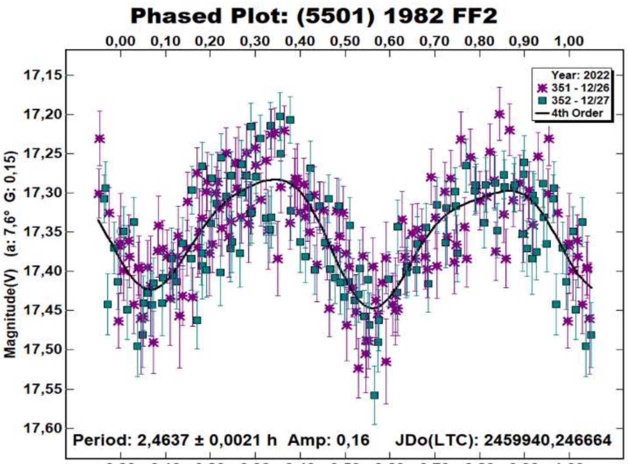


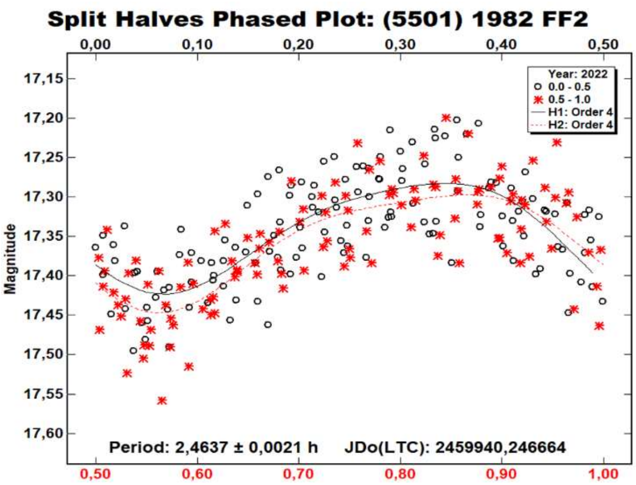


(5643) Roques. This Main-Belt asteroid (inner) of the FLO category was discovered on 1990 Aug 22 by H. E. Holt at Palomar Observatory, California. We made observations on 2022 May 8-10. From our data we derive a rotation period of 7.49 ± 0.03 h and an amplitude of 0.13 mag. Chang et al. (2016) found an ambiguous period of 3.89 / 7.78 h. with incomplete data (U=1).

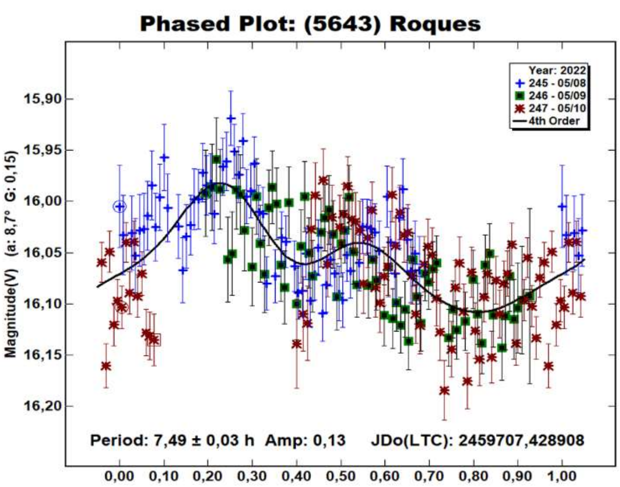


(7195) Danboice. This-Main Belt asteroid (inner) was discovered on 1994 Jan 2 by H. E. Holt at Palomar Observatory, California. We made observations on 2022 May 10-14. From our data we derive a rotation period of 8.689 ± 0.0075 h and an amplitude of 0.29 mag. Chang et al. (2014) found a period of 8.67 h with incomplete data (U=1+), which is consistent with our observations.

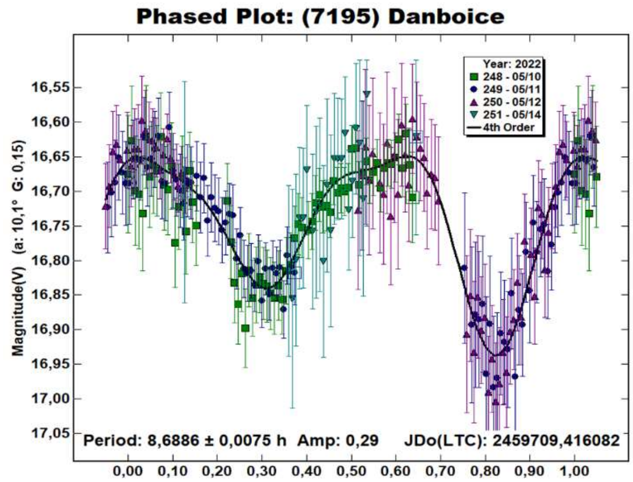


(7317) Cabot. This Main-Belt asteroid (inner) was discovered on 1940 March 12 by G. Kulin from the Konkoly Obs, Hungary. We made observations on 2022 Aprl 4-10. From our data we derive a rotation period of 2.345 ± 0.002 h and an amplitude of 0.08 mag. Waszczak et al. (2015) found a period of 2.237 h with incomplete data (U=1).

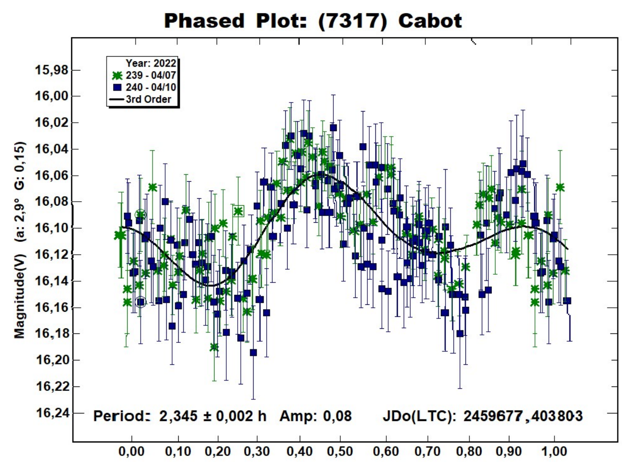


(12999) Torun. This Main-Belt asteroid (inner) of the FLO family was discovered on 1981 Aug 30 by E. Bowell at Anderson Mesa observatory in USA. We made observations on 2022 Aug 14-24. From our data we derive a rotation period of 4.020 ± 0.003 h and an amplitude of 0.06 mag. Waszczak et al. (2015) found a period of 3.552 h with incomplete data (U=1). We note these data are near the limit of our equipment.

| Number | Name | mm/dd | Pts | Phase | $L_{PAB}$ | $B_{PAB}$ | Period(h) | P.E. | Amp | A.E. | Grp |
|---|---|---|---|---|---|---|---|---|---|---|---|
| 1055 | Tynka | 22/05/02-06/04 | 805 | 11.08 | 224.7 | 7.4 | 11.893 | 0.001 | 0.07 | 0.01 | MB-I |
| | (from Stephens) | 2012 03/27-05/09 | | | | | | | | | |
| 1417 | Walinskia | 22/12/25 | 156 | 6.94 | 113.2 | 2.4 | --- | --- | --- | --- | MB-O |
| 1500 | Jyvaskyla | 2022/11/6-23 | 922 | 6.84-8.22 | 51.5 | 6.2 | 8.8268 | 0.0002 | 0.95 | 0.05 | MB-I |
| 2003 | Harding | 2022/04/04-05/05 | 250 | 4.73-6.27 | 195.9 | 0.35 | 4.453 | 0.001 | 0.08 | 0.01 | MB-O |
| 2695 | Christabel | 2022/05/ 5-7 | 250 | 3.98-4.23 | 219.4 | 7.3 | 5.623 | 0.004 | 0.73 | 0.05 | MB-M |
| 3686 | Antoku | 2019/03/13-16 | 340 | 24.69-24.55 | 240.9 | 6.45 | 6.744 | 0.006 | 0.3 | 0.05 | MB-M |
| 4528 | Berg | 2022/05/16-25 | 363 | 24.05-24.65 | 174.95 | 4.35 | 3.564 | 0.001 | 0.28 | 0.05 | MB-M |
| | (from Polakis) | 2018/02/27-02/12 | | | | | | | | | |
| 5501 | 1982 FF2 | 2022/12/26-27 | 255 | 20.77-20.85 | 28.1 | 1.2 | 2.464 | 0.002 | 0.16 | 0.02 | MB-I |
| 5643 | Roques | 2022/05/8-10 | 206 | 8.22-7.37 | 236.15 | 7.3 | 7.49 | 0.03 | 0.13 | 0.02 | MB-I |
| 7195 | Danboice | 2022/05/10-14 | 238 | 9.75-8.38 | 245.05 | 10.9 | 8.689 | 0.007 | 0.29 | 0.01 | MB-I |
| 7317 | Cabot | 2022/04/4-10 | 227 | 7.37-1.49 | 201.1 | 1.8 | 2.345 | 0.002 | 0.08 | 0.01 | MB-I |
| 12999 | Torun | 2022/08/14-24 | 205 | 6.05-11.77 | 313.85 | 2.2 | 4.020 | 0.002 | 0.06 | 0.01 | MB-I |
| 15476 | Narendra | 2022/12/28 | 137 | 10.36 | 80.8 | -7.4 | --- | --- | --- | --- | MB-I |
| 19750 | 2000 CM62 | 2022/06-5/7-6 | 149 | 11.65-12.63 | 267 | 19.7 | 6.518 | 0.001 | 0.22 | 0.05 | MB-M |
| 23892 | 1998 SH49 | 2022/07/3-22 | 270 | 11.25-15.57 | 280 | 18.1 | 3.722 | 0.001 | 0.11 | 0.02 | MB- |
| 33697 | 1999 KJ11 | 2022/12/23-24 | 235 | 6.09-5.54 | 102.4 | 0.55 | 4.876 | 0.003 | 0.36 | 0.05 | MB-I |

Table I. Observing circumstances and results. Pts is the number of data points. The phase angle values are for the first and last date. $L_{PAB}$ and $B_{PAB}$ are the approximate phase angle bisector longitude and latitude at mid-date range (see Harris et al., 1984). Grp is the asteroid family/group (Warner et al., 2009). ERI: Erigone; EUN: Eunomia; MB-I/O: Main-belt inner/outer; MC: Mars-crosser; NEA: near-Earth; THM: Themis; TRJ: Jupiter Trojan.

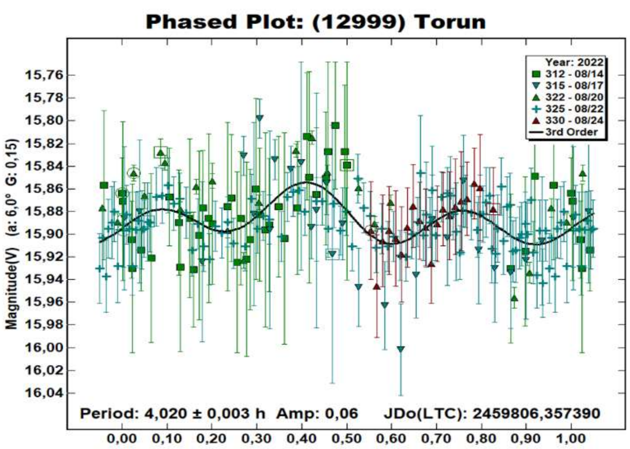


(15476) Narendra. This Main-Belt asteroid (inner) was discovered on 1999 Jan 18 by LINEAR at Socorro, USA. We made observations on 2022 December 28. From our data we are not able to derive any rotation period. In ALCDEF a period of Waszczak et al. (2015) appears, but when consulting the data we found that it is classified as uncertain U=1. We can only confirm the uncertain character. Of course, we cannot confirm the period shown by ALCDEF with 3.036 h and with A=0.08.

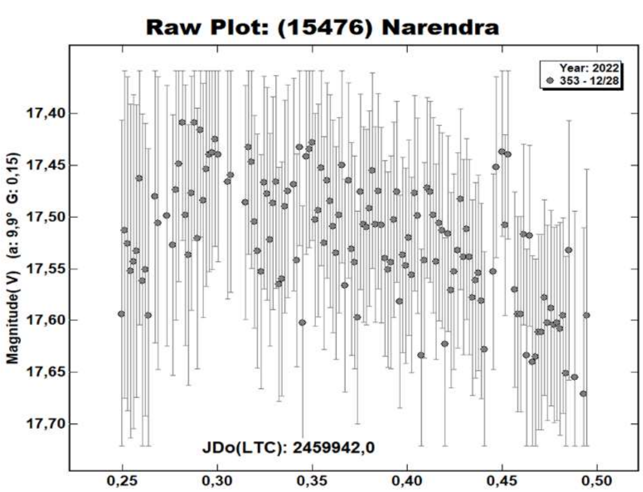


(19750) 2000 CM62. This Main-Belt asteroid (middle) of the MAR family was discovered on 2000 Feb 2 by LINEAR at Socorro in USA. We made observations on 2022 Jun 05 - Jul 06. From our data we derive a rotation period of 6.518 ± 0.001 h and an amplitude of 0.22 mag. Waszczak et al. (2015) found a period of 6.462 h which agrees with our observations.

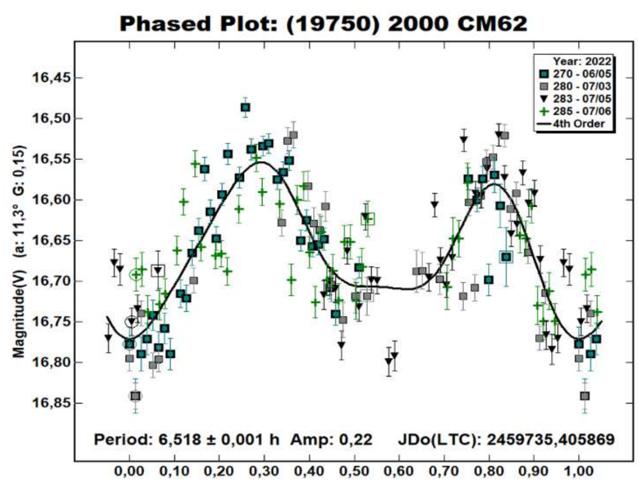


(23892) 1998 SH49. This Main-Belt asteroid (outer) was discovered in 1998 Sep 23 by T. Pawels at the Royal Observatory of Belgium. We made observations on 2022 Jul 3-22. From our data we derive a rotation period of 3.722 ± 0.001 h and an amplitude of 0.11 mag. Waszczak et al. (2015) found a period of 3.72 h which agrees with our observations.

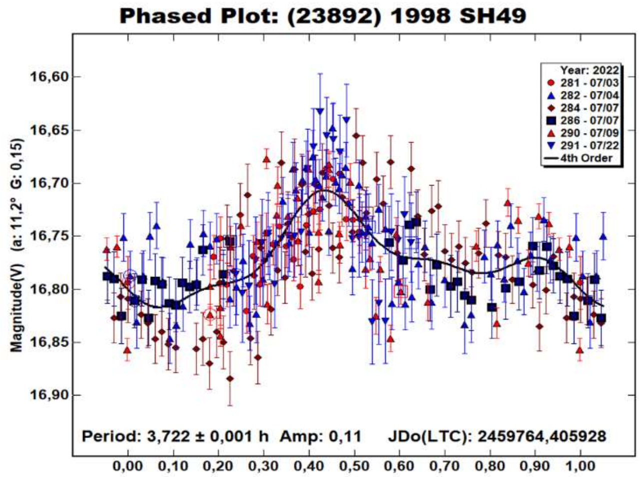


<u>(33697) 1999 KJ11</u>. This Main-Belt asteroid (inner) was discovered on 1999 May 18 at the LINEAR Observatory, Socorro, USA. We made observations on 2022 December 23-24. From our data we derive a rotation period of 4.876 ± 0.003 h and an amplitude of 0.36 mag. Pál et al. (2020) found a period of 4.888 h with U=1.

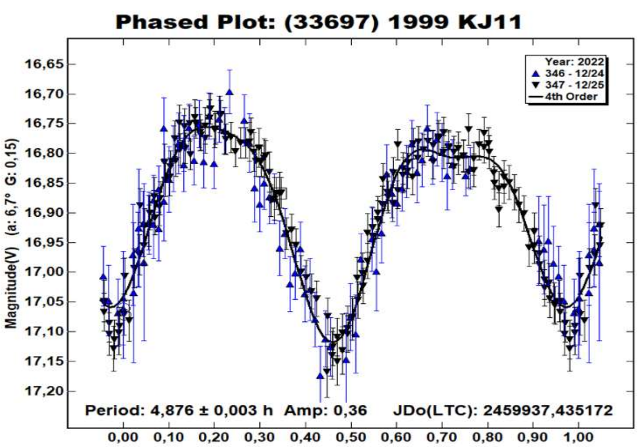


Acknowledgements

We would like to express our gratitude to Brian Warner for supporting the CALL web site and his suggestions.

References

Alvarez-Candal, A.; Duffard, R.; Angeli, C.A.; Lazzaro, D.; Fernández, S. (2004). “Rotational lightcurves of asteroids belonging to familie.” *Icarus* **172**, 388-401.

Behrend, R. (2006web, 2012web, 2018web, 2019web, 2021web). Observatoire de Genève web site. *http://obswww.unige.ch/~behrend/page_cou.html*

Chang, C.-K.; Ip, W.-H.; Lin, H.-W.; Cheng, Y.-C.; Ngeow, C.-C.; Yang, T.-C.; Waszczak, A.; Kulkarni, S.R.; Levitan, D.; Sesar, B.; Laher, R.; Surace, J.; Prince, T.A. (2014). “313 new asteroid rotation periods from Palomar Transient Factory Observations.” *Astrophys. J.* **788**, A17.

Chang, C.-K.; Ip, W.-H.; Lin, H.-W.; Prince, T.A.; Kulkarni, S.R.; Levitan, D.; Laher, R.; Surace, J.; (2016). “Large super-fast rotator hunting using the Intermediatae Palomar Transient Facility.” *Astrophys. J. Supp.* **227**, A20.

Durech, J.; Hanuš, J.; Oszkiewicz, D.; Vančo, R. (2016). “Asteroid models from the Lowell photometric database.” *Astron. Astrophys.* **587**, A48.

Durech, J.; Tonry, J.; Erasmus, N.; Denneau, L.; Heinze, A.N.; Flewelling, H.; Vančo, R. (2020). “Asteroid models reconstructed from ATLAS photometry.” *Astron. Astrophys.* **643**, A59.

Harris, A.W.; Young, J.W.; Scaltriti, F.; Zappala, V. (1984). “Lightcurves and phase relations of asteroids 82 Alkmene and 444 Gyptis.” *Icarus* **57**, 251-258.

Higgins, D.; Pilcher, F. (2009). “Lightcurve analisys of 48 Doris and 1055 Tynka.” *Minor Planet Bull.* **36**, 143-144.

Kryszczynska, A.; Colas, F.; Polinska, M.; Hirsch, R. and 26 colleagues (2012). “Do Silvan states exist in the Flora Family? I. Photometric Survey of the Flora region.” *Astron. Astrophys.* **546**, A72.

Pál, A.; Szakáts, R.; Kiss, C.; Bódi, A.; Bognár, Z.; Kalup, C.; Kiss, L.L.; Marton, G.; Molnár, L.; Plachy, E.; Sárneczky, K.; Szabó, G.M.; Szabó, R. (2020). “Solar System Objects Observed with TESS - First Data Release: Bright Main-belt and Trojan Asteroids from the Southern Survey.” *Ap. J.* **247**, A26.

Polakis, T. (2018). “Lightcurve analysis for eleven main-belt minor planets.” *Minor Planet Bull.* **45**, 269-273.

Stecher, G.; Ford, L.; Bluem, J.; Smith, B.; Fahey, S. (2015). “The rotation period of 4528 Berg.” *Minor Planet Bull.* 42, 148.

Warner, B.D.; Harris, A.W.; Pravec, P. (2009). “The Asteroid Lightcurve Database.” *Icarus* **202**, 134-146. Updated 2016 Sep. *http://www.minorplanet.info/lightcurvedatabase.html*

Waszczak, A.; Chang, C.-K.; Ofek, E.O.; Laher, R.; Masci, F.; Levitan, D.; Surace, J.; Cheng, Y.-C.; Ip, W.-H.; Kinoshita, D.; Helou, G.; Prince, T.A.; Kulkarni, S. (2015). “Asteroid light curves from the Palomar Transient Factory survey: rotation periods and phase functions from sparse photometry.” *Astronomical Journal* **150**, 75.

# LIGHTCURVE ANALYSIS OF THE KORONIS FAMILY MEMBER 1840 HUS

Gonzalo Fornas, Alvaro Fornas, AVA - J57, CAAT
Centro Astronómico del Alto Turia, Aras de los Olmos, Spain
gon@iicv.es

Enrique Arce, AVA - J67
Vallbona Observatory, Puebla de Vallbona, Spain

Fernando Huet, AVA - Z93
Polop de la Marina, Spain

(Received: 2023 April 10)

We report rotation lightcurves of 1840 Hus observed during its apparition in 2023. We have analyzed our data to calculate the synodic period with the *Canopus* software. Our conclusion with the available data is that the synodic rotation period is 4.7491 h

In the present study we report the data obtained during the observation campaign of the asteroid 1840 Hus carried out during the apparition of 2023. This work has been done from:

- Astronomical Center Alto Turia (CAAT), with the MPC code J57, located in Aras de los Olmos, Valencia
- Vallbona Observatory, with the MPC code J67, located at Puebla de Vallbona, Valencia.

All of them operated by members of the Valencian Astronomy Association (AVA) (*http://www.astroava.org*).

| Observatory | Telescope (m) | CCD (filter) | Observations |
|---|---|---|---|
| C.A.A.T. J57 | 43 cm DK | SBIG STXL-11002 C filter | 02/16 02/17 02/18 02/19 02/20 03/14 03/15 03/18 |
| C.A.A.T. J57 | 106 mm Refr | ZWO ASI 1600 L filter | 01/11 |
| J67 | SC 10” | ZWO ASI194 C filter | 01/25 01/27 03/14 |

Table I. List of instruments and observations

This study is intended as a continuation of the observations made by Slivan et al. (2021) on the apparition in 2020. He calculated a rotation period of 4.7483 ± 0.0008 h. In the LCDB (Warner et al., 2009) we find statistical analyses of “sparse data” from surveys: Erasmus et al. (2020) report a period of 4.749 ± 0.001h. Durech et al. (2016) using Lowell data reports a sidereal period of 4.749057 ± 0.00001h.

Our observations were made in 10 nights in 2023 Jan 11 - March 18. Our analysis with *Canopus* shows a synodic rotation period of 4.7491 ± 0.0001 h.

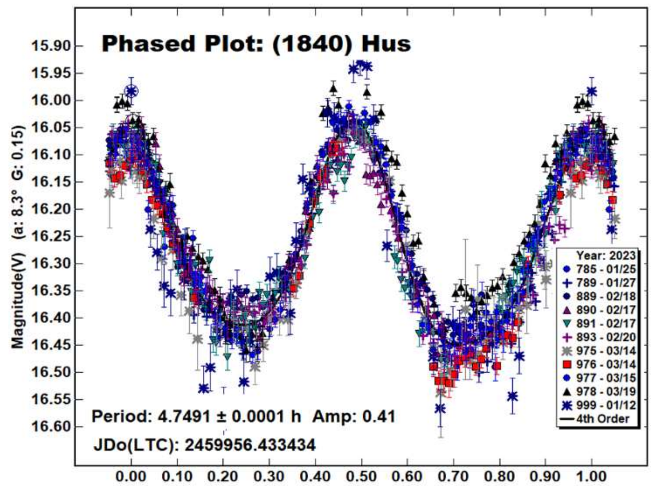


Acknowledgements

We would like to express our gratitude to Brian Warner for supporting the CALL web site and his suggestions and to Dr. Stephen Slivan for his advice.

References

Durech, J.; Hanus, J.; Oszkiewsicz, D.; Vanco, R. (2016). “Asteroid models from the Lowell photometric database.” *Astron. Astrophys.* **587**, A48.

Erasmus, N.; Navarro-Meza, S.; McNeill, A.; Trilling, D.E.; Sickafoose, A.A.; Denneau, L.; Flewelling, H.; Heinze, A.; Tonry, J.L. (2020). “Investigating Taxonomic Diversity within Asteroid Families through ATLAS Dual-band Photometry.” *Ap. J. Suppl. Ser.* **247**, A13.

Slivan, S.M.; McLellan-Cassivi, C.; Shishido, R.; Wang, N. (2021). “Rotation Period of Koronis Family Member 1840 Hus.” *Minor Planet Bull.* **48**, 112-113.

Warner, B.D.; Harris, A.W.; Pravec, P. (2009). “The Asteroid Lightcurve Database.” *Icarus* **202**, 134-146. Updated 2016 Sep. *http://www.minorplanet.info/lightcurvedatabase.html*

| Number | Name | yyyy mm/dd | Phase | $L_{PAB}$ | $B_{PAB}$ | Period(h) | P.E. | Amp | A.E. | Grp |
|---|---|---|---|---|---|---|---|---|---|---|
| 1840 | Hus | 2023/01/11-03/18 | 8.3,11.9 | 145.5 | 2.8 | 4.7491 | 0.0001 | 0.41 | 0.05 | MB-O |

Table II. Observing circumstances and results. The phase angle is given for the first and last date. $L_{PAB}$ and $B_{PAB}$ are the approximate phase angle bisector longitude/latitude at mid-date range. Grp is the asteroid family/group (Warner et al., 2009).

# LIGHTCURVE AND CONSTRAINTS ON THE SPIN VECTOR OF KORONIS FAMILY MEMBER (1840) HUS: ILLUSTRATING ANALYSIS OF A COMBINED DATA SET

Stephen M. Slivan, Claire J. McLellan-Cassivi
Massachusetts Institute of Technology
Dept. of Earth, Atmospheric, and Planetary Sciences
77 Mass. Ave. Rm. 54-424, Cambridge, MA 02139
slivan@mit.edu

Miquel Serra-Ricart, M.R. Alarcón
Instituto de Astrofísica de Canarias
La Laguna, Tenerife, Spain

(Received: 2023 April 10)

A new lightcurve of Koronis asteroid family member (1840) Hus records two consecutive rotations and confirms the resolution by Slivan et al. (2021) of the rotation period alias. The data are analyzed together with additional new lightcurves (Fornas et al., 2023) as well as observations from earlier apparitions as a case study to illustrate a spin vector determination described in detail, and as an example of an analysis that is documented so that a reader can understand what level of confidence is merited for the results. The Hus data set yields an unambiguous count of rotations back to 2001, a sidereal rotation period of 4.749052 ± 0.000002 h, and indicates that the spin is prograde with a high-latitude pole.

The rotation period determination for Koronis family member (1840) Hus reported by Slivan et al. (2021) was identified as being the only solution that is consistent with the published lightcurve observations, but suitable single-night coverage of a full rotation period was not available to directly check the result. During its apparition in 2023, Hus was observed to obtain a low-noise lightcurve recording nearly two consecutive rotations on a single night which confirms the period. Also, during the same apparition in 2023, Fornas et al. (2023) observed Hus during three lunations to more precisely determine a synodic rotation period. This paper documents in detail as a case study an analysis of all of the 2023 data together with observations from previous apparitions to count sidereal rotations, determine the sense of spin and sidereal rotation period, and constraints on the spin vector orientation, including at each step an assessment of the suitability of the data set to proceed.

Hus was observed on the night of UT 2023 Jan 23-24 at the Teide Observatory at Tenerife, Spain as part of a project during the MIT Astronomy Field Camp subject, using an 0.8-m testing telescope for the Two-Meter Twin Telescope (TTT) project. An Andor iKon-L 936 CCD camera was mounted at a Nasmyth focus, imaging a 17′×17′ field for an unbinned image scale of 0.51 arcsec/pix. Image integrations were 60 s using an *r′* filter. The images were processed for bias, dark, and flat corrections using the TTT data pipeline, and measured using *AstroImageJ* (Collins et al., 2017). A comparison star from the APASS DR9 catalog (Henden et al., 2015) comparable to solar color was used to determine the zero-point calibration to *r′* magnitudes. The resulting lightcurve (Fig. 1) was reduced for light-time and to unit distances. The single-night observed span of 9.0 h records just over 1.9 rotations for unambiguous redundant coverage in rotation phase, yielding a synodic rotation period of 4.75 ± 0.02 h and confirming the alias resolution of Slivan et al. (2021).

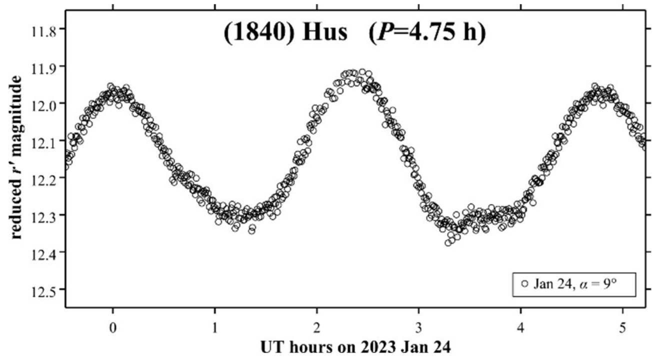


Figure 1. Folded composite lightcurve of (1840) Hus during its 2023 apparition, light-time corrected, showing one rotation period plus the earliest and latest 10% repeated. The estimated error in the *r′* zero-point calibration is 0.03 mag. The legend gives UT date of observation and solar phase angle *α*.

The observations of Hus in 2023 comprise its third apparition of dedicated lightcurves, recording a viewing aspect not included among the published lightcurves from the apparitions observed in 2009 (Clark, 2010) and 2020 (Slivan et al., 2021). The calculation given by Slivan (2012; Eqs. 3-5) can be used to test whether the previously published synodic period is precise enough to unambiguously count rotations between the closest-in-time observed apparitions in the data set, which are those in 2020 and 2023. For $\sigma_{99}(P_{\mathrm{syn}})$ = 0.002 h and $P_{\mathrm{syn}}$ = 4.748 h with the epochs given in Table I, $\Delta t$ = 21554 h and the result is an ambiguity among $N_{\mathrm{per}}$ = 9 possible solutions. However, during its 2023 apparition Hus also was observed by Fornas et al. (2023) who recorded data spanning three lunations to maximize the precision of the derived synodic rotation period. Combining all of the 2023 data for analysis gives a derived synodic period of 4.7491 ± 0.0001 h, for $\sigma_{99}(P_{\mathrm{syn}})$ = 0.00025 h and $N_{\mathrm{per}}$ = 1 solution indicating that an unambiguous rotation count between the two apparitions has been achieved.

The next test is whether the rotation counting can be expanded across the entire data set, in this case back to the epoch from 2009. In this context it is important that the uncertainties of the epochs be carefully estimated. The epoch errors given in Table I are based on the RMS error of the corresponding unfiltered Fourier series fit model to the lightcurve data, calculating the corresponding error along the time axis by dividing by the steepest slope on the filtered model; that is, the slope at its mean value crossing. Using these error estimates, the "sieve algorithm" of Slivan (2013) reveals that the sidereal rotation count from 2009 to 2023 is indeed unambiguous (Fig. 2).

Having confirmed that the data set satisfies both rotation-counting tests, the third test is to see whether the available data can also begin to constrain the spin pole orientation by distinguishing whether the direction of spin is prograde or retrograde; that is, identify whether the spin pole lies in the northern or the southern ecliptic hemisphere, respectively. Constraining pole location involves greater demands on the data set, and three viewing geometries is too few to provide enough information for a credible result. To proceed, the Minor Planet Center Orbits/Observations Database was searched for photometry of Hus that yields suitable composite lightcurves from additional apparitions. Lightcurves from the apparitions in 2019 (similar aspect to the noisy data from 2009) and in 2021 (an aspect lacking dedicated lightcurves) were assembled from data recorded by the ATLAS sky survey (Tonry et al., 2018) and are shown in the upper panels of Fig. 3. The polar graph of the corresponding phase angle bisector (PAB) longitudes in Fig. 4 shows an unusually symmetric pattern of longitudes always close to 90 degrees apart; this is a consequence of the asteroid's orbit period 4.98 years being nearly 5:1 commensurate with Earth's orbit period, and means that the data set lacks observations from intermediate longitudes having information to break the symmetry and distinguish the direction of spin. A second consequence is that the viewing aspect changes by only a small angle for each successive asteroid orbit (2 to 3 degrees per decade for two orbits), so that multiple asteroid orbits must elapse to assemble coverage of intermediate longitudes. The MPC Database then was checked specifically for additional suitable lightcurves of Hus from apparitions as far back in time as possible, in order to maximize the differences in PAB longitude from the most recent apparitions. Usable composite lightcurves from the apparitions in 2001 in 2003 were assembled from data recorded at the USNO Flagstaff station and are shown in the lower panels of Fig. 3.

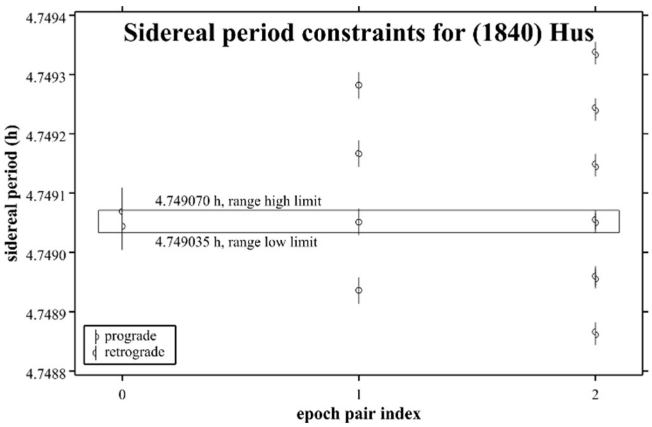


Figure 2. Ranges of possible sidereal rotation periods allowed by the three epochs in Part A of Table I. Each horizontal coordinate index represents the time interval between a pair of epochs (Table II), with longer intervals to the right. Points and range bars represent sidereal periods calculated from every possible number of rotations that could elapse during the interval. The thin horizontal rectangle identifies the single range of periods that is allowed by all three time intervals.

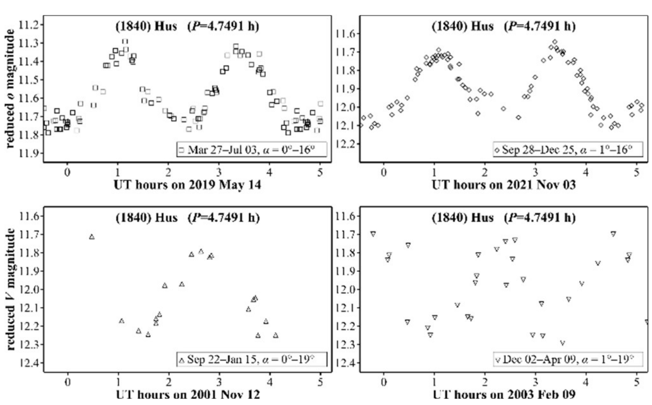


Figure 3. Composite lightcurves of data from sky surveys. (Upper panels) Reduced *o*-band data from ATLAS, selecting the subsets of data points that were recorded between the stationary points of the apparitions. The slope parameter $G_o$ values used to reduce for changing solar phase angle, 0.23 for 2019 and 0.26 for 2021, were determined from the data by fitting the Lumme-Bowell model (Bowell et al., 1989) using the approach described by Slivan et al. (2008). (Lower panels) Reduced *V*-band data from USNO Flagstaff Station. The slope parameter $G$ = 0.23 for S-type objects (Lagerkvist and Magnusson, 1990) was used to reduce for changing solar phase angle.

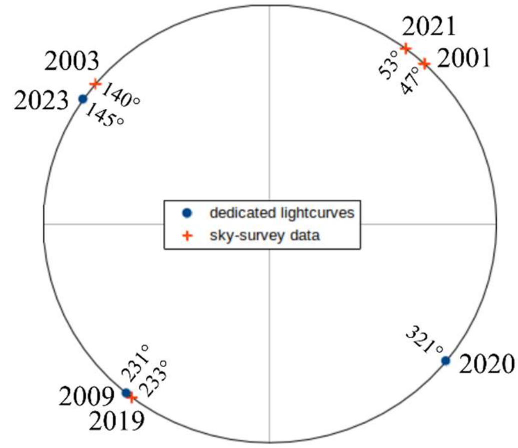


Figure 4. Angular distribution of ecliptic longitudes of PABs for epochs in Table I. Each apparition of sky survey data is represented by a single longitude calculated for the "median date" of the UT dates of observations, reflecting that the information content of these data comes from the nights in combination rather than each night taken individually.

Sidereal photometric astrometry (SPA) (Slivan, 2014; Drummond et al., 1988) was used to calculate the contour graph in Fig. 5 from the expanded set of all seven epochs, which indicates prograde spin and a high ecliptic latitude for the pole. Information about the pole longitude is less clear, partly because longitudes from epoch analyses can be subject to systematic errors even for a plentiful data set, and partly because in this case the symmetry of the observing aspect coverage in ecliptic longitude skews the pattern of contours. The ambiguity of the two pole regions cannot be resolved by the lightcurves because of the small orbit inclination of Hus, about 2 degrees. Crudely estimating from the pole regions graph in Fig. 5, the pole solution $P_1$ latitude is about +70°, longitude between about 335° and 35°; solution $P_2$ latitude is about +74°, longitude between about 165° and 225°. In the absence of a clear pole solution, the most secure sidereal period result comes from applying the sieve algorithm to the expanded set of all seven epochs in Table I, which yields 4.749052 ± 0.000002 h for prograde rotation. A summary of the results is presented in Table III, in which the estimated ranges of the pole longitudes are represented as larger uncertainties, and the coarse estimate of the *a*/*b* axial ratio is based on a triaxial ellipsoid model. The poor constraint on pole longitudes limits the possibilities for more meaningful shape modeling; in particular, the restricted set of viewing geometries falls short of what would be needed for reliable pole and shape model results from convex inversion.

The published sidereal period result that Ďurech et al. (2016) determined for Hus using an ellipsoidal model shape satisfies the same rotation count constraint determined in this work using the sieve algorithm, but the retrograde period value corresponds to an alias sidereal period from our analysis. The accompanying single pole solution that they obtained using convex inversion (Kaasalainen et al., 2001) is about 150° away in pole latitude from our solutions in the opposite ecliptic hemisphere, and thus is not consistent with the constraints from the epochs analysis.

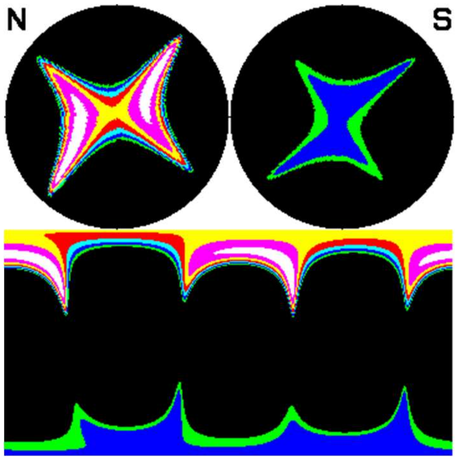


Figure 5. Contour graphs of RMS error of trial poles for the SPA analyses of the seven epochs in Table I. In the lower half of the figure the celestial sphere is projected on a rectangular grid of ecliptic longitude and latitude; the same data in a polar format undistorted near the ecliptic poles appear in the upper half of the graph where north and south hemispheres are plotted separately. Best-fit regions are colored white. The results locate a symmetric pair of high-latitude prograde pole regions, although the skewed pattern of contours also reflects the very incomplete observing aspect coverage in ecliptic longitude.

| UT date | Epoch (UT h) | PAB λ,β(°) | Data ref. |
|---|---|---|---|
| Part A: Dedicated lightcurves | | | |
| 2009 Jun 15 | 1.89 ± 0.35 | 230.8 -0.8 | a |
| 2020 Aug 09 | 0.80 ± 0.11 | 321.1 -3.0 | b |
| 2023 Jan 24 | 2.39 ± 0.03 | 145.4 +2.9 | c |
| Part B: Sky survey lightcurves sparse-in-time | | | |
| 2001 Nov 12 | 2.69 ± 0.14 | 47.0 +0.4 | d |
| 2003 Feb 09 | 2.23 ± 0.21 | 140.3 +3.0 | d |
| 2019 May 14 | 3.46 ± 0.07 | 232.5 -0.6 | e,f |
| 2021 Nov 03 | 3.47 ± 0.07 | 53.2 +0.5 | e,f |

Table I. Summary of lightcurve epochs, in each case locating a maximum from the second harmonic of a Fourier series model fit to the lightcurves. PAB *λ,β* are the J2000.0 ecliptic longitude and latitude of the phase angle bisector. Data references are a, Clark (2010); b, Slivan et al. (2021); c, this work; d, USNO Flagstaff station; e, ATLAS-MLO *o*-band; f, ATLAS-HKO *o*-band. Photometry from USNO Flagstaff and from the ATLAS survey was retrieved from the MPC Orbits/Observations Database.

| Epoch pair index | Interval (d) | Interval (app.) | Epochs source apparitions |
|---|---|---|---|
| 0 | 898.1 | 2 | 2020, 2023 |
| 1 | 4073.0 | 9 | 2009, 2020 |
| 2 | 4971.0 | 11 | 2009, 2023 |

Table II. Time intervals between lightcurve epochs used to identify the ranges of possible sidereal periods in Fig. 2. Columns are: epoch pair index label in Fig. 2, interval length rounded to 0.1 d, the corresponding integer count of elapsed apparitions, and the apparitions from which the defining epochs were measured.

| | | | |
|---|---|---|---|
| sidereal period: | 4.749052 ± 0.000002 h | | |
| | | λ(°) | β(°) |
| spin poles: | $P_1$ | 5 ± 15 | +70 ± 5 |
| | $P_2$ | 195 ± 15 | +74 ± 5 |
| model axial ratio *a*/*b*: | ~1.4 | | |

Table III. Summary of period and pole results. The errors for the pole coordinates are given in degrees of arc and were estimated based on the RMS error distribution of the SPA fits to trial poles.

## Acknowledgments

We thank Dr. Michael Person for organizing and conducting the Field Camp, and G. Fornas for providing his data prior to publication. This article includes observations made at the Two-Meter Twin Telescope (TTT) at the Teide Observatory (managed by the Instituto de Astrofísica de Canarias) that Light Bridges, SL, operates on the Island of Tenerife, Canary Islands (Spain). This research has made use of the VizieR catalogue access tool, CDS, Strasbourg, France (*DOI:10.26093/cds/vizier*). This work also has made use of data and services provided by the International Astronomical Union's Minor Planet Center; specifically, the brightnesses accompanying astrometry from the USNO Flagstaff station and from the Asteroid Terrestrial-impact Last Alert System (ATLAS) survey observing program.

## References

Bowell, E.; Hapke, B.; Domingue, D.; Lumme, K.; Peltoniemi, J.; Harris, A.W. (1989). "Application of Photometric Models to Asteroids." In *Asteroids II* (R.P. Binzel; T. Gehrels; M.S. Matthews, eds.) pp. 524-556. Appendix: The IAU Two-Parameter Magnitude System for Asteroids. U. of Arizona Press, Tucson, AZ.

Clark, M. (2010). "Asteroid Lightcurves from the Chiro Observatory." *Minor Planet Bull.* **37**, 89-92.

Collins, K.A.; Kielkopf, J.F.; Stassun, K.G.; Hessman, F.V. (2017). "AstroimageJ: Image Processing and Photometric Extraction for Ultra-precise Astronomical Light Curves." *Astron. J.* **153**, A77.

Drummond, J.D.; Weidenschilling, S.J.; Chapman, C.R.; Davis, D.R. (1988). "Photometric geodesy of main-belt asteroids. II. Analysis of lightcurves for poles, periods, and shapes." *Icarus* **76**, 19-77.

Ďurech, J.; Hanuš, J.; Oszkiewicz, D.; Vančo, R. (2016). "Asteroid Models from the Lowell Photometric Database." *Astron. Astrophys.* **587**, A48.

Fornas, G.; Fornas, A.; Arce, E.; Huet, F. (2023). "Lightcurve Analysis of the Koronis Family Member 1840 Hus." *Minor Planet Bull.* **50**, 189.

Henden, A.A.; Levine, S.; Terrell, D.; Welch, D.L. (2015). "APASS - The Latest Data Release." *American Astronomical Society 225th Meeting*, id 336.16.

| Number | Name | yyyy mm/dd | Phase | $L_{PAB}$ | $B_{PAB}$ | Period(h) | P.E. | Amp | A.E. |
|---|---|---|---|---|---|---|---|---|---|
| 1840 | Hus | 2023 01/24-01/24 | 8.7 | 145 | 3 | 4.75 | 0.02 | 0.40 | 0.02 |

Table IV. Observing circumstances and results. Phase is the solar phase angle. $L_{PAB}$ and $B_{PAB}$ are the approximate phase angle bisector longitude and latitude.

Kaasalainen, M.; Torppa, J.; Muinonen, K. (2001). “Optimization methods for asteroid lightcurve inversion. II. The complete inverse problem.” *Icarus* **153**, 37-51.

Lagerkvist, C.I.; Magnusson, P. (1990). “Analysis of asteroid lightcurves. II. Phase curves in a generalized HG-system.” *Astron. Astrophys. Suppl.* **86**, 119-165.

Slivan, S.M.; Binzel, R.P.; Boroumand, S.C.; Pan, M.W.; Simpson, C.M.; Tanabe, J.T.; Villastrigo, R.M.; Yen, L.L.; Ditteon, R.P.; Pray, D.P.; Stephens, R.D. (2008). “Rotation Rates in the Koronis Family, Complete to $H \approx 11.2$.” *Icarus* **195**, 226-276.

Slivan, S.M. (2012). “Epoch Data in Sidereal Period Determination. I. Initial Constraint from Closest Epochs.” *Minor Planet Bull.* **39**, 204-206.

Slivan, S.M. (2013). “Epoch data in sidereal period determination. II. Combining epochs from different apparitions.” *Minor Planet Bull.* **40**, 45-48.

Slivan, S.M. (2014). “Sidereal Photometric Astrometry as Efficient Initial Search for Spin Vector.” *Minor Planet Bull.* **41**, 282-284.

Slivan, S.M.; McLellan-Cassivi, C.; Shishido, R.; Wang, N. (2021). “Rotation Period of Koronis Family Member 1840 Hus.” *Minor Planet Bull.* **48**, 112-113.

Tonry, J.L.; Denneau, L.; Heinze, A.N.; Stalder, B.; Smith, K.W.; Smartt, S.J.; Stubbs, C.W.; Weiland, H.J.; Rest, A. (2018). “ATLAS: A High-cadence All-sky Survey System.” *PASP* **130**, 064505.

## AN IMPROVED LIGHTCURVE AND ROTATION PERIOD OF 1178 IRMELA

Frederick Pilcher
Organ Mesa Observatory (G50)
4438 Organ Mesa Loop
Las Cruces, NM 88011 USA
fpilcher35@gmail.com

Lorenzo Franco
Balzaretto Observatory (A81), Rome, ITALY

Giulio Scarfi
Iota Scorpii Observatory (K78), La Spezia, ITALY

Paolo Bacci, Martina Maestripieri
GAMP - San Marcello Pistoiese (104), Pistoia, ITALY

Paolo Fini, Guido Betti
Beato Ermanno Astronomical Observatory (L73)
Impruneta, ITALY

Alessandro Marchini
Astronomical Observatory, University of Siena (K54)
Via Roma 56, 53100 - Siena, ITALY

(Received: 2023 Feb 26)

A collaboration of observers from North America and Europe has produced a lightcurve of 1178 Irmela with synodic period 11.992 ± 0.001 hours, amplitude 0.29 ± 0.02 magnitudes, and full phase coverage.

Previously published period determinations for 1178 Irmela are reported by Binzel (1987), 19.17 hours; Stephens (2012), 11.989 hours; and Polakis (2019), 11.985 hours. The lightcurves published by Stephens (2012) and by Polakis (2019) were made from a single observatory and therefore show only about 2/3 phase coverage for an Earth-commensurate period. Stephens (2012) showed that the 19.17-hour period published by Binzel (1987), based upon sparse lightcurves widely spaced in time, is an 8/5 alias of a period near 11.99 hours.

The authors of this paper, widely spaced in longitude in North America and Europe, respectively, agreed to collaborate to obtain full phase coverage. An equipment list for all observers is provided in table II. Ten sessions 2023 Jan. 26 - Feb. 17 provide a very good fit to bimodal lightcurve with synodic period 11.992 ± 0.001 hours and amplitude 0.29 ± 0.02 magnitudes with full phase coverage. This result is very close to the periods published by Stephens (2012) and by Polakis (2019), and to 5/8 of the period by Binzel (1987).

On 2023 Jan. 31, P. Bacci and M. Maestripieri obtained alternating data points in the V and R filters that show V-R = 0.40. This value is within the usual range 0.38 ± 0.05 for asteroids with C-type taxonomic classifications (Shevchenko and Lupishko, 1998).

| Number | Name | yyyy/mm/dd | Phase | LPAB | BPAB | Period(h) | P.E | Amp | A.E. |
|---|---|---|---|---|---|---|---|---|---|
| 1178 | Irmela | 2023/01/26-02/17 | * 7.4, 5.8 | 138 | -5 | 11.992 | 0.001 | 0.29 | 0.02 |

Table I. Observing circumstances and results. The phase angle is given for the first and last date, unless a minimum (second value) was reached. LPAB and BPAB are the approximate phase angle bisector longitude and latitude at mid-date range (see Harris et al., 1984).

| Observatory (MPC code) | Telescope | CCD | Filter |
|---|---|---|---|
| Organ Mesa Observatory (G50) | 0.35-m SCT f/10 | SBIG STL-1001E | C |
| Iota Scorpii (K78) | 0.40-m RCT f/8 | SBIG STXL-6303e (bin 2×2) | Rc |
| GAMP (104) | 0.60-m NRT f/4 | Apogee Alta | V,Rc |
| Beato Ermanno Astronomical Observatory (L73) | 0.30-m SCT f/6 | QHY174M CMOS (bin 2×2) | Rc |
| Astronomical Observatory, University of Siena (K54) | 0.30-m MCT f/5.6 | SBIG STL-6303e (bin 2×2) | C |

Table II. Observing Instrumentations. MCT: Maksutov-Cassegrain, NRT: Newtonian Reflector, RCT: Ritchey-Chretien, SCT: Schmidt-Cassegrain.

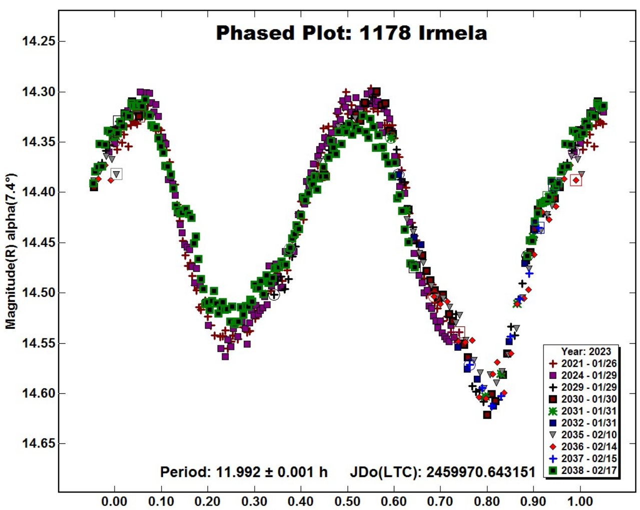


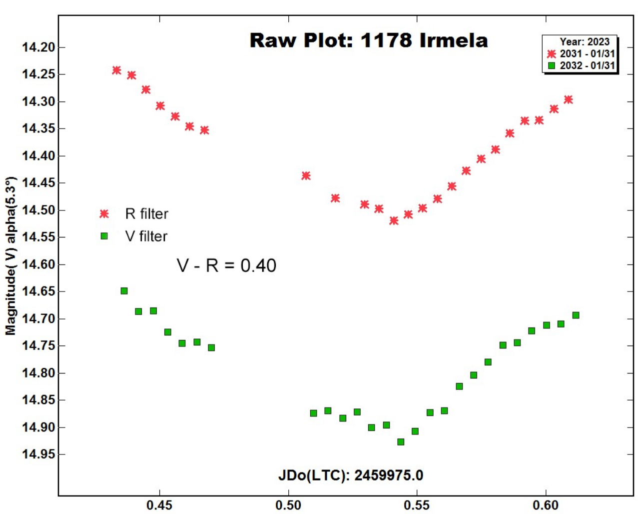


References

Binzel, R.P. (1987). "A Photoelectric Survey of 130 Asteroids." *Icarus* **72**, 135-208.

Harris, A.W.; Young, J.W.; Scaltriti, F.; Zappala, V. (1984). "Lightcurves and phase relations of the asteroids 82 Alkmene and 444 Gyptis." *Icarus* **57**, 251-258.

Polakis, T. (2019). "Photometric observations of seventeen minor planets." *Minor Planet Bull.* **46**, 400-406.

Shevchenko, V.G.; Lupishko, D.F. (1998). "Optical properties of Asteroids from Photometric Data." *Solar System Research* **32**, 220-232.

Stephens, R. (2012). "Asteroids observed from GMARS and Santana Observatories: 2011 October - December." *Minor Planet Bull.* **39**, 80-82.

## ROTATION PERIOD DETERMINATION FOR THE MARS-CROSSING ASTEROID (97514) 2000 DL1

Alessandro Marchini, Riccardo Papini
Astronomical Observatory, DSFTA - University of Siena (K54)
Via Roma 56, 53100 - Siena, ITALY
marchini@unisi.it

Lorenzo Franco
Balzaretto Observatory (A81), Rome, ITALY

(Received: 2023 April 15)

Photometric observations of the Mars-crossing asteroid (97514) 2000 DL1 were conducted in order to determine its synodic rotation period. The asteroid is certainly a slow rotator and the period has not been completely covered by our observations. We present the most likely bimodal solution with a period of P = 163.6 ± 0.3 h, A = 0.47 ± 0.09 mag.

CCD photometric observations of the Mars-crossing asteroid (97514) 2000 DL1 were carried out in 2023 February-April at the Astronomical Observatory of the University of Siena (K54). We used a 0.30-m *f*/5.6 Maksutov-Cassegrain telescope, SBIG STL-6303E NABG CCD camera, and clear filter; the pixel scale was 2.30 arcsec when binned at 2×2 pixels and all exposures were 300 seconds.

Data processing and analysis were done with *MPO Canopus* (Warner, 2018). All images were calibrated with dark and flat-field frames and the instrumental magnitudes converted to R magnitudes using solar-colored field stars from a version of the CMC-15 catalogue distributed with *MPO Canopus*. Table I shows the observing circumstances and results.

A search through the asteroid lightcurve database (LCDB; Warner et al., 2009) indicates that our result may be the first reported lightcurve observations and results for this asteroid.

(97514) 2000 DL1 was discovered on 2000 February 25 by LINEAR at Socorro. It is a Mars-crossing asteroid with a semi-major axis of 2.018 AU, eccentricity 0.272, inclination 35.375°, and an orbital period of 2.87 years. Its absolute magnitude is $H$ = 14.10 (JPL, 2023). In the asteroid lightcurve database (Warner et al., 2009) we found a diameter $D$ = 9.46 km using an absolute magnitude $H$ = 13.90 (Alí-Lagoa and Delbo, 2017).

Observations were conducted over fourteen nights and collected 951 data points. The strongest peak in the period spectrum is situated at about 232 hours, which yields a highly "noisy" and asymmetric tri-modal solution. The mono-modal solution at about 75 hours is highly dispersed and noisy, too. There is a third prominent peak at about 100 hours, but the solution is meaningless. None of them is satisfying since the plots still have large gaps which weaken Fourier interpolation. Given our limited amount of data, we present the bimodal solution with a period of $P$ = 163,6 ± 0.3 h, $A$ = 0.47 ± 0.09 mag as the most likely. However, a few sessions still clearly look as outliers when compared to the mean lightcurve and might suggest a more peculiar behavior of this asteroid. Further observations are strongly recommended and encouraged.

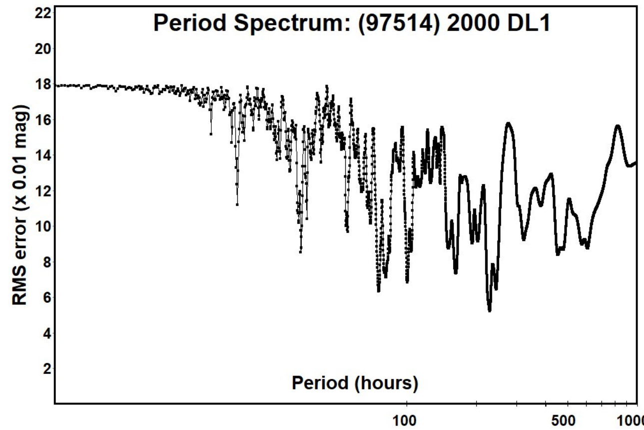


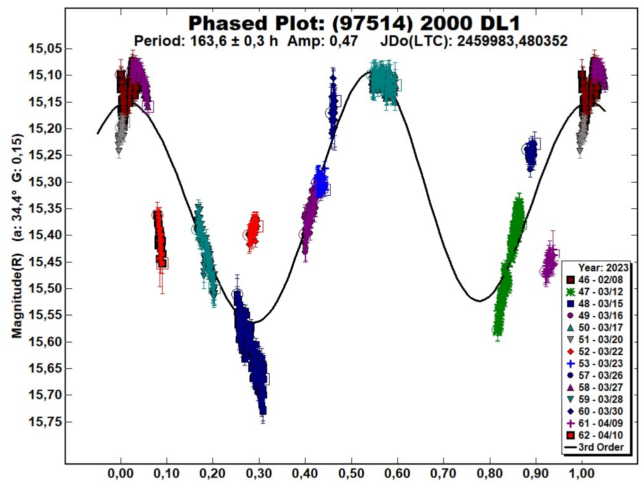


| Number | Name | 2023/mm/dd | Phase | $L_{PAB}$ | $B_{PAB}$ | Period(h) | P.E. | Amp | A.E. | Grp |
|---|---|---|---|---|---|---|---|---|---|---|
| 97514 | 2000 DL1 | 02/07-04/10 | *34.5,21.0 | 174 | 17 | 163.6 | 0.3 | 0.47 | 0.09 | MarsC |

Table I. Observing circumstances and results. The phase angle is given for the first and last date. If preceded by an asterisk, the phase angle reached an extrema during the period. $L_{PAB}$ and $B_{PAB}$ are the approximate phase angle bisector longitude/latitude at mid-date range (see Harris et al., 1984). Grp is the asteroid family/group (Warner et al., 2009).

References

Alí-Lagoa, V.; Delbo, M. (2017). "Sizes and albedos of Mars-crossing asteroids from WISE/NEOWISE data." *Astronomy & Astrophysics* **603**, A55.

Harris, A.W.; Young, J.W.; Scaltriti, F.; Zappala, V. (1984). "Lightcurves and phase relations of the asteroids 82 Alkmene and 444 Gyptis." *Icarus* **57**, 251-258.

JPL (2023). Small Body Database Search Engine. *https://ssd.jpl.nasa.gov*

Warner, B.D.; Harris, A.W.; Pravec, P. (2009). "The Asteroid Lightcurve Database." *Icarus* **202**, 134-146. Updated 2021 Dec. *https://minplanobs.org/mpinfo/php/lcdb.php*

Warner, B.D. (2018). MPO Software, MPO Canopus v10.7.7.0. Bdw Publishing. *http://bdwpublishing.com/*

# BROAD-BAND PHOTOMETRIC MONITORING OF 2500 ALASCATTALO

Misty C. Bentz, Nabanita Das, Thomas Gregoire,
Jessica Hamilton, Sakib Hossain, Tim Johns, Madison LeBlanc,
Shanice Mack, Blake L. Norrington, Alton Patrick, Garrett Polack,
Tamima Saba, Yasmeen Sherif, Melodie Sloneker,
Sepehr Vahdatinia, Ashley Wheeler
Department of Physics and Astronomy
Georgia State University
25 Park Place, Suite 605
Atlanta, GA 30303 USA
bentz@astro.gsu.edu

(Received: 2023 April 15)

Broad-band photometric monitoring of the stony asteroid 2500 Alascattalo was carried out over three nights in 2023 February. We find a typical color of V–R = 0.44 ± 0.05 mag, which is in good agreement with expectations for S-class asteroids. We also report a rotation period of 2.751 ± 0.001 h and a V-band variability amplitude of 0.16 ± 0.02 mag, which are in excellent agreement with previously reported measurements.

2500 Alascattalo was discovered on 1926 April 2 by Karl Wilhelm Reinmuth at the Heidelberg Observatory (JPL, 2023). It is a member of the Flora family of stony asteroids in the innermost asteroid belt, and the collision that formed the Flora family is possibly the source of many large asteroids that impacted the Earth during the mid-Proterozoic era (Vokrouhlický et al., 2017). Recently, 2500 Alascattalo was found to have a satellite that is roughly 40% its diameter (Benishek et al., 2020), making it a binary asteroid system.

Observations of 2500 Alascattalo were obtained as part of the course work for the Georgia State University class *Astronomical Techniques and Instrumentation* at GSU's Hard Labor Creek Observatory in Rutledge, GA. Monitoring was carried out with the 24-inch Miller Telescope, an *f*/6.5 Planewave Corrected Dall-Kirkham Astrograph, equipped with an FLI ProLine CCD with 2048×2048 pixels, giving a field of view of 26.3 arcmin × 26.3 arcmin and a pixel scale of 0.77 arcsec. Images through the Johnson-Cousins *R* filter were collected on UT date 2023 Feb 4 under bright Moon conditions, with a typical exposure time of 300 s for each of the 50 good frames. Darker skies were present when observations through the Johnson *V* filter were collected on UT date 2023 Feb 18, with each of the 67 frames acquired with a typical exposure time of 300 s, and on UT date 2023 Feb 20, with 31 frames acquired using a typical exposure time of 240 s.

All images were reduced in IRAF following standard procedures, which included bias and overscan subtraction, dark subtraction, and flat fielding. Aperture photometry of the asteroid and 6-7 field stars was carried out in IRAF. APASS *V*-band photometry of field stars (Henden et al., 2008) was used to convert instrumental *V* magnitudes to calibrated *V* magnitudes, while the transformation equations of Jordi et al. (2006) for Population I stars were used to determine the effective *R* magnitudes for field stars, and thus the asteroid, using the Sloan *r′* magnitudes and the *g′*–*r′* colors from APASS. We find a typical color for 2500 Alascattalo of V–R = 0.44 ± 0.05 mag. This color agrees well with the expected value 0.475 for stony, or S-type, asteroids (Dandy et al., 2003).

The rotation period and variability amplitude of the asteroid were determined using *MPO Canopus*, which implements the Fourier Analysis of Light Curves (FALC) algorithm of Harris et al. (1989). A rotation period of 2.751 ± 0.001 h and a variability amplitude of 0.16 ± 0.02 mag was determined by offsetting the *R*-band light curve to match the *V* band and then fitting both bands simultaneously. Given the lower signal-to-noise of the *R*-band measurements (blue triangles in the figure below) due to the nearly full Moon on that night, we also fit each band separately:

*V*: rotation period = 2.751 ± 0.001 h, amplitude = 0.16 ± 0.02 mag.
*R*: rotation period = 2.786 ± 0.050 h, amplitude = 0.18 ± 0.02 mag.

While the uncertainties are larger for the period and amplitude derived from the R-band measurements, the results of analyzing each band separately agree with the results derived from fitting both bands together. Our reported rotation period agrees extremely well with previous findings, which include 2.754 ± 0.007 h (Behrend, 2013web), 2.751 ± 0.002 h (Liu, 2016), and 2.75123 ± 0.00009 h (Benishek et al., 2020). The observations we describe here appear to be the first filtered observations of 2500 Alascattalo, but we find a similar amplitude of variability as reported by these earlier studies through a clear filter.

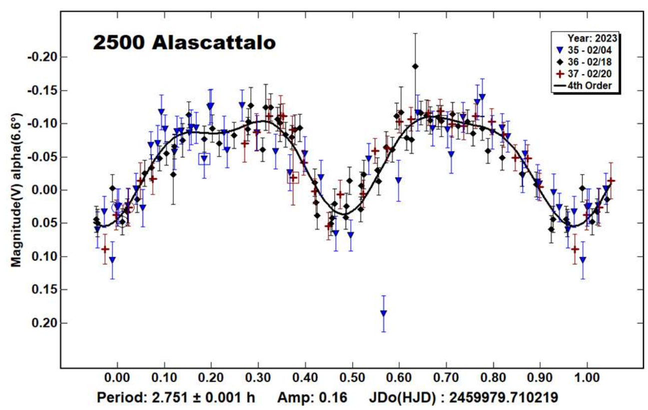


Acknowledgements

IRAF was distributed by the National Optical Astronomy Observatory, which is operated by the Association of Universities for Research in Astronomy (AURA) under a cooperative agreement with the National Science Foundation. This research was made possible in part based on data from the AAVSO Photometric All-Sky Survey (APASS), funded by the Robert Martin Ayers Sciences Fund and NSF AST-1412587.

| Number | Name | 2023 mm/dd | Phase | $L_{PAB}$ | $B_{PAB}$ | Period(h) | P.E. | Amp | A.E. | Grp |
|---|---|---|---|---|---|---|---|---|---|---|
| 2500 | Alascattalo | 02/04-02/20 | *6.61,8.53 | 140 | 10 | 2.751 | 0.001 | 0.16 | 0.02 | 402 |

Table I. Observing circumstances and results. The phase angle is given for the first and last date. If preceded by an asterisk, the phase angle reached an extrema during the period. $L_{PAB}$ and $B_{PAB}$ are the approximate phase angle bisector longitude/latitude at mid-date range (see Harris et al., 1984). Grp is the asteroid family/group (Warner et al., 2009).

References

Benishek, V.; Pravec, P.; Pilcher, F.; Marchini, A.; Papini, R.; Salvaggio, F.; Oey, J.; Pray, D.; Durkee, R.; Cooney, W.; Gross, J.; Terrell, D.; Goncalves, R.; Aznar, A.; and 2 colleagues. (2020). "(2500) ALASCATTALO." *CBET* **4791**.

Behrend, R. (2013web). Courbes de rotation d'astéroïdes et de comètes. *http://obswww.unige.ch/~behrend/page_cou.html*

Dandy, C.L.; Fitzsimmons, A.; Collander-Brown, S.J. (2003). "Optical colors of 56 near-Earth objects: trends with size and orbit." *Icarus* **163**, 363-373.

Harris, A.W.; Young, J.W.; Scaltriti, F.; Zappala, V. (1984). "Lightcurves and phase relations of the asteroids 82 Alkmene and 444 Gyptis." *Icarus* **57**, 251-258.

Harris, A.W.; Young, J.W.; Bowell, E.; Martin, L.J.; Millis, R.L.; Poutanen, M.; Scaltriti, F.; Zappala, V.; Schober, H.J.; Debehogne, H.; Zeigler, K.W. (1989). "Photoelectric Observations of Asteroids 3, 24, 60, 261, and 863." *Icarus* **77**, 171-186.

Henden, A.A.; Terrell, D.; Levine, S.E.; Templeton, M.; Smith, T.C.; Welch, D.L. (2009). "APASS: The AAVSO Photometric All-Sky Survey." *http://www.aavso.org/apass*

Jordi, K.; Grebel, E.K.; Ammon, K. (2006). "Empirical color transformations between SDSS photometry and other photometric systems." *Astron. Astrophys.* **460**, 339-347.

JPL (2023). "Small-Body Database Browser." *https://ssd.jpl.nasa.gov/tools/sbdb_lookup.html*

Liu, J. (2016). "Rotation Period Analysis for 2500 Alascattalo." *Minor Planet Bull*. **43,** 111.

Vokrouhlický, D.; Bottke, W.F.; Nesvorný, D. (2017). "Forming the Flora Family: Implications for the Near-Earth Asteroid Population and Large Terrestrial Planet Impactors." *Astron. J.* **153**, 172.

Warner, B.D.; Harris, A.W.; Pravec, P. (2009). "The Asteroid Lightcurve Database." *Icarus* **202**, 134-146. Updated 2023 April. *http://www.MinorPlanet.info/php/lcdb.php*


# LIGHTCURVES AND ROTATION PERIODS OF 111 ATE, 169 ZELIA, 421 ZAHRINGIA, AND 580 SELENE


Frederick Pilcher
Organ Mesa Observatory (G50)
4438 Organ Mesa Loop
Las Cruces, NM 88011 USA
fpilcher35@gmail.com


(Received: 2023 March 27)


Synodic rotation periods and amplitudes at their early 2023 oppositions are found for 111 Ate 22.068 ± 0.001 hours, 0.11 ± 0.01 magnitudes; 169 Zelia 14.539 ± 0.001 hours, 0.17 ± 0.01 magnitudes; 421 Zahringia 25.509 ± 0.002 hours, 0.14 ± 0.01 magnitudes; 580 Selene 9.494 ± 0.001 hours, 0.19 ± 0.01 magnitudes.


The new observations to produce the results reported in this paper were made at the Organ Mesa Observatory with a Meade 35 cm LX200 GPS Schmidt-Cassegrain, SBIG STL-1001E CCD, 60 to 120 second exposures, unguided, R filter for 11$^{th}$ magnitude 111 Ate, clear filter for all other targets. Image measurement and lightcurve construction were with *MPO Canopus* software with calibration star magnitudes for solar colored stars from the CMC15 catalog reduced to the Cousins R band. Zero-point adjustments of a few × 0.01 magnitude were made for best fit. To reduce the number of data points on the lightcurves and make them easier to read, data points have been binned in sets of 3 with maximum time difference 6 minutes.

111 Ate. Previously published rotation periods for 111 Ate are by Harris and Young (1983), 22.2 hours; Behrend (2006web), 20 hours; Pilcher (2010), 22.072 hours; Pilcher (2011), also 22.072 hours; Szabó et al. (2016), 20.63 hours; Pál et al. (2020), 22.0497 hours. New observations on 8 nights 2023 Jan. 27 - March 10 provide an excellent fit to a lightcurve with period 22.068 ± 0.001 hours, amplitude 0.11 ± 0.01 magnitudes and four unequal maxima and minima per rotational cycle. This value is in good agreement with most of the previously found periods.

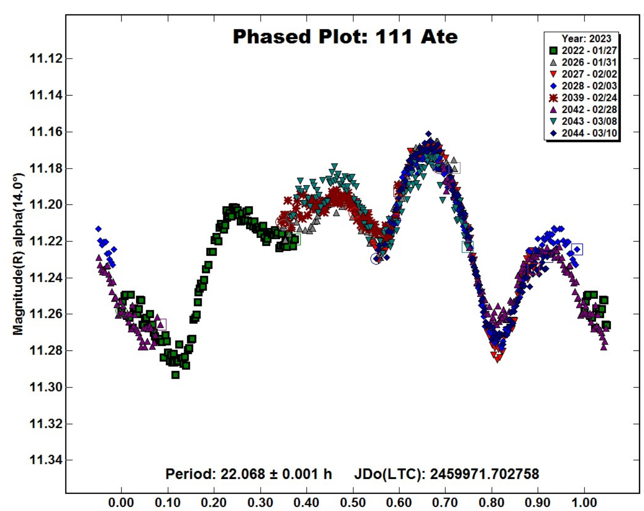

| Number | Name | yyyy/mm/dd | Phase | LPAB | BPAB | Period(h) | P.E | Amp | A.E. |
|---|---|---|---|---|---|---|---|---|---|
| 111 | Ate | 2023/01/27-2023/03/10 | *14.0 - 6.7 | 156 | - 3 | 22.068 | 0.001 | 0.11 | 0.01 |
| 169 | Zelia | 2023/01/28-2023/02/15 | 10.2 - 2.6 | 151 | 3 | 14.539 | 0.001 | 0.17 | 0.01 |
| 421 | Zahringia | 2009/07/12-2009/08/15 | * 7.7 - 11.9 | 301 | 10 | 25.460 | 0.003 | 0.16 | 0.03 |
| 421 | Zahringia | 2022/12/20-2023/01/25 | 18.9 - 5.0 | 125 | -10 | 25.509 | 0.002 | 0.14 | 0.01 |
| 580 | Selene | 2023/02/25-2023/03/19 | 8.4 - 1.8 | 180 | 4 | 9.494 | 0.001 | 0.19 | 0.01 |

Table I. Observing circumstances and results. The phase angle is given for the first and last date, unless a minimum (second value) was reached. LPAB and BPAB are the approximate phase angle bisector longitude and latitude at mid-date range (see Harris *et al.*, 1984).

169 Zelia. Previously published rotation periods for 169 Zelia are by Harris et al. (1992), > 16 hours; Love (1997), 13.27 hours; Stephens and Pilcher (2009), 14.537 hours; and Behrend (2019web), 14.547 hours. New observations on four nights 2023 Jan. 28 - Feb. 15 provide an excellent fit to an unsymmetric bimodal lightcurve with period 14.539 ± 0.001 hours, amplitude 0.17 ± 0.01 magnitudes. This value is in very good agreement with Stephens and Pilcher (2009) and with Behrend (2019web), and rules out the periods by Harris et al. (1992) and Love (1997).

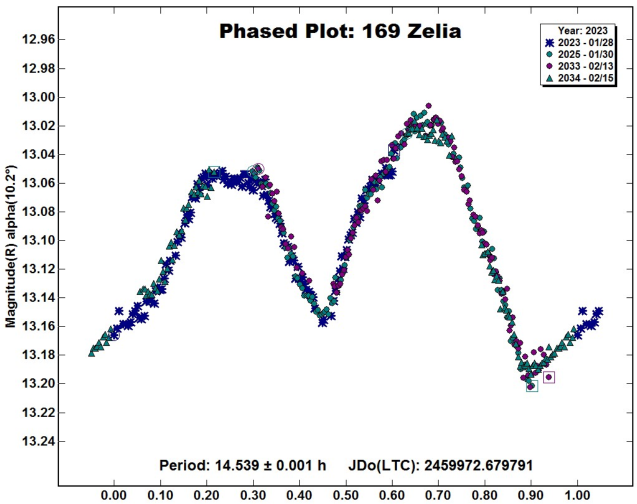


421 Zahringia. Earlier published rotation periods for 421 Zahringia are by Behrend (2001web and 2005web), 17.49 hours; Robinson (2002), 15.5 hours; and Warner (2010), 6.42 hours. This author obtained seven sessions on 421 Zahringia 2009 July 12-Aug. 15 in the poor weather of the local rainy/cloudy season. He was unable to fit the data to a shorter period and did not publish at that time.

Several years later, Waszczak et al. (2015), using sparse data from the Palomar Transient Survey, found a period of 25.489 hours. Durech et al. (2020), on the basis of ATLAS photometry, obtained a sidereal period of 25.5041 hours. On the basis of a likely period near 25.5 hours, this author reexamined his uncalibrated year 2009 data. With *MPO Canopus* software the zero points were adjusted to best fit between 24.5 hours and 26.5 hours and a fit to a period of 25.46 hours, amplitude 0.16 magnitudes, was obtained. The lightcurve was very noisy with nearly 1/3 of the total phase coverage missing, but otherwise looked like 2/3 of a usual bimodal lightcurve. Attempts to fit the data to all of the other narrow minima on a period spectrum between 5 hours and 35 hours produced wildly unrealistic lightcurves.

Eleven sessions on 421 Zahringia were obtained 2022 Dec. 20 to 2023 Jan. 25, phase angles 18.9° to 5.0°. They provide an excellent fit to a slightly asymmetric bimodal lightcurve with period 25.509 ± 0.002 hours and amplitude 0.14 ± 0.01 magnitudes. The entire double period was covered and the split halves plot, not presented here but available from the author on request, shows that the two halves are identical except for the small change of amplitude commonly encountered with a phase angle change as large as was encountered here. This new result is very close to the values found by Durech et al. (2020) and to Waszczak et al. (2015) and rules out all of the earlier published shorter periods.

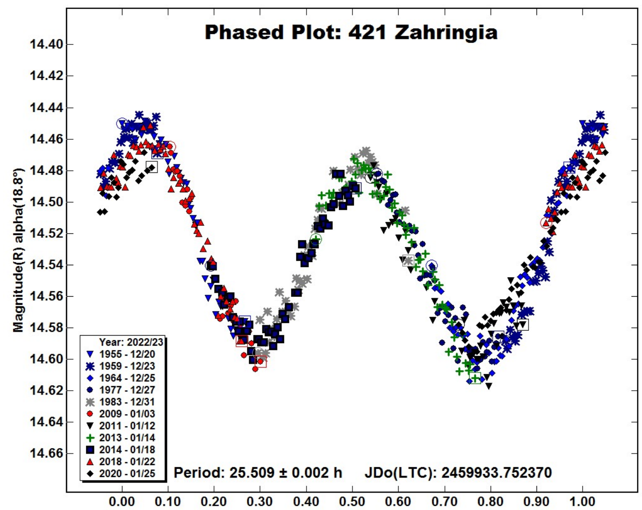


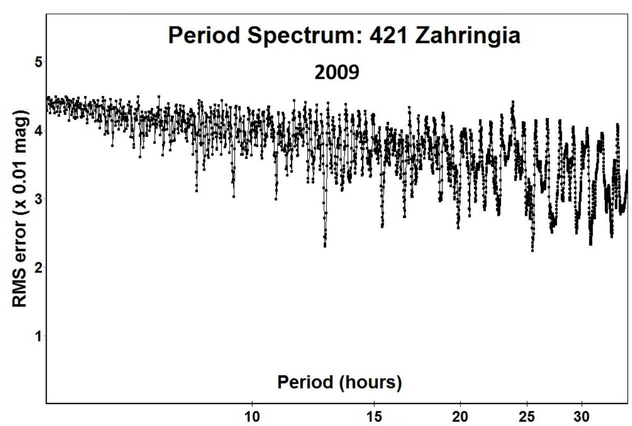

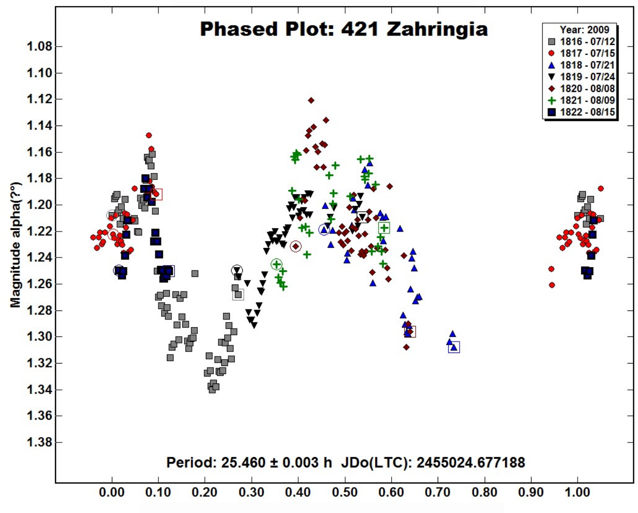


580 Selene. A lightcurve published by Behrend (2005web) provided a synodic period of 9.47 hours. Durech et al. (2019) utilized lightcurve inversion of sparse data to obtain a sidereal period of 9.49285 hours. New observations on five nights 2023 Feb. 25 - March 19 provide a good fit to an unsymmetric bimodal lightcurve with period 9.494 ± 0.001 hours, amplitude 0.19 ± 0.01 magnitudes. This value is in very good agreement with previously published periods.

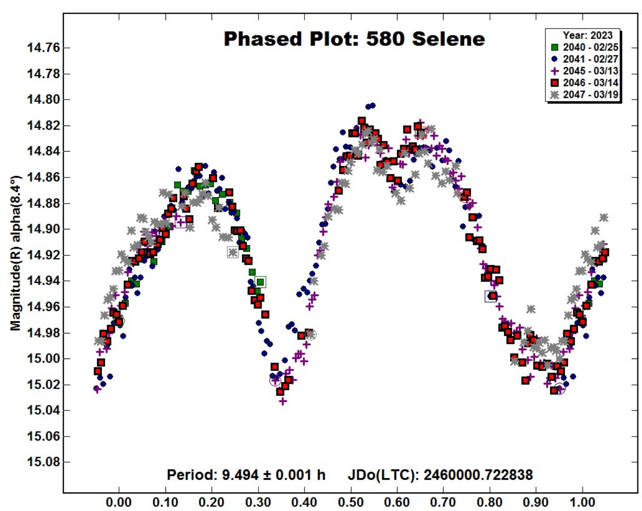


References


Behrend, R. (2001web, 2005web, 2006web, 2019web). Observatoire de Geneve web site. *http://*obswww.unige.ch/*~behrend/page_cou.html*

Durech, J.; Hanus, J.; Vančo, R. (2019). "Inversion of asteroid photometry from the Gaia DR2 and the Lowell Observatory photometric database." *Astron. Astrophys.* **631**, A2.

Durech, J.; Tonry, J.; Erasmus, N.; Denneau, L.; Heinze, A.N.; Flewelling, H.; Vančo, R. (2020). "Asteroid models reconstructed from ATLAS photometry." *Astron. Astrophys.* **643**, A59.

Harris, A.W.; Young, J.W. (1983). "Asteroid Rotation IV. 1979 Observations." *Icarus* **54**, 59-109.

Harris, A.W.; Young, J.W.; Scaltriti, F.; Zappala, V. (1984). "Lightcurves and phase relations of the asteroids 82 Alkmene and 444 Gyptis." *Icarus* **57**, 251-258.

Harris, A.W.; Young, J.W.; Dockweiler, T. (1992). "Asteroid Lightcurve Observations from 1981." *Icarus* **95**, 115-147.

Love, T. (1997). "CCD Photometry of 169 Zelia." *Minor Planet Bull*. **24**, 11-12.

Pál, A.; Szakáts, R.; Kiss, C.; Bódi, A.; Bognár, Z.; Kalup, C.; Kiss, L.L.; Marton, G.; Molnár, L.; Plachy, E.; Sárneczky, K.; Szabó, G. M.; Szabó, R. (2020). "Solar System Objects Observed with TESS - First Data Release: Bright Main-belt and Trojan Asteroids from the Southern Survey." *Ap. J.* **247**, A26.

Pilcher, F. (2010). "Period Determinations for 11 Parthenope, 35 Leukothea, 38 Leda, 111 Ate, 194 Prokne, 262 Valda, 728 Leonisis, and 747 Winchester." *Minor Planet Bull*. **37**, 119-122.

Pilcher, F. (2011. "Rotation period determinations for 11 Parthenope, 38 Leda, 99 Dike, 111 Ate, 194 Prokne, 217 Eudora, and 224 Oceana." *Minor Planet Bull.* **38**, 183-185.

Robinson, L.E. (2002), "Photometry of five difficult asteroids: 309 Fraternitas, 366 Vincentina, 421 Zahringia, 578 Happelia, 959 Arne." *Minor Planet Bull.* **29**, 30-31.

Stephens, R.D.; Pilcher, F. (2009). "Photometric observations of 169 Zelia." *Minor Planet Bull.* **36**, 161.

Szabó, R.; Pál, A.; Sárneczky, K.; Szabó, G.M.; Molnár, L.; Kiss, L.L.; Hanyecz, O.; Plachy, E.; Kiss, C. (2016). "Uninterrupted optical lightcurves of main-belt asteroids from the K2 mission." *Astron. Astrophys.* **596**, A40.

Warner, B.D. (2010). "Upon further review I. An examination of previous lightcurve analysis from the Palmer Divide Observatory." *Minor Planet Bull.* **37**, 127-130.

Waszczak, A.; Chang, C.-K.; Ofek, E.O.; Laher, R.; Masci, F.; Levitan, D.; Surace, J.; Cheng, Y.-C.; Ip, W.-H.; Kinoshita, D.; Helou, G.; Prince, T.A.; Kulkarni, S. (2015). "Asteroid Light Curves from the Palomar Transient Factory Survey: Rotation Periods and Phase Functions from Sparse Photometry." *Astron. J.* **150**, A75

# PHOTOMETRY AND LIGHTCURVE ANALYSIS OF TWO MARS-CROSSING ASTEROIDS: (106848) 2000 YP16 AND (133090) 2003 MS9

Jonatan Michimani, Daniela Lazzaro, Filipe Monteiro,
Eduardo Rondón, Plícida Arcoverde, Marçal Evangelista-Santana,
Weslley Pereira, Wesley Mesquita, Tatiane Corrêa,
Roberto Souza, Teresinha Rodrigues
Observatório Nacional, COAA,
Rua Gal. José Cristino 77, 20921-400,
Rio de Janeiro, Brasil.
jonatangarcia@on.br

(Received: 2023 March 22)

Lightcurves and rotational periods for Mars-Crossing asteroids (106848) 2000 YP16 and (133090) 2003 MS9 were obtained at the Observatório Astronômico do Sertão de Itaparica (MPC code Y28, OASI) in 2021 January-February and October-December, respectively.

CCD photometric observations of two Mars-crossers (MCs) were made at the Observatório Astronômico do Sertão de Itaparica (MPC Y28) between 2021 January-February and October-December. Images were obtained with the 1.0m f/8 telescope of the IMPACTON project and an FLI PL424 CCD camera (2048×2048 pixels) set to 2×2 binning (Rondón et al., 2020) and Johnson-Cousins R filter. The reduction process included calibration of raw images with dark and flat frames via IRAF. MPO Canopus (Warner, 2017) was used for brightness measurements, Fourier analysis (Harris et al., 1989) and to produce the final lightcurves.

Table I shows the date of the observations for each object, as well as the derived rotation period and amplitude of the lightcurve. Individual results are discussed below. The phased rotational lightcurve and the periodogram are shown for each object.

(106848) 2000 YP16. A search in the Asteroid Lightcurve Database (LCDB; Warner et al., 2009) did not find any previously reported period for this MC. This object was observed over several nights in 2021 January and February. Our photometric analysis allowed us to derive a rotational period of 2.199 ± 0.002 h. The lightcurve shows a well-defined bimodal shape and a low maximum amplitude of 0.08 mag.

The period found places the asteroid just above the so-called "spin barrier," of about P = 2.2 h (Pravec and Harris 2000), which might have implications of the cohesive forces of the object (gravitationally-bound or strength-bound). In order to clarify the nature of the object, we believe this MC is an interesting target for future observations.

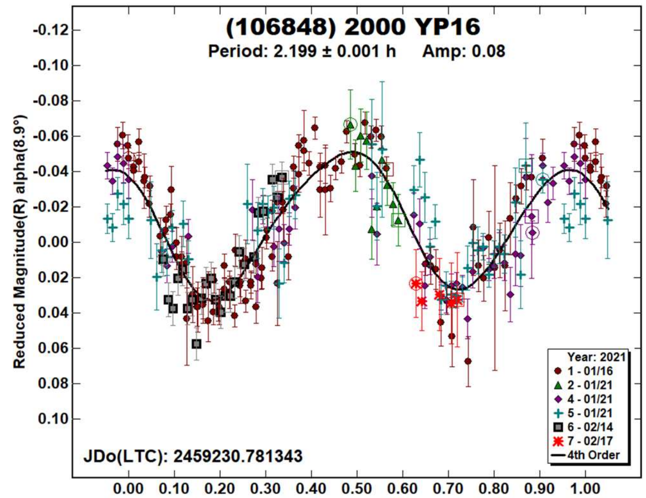


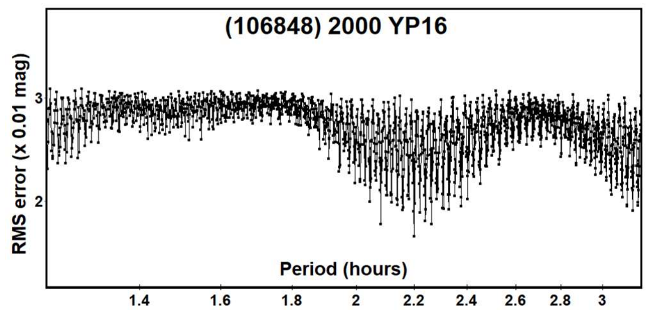


(133090) 2003 MS9. No rotational period has been found in the LCDB (Warner et al., 2009) for this object. In order to get the best possible fit, we grouped the observations into two sets. First, we adjusted a period based on the data obtained over four nights in October 2021. This data showed a period of 4.915 ± 0.005 h and an amplitude of 0.11 mag. Next, we fit the data acquired over three nights in December of the same year and found a period of 4.90 ± 0.01 h with an amplitude of 0.13 mag. Given the small variation in amplitude between the lightcurves with data in October and December, we then performed a new fit including all the data. The period found and the one adopted for this paper is 4.914 ± 0.001 h and an amplitude of 0.10 mag. We present the three fits below.

| Number | Name | 2021 mm/dd | Phase | $L_{PAB}$ | $B_{PAB}$ | Period(h) | P.E. | Amp | A.E. | U |
|---|---|---|---|---|---|---|---|---|---|---|
| 106848 | 2000 YP16 | 01/16-02/17 | * 8.4,18.4 | 131 | -2 | 2.199 | 0.002 | 0.08 | 0.01 | 2+ |
| 133090 | 2003 MS9 | 10/03-12/12 | *29.4,17.3 | 48 | 0 | 4.914 | 0.001 | 0.10 | 0.02 | 2 |

Table I. Observing circumstances and results. The phase angle is given for the first and last date. If preceded by an asterisk, the phase angle reached an extrema during the period. $L_{PAB}$ and $B_{PAB}$ are the approximate phase angle bisector longitude/latitude at mid-date range (see Harris et al., 1984).

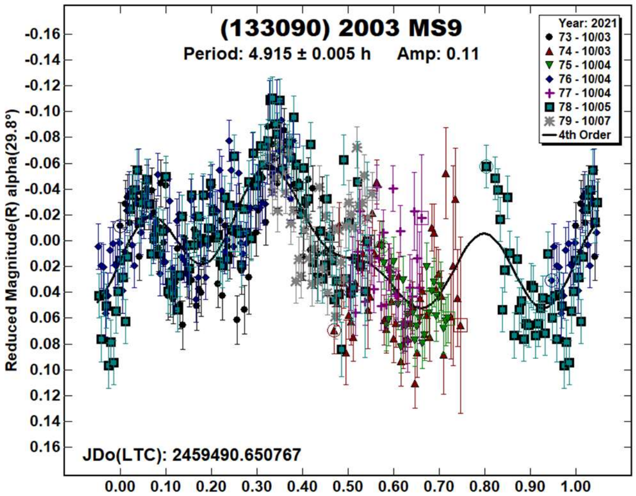


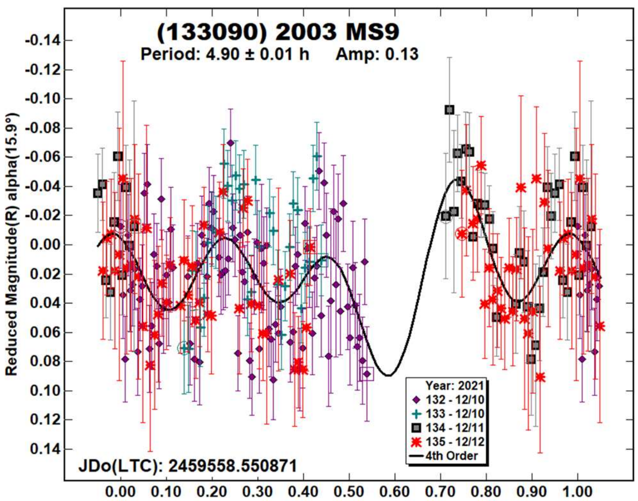


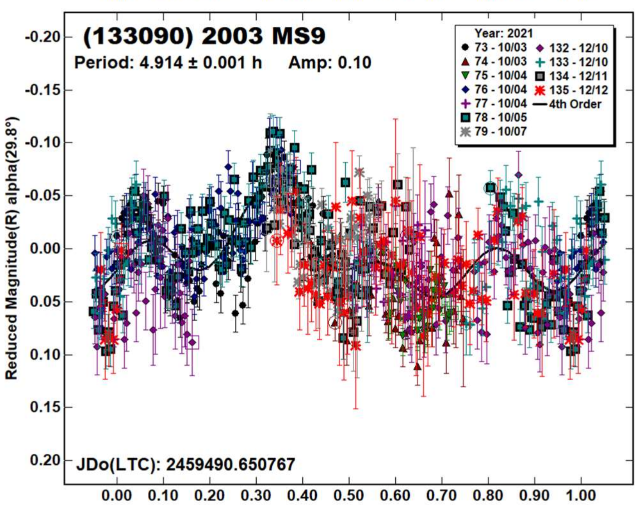


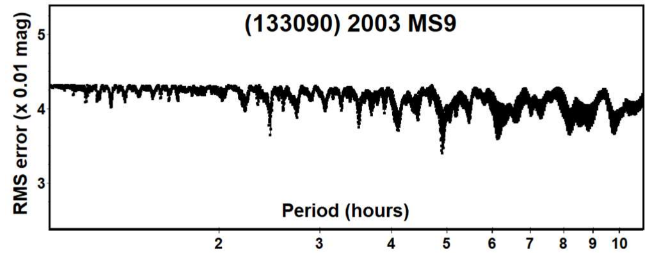



Acknowledgements

The authors acknowledge CNPq, CAPES and FAPERJ for supporting this work through diverse fellowships and grants. Support by CNPq (proc. 310964/2020-2) and FAPERJ (proc. E-26/201.001/2021) is acknowledged by D.L. Technical support at OASI is also recognized, in particular, A. Santiago and J. dos Santos.


References


Harris, A.W.; Young, J.W.; Scaltriti, F.; Zappala, V. (1984). "Lightcurves and phase relations of asteroids 82 Alkmene and 444 Gyptis." *Icarus* **57**, 251-258.

Harris, A.W.; Young, J.W.; Bowell, E.; Martin, L.J.; Millis, R.L.; Poutanen, M.; Scaltriti, F.; Zappala, V.; Schober, H.J.; Debehogne, H.; Zeigler, K.W. (1989). "Photoelectric Observations of Asteroids 3, 24, 60, 261 and 863." *Icarus* **77**, 171-186.

Pravec, P., Harris, A.W. (2000). "Fast and Slow Rotation of Asteroids." *Icarus* **148**, 12-20.

Rondón, E.; Lazzaro, D.; Rodrigues, T.; Carvano, J.M.; Roig, F.; Monteiro, F.; Arcoverde, P.; Medeiros, H.; Silva, J.; Jasmin, F.; de Prá, M.; Hasselmann, P.; Ribeiro, A; Dávalos, J.; Souza, R. (2020). "OASI: A Brazilian Observatory Dedicated to the Study of Small Solar System Bodies - Some Results of NEOs Physical Properties." *PASP* **132**, 065001.

Warner, B.D.; Harris, A.W.; Pravec, P. (2009). "The Asteroid Lightcurve Database." *Icarus* **202**, 134-146. Updated 2016 Sep. *http://www.minorplanet.info/lightcurvedatabase.html*

Warner, B.D. (2017). *MPO Canopus* Software, version 10.7.11.1, BDW Publishing. *http://www.bdwpublishing.com*

# LIGHTCURVE ANALYSIS FOR TWO NEAR-EARTH ASTEROIDS OBSERVED IN JANUARY 2023

Peter Birtwhistle
Great Shefford Observatory
Phlox Cottage, Wantage Road
Great Shefford, Berkshire, RG17 7DA
United Kingdom
peter@birtwhistle.org.uk

(Received: 2023 March 31)

Lightcurves and amplitudes for 2 small near-Earth asteroids observed from Great Shefford Observatory during close approaches in January 2023 are reported. Both are superfast rotators with periods shorter than 3 minutes, one with reliably detected tumbling rotation.

Photometric observations of near-Earth asteroids during close approaches to Earth in January 2023 were made at Great Shefford Observatory using a 0.40-m Schmidt-Cassegrain and Apogee Alta U47+ CCD camera. All observations were made unfiltered and with the telescope operating with a focal reducer at f/6. The 1K×1K, 13-micron CCD was binned 2×2 resulting in an image scale of 2.16 arc seconds/pixel. All the images were calibrated with dark and flat frames and *Astrometrica* (Raab, 2018) was used to measure photometry using APASS Johnson V band data from the UCAC4 catalogue (Zacharias et al., 2013) in *MPO Canopus* (Warner, 2022), incorporating the Fourier algorithm developed by Harris (Harris et al., 1989) was used for lightcurve analysis.

No previously reported results have been found in the Asteroid Lightcurve Database (LCDB) (Warner et al., 2009), from searches via the Astrophysics Data System (ADS, 2023) or from wider searches unless otherwise noted. All size estimates are calculated using H values from the Small-Body Database Lookup (JPL, 2023), using an assumed albedo for NEAs of 0.2 (LCDB readme.pdf file) and are therefore uncertain and offered for relative comparison only.

2023 AQ. This Apollo was discovered by the Mt. Lemmon Survey on 2023 Jan 13.53 UTC and made its closest approach 3.5 days later at 11 Lunar Distances (LD) from Earth (Melnikov et al., 2023). It was observed over a period of 1.6 h starting 2023 Jan 15.02 UTC when it was 17th mag and due to its apparent speed of 35 arcsec/min, exposures were limited to 15 seconds to keep trailing of the target within the measurement aperture of *Astrometrica*. Analysis with *MPO Canopus* reveals a relatively short, 124.7 second rotation period for an object with H = 22.78 (est. dia. ~83 m) and an amplitude of 0.9.

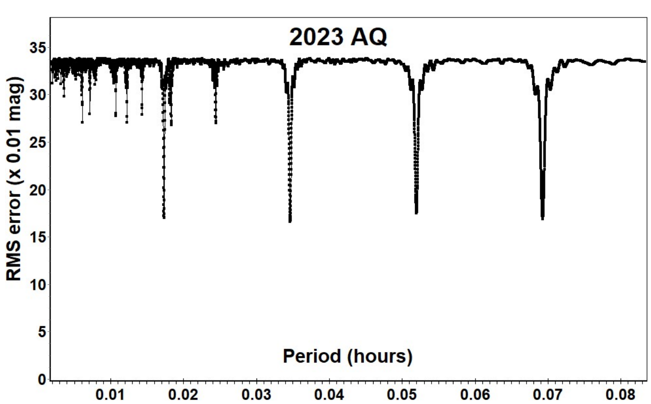


As well as the strong signals related to the derived period the period spectrum includes a number of weaker RMS minima which are all multiples of either 12.89 or 21.98 seconds and have similar strengths. These are suggestive of low amplitude tumbling motion but are discounted here as possible artifacts of the cadence of the exposures taken but also because any signal from real periodicity would be expected to be drastically degraded or completely obscured due to lightcurve smoothing for periods below ~0.0125 h, where the exposure length is potentially 1/3 or more of the indicated periods (Pravec et al., 2000).

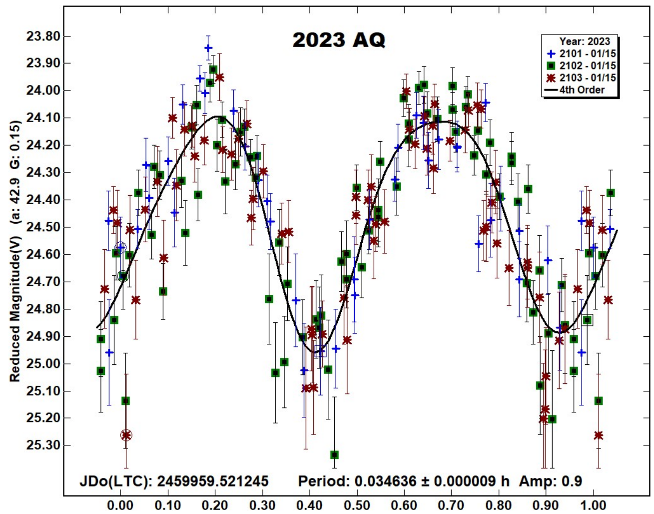


2023 BU. Discovered by G. Borisov at MARGO, Nauchnij, Crimea 5 days before an exceptionally close approach to 3,600 km above the Earth's surface on 2023 Jan 27.02 UTC (Zoltowski et al., 2023). With H = 29.7 it has an estimated dia. of ~3 m and was 17th mag when observed over a period of 3 h starting 2023 Jan 25.96 UTC and as bright as 12th mag the next night, the night of closest approach, when it was followed for 42 min starting at 2023 Jan 26.93 UTC. Exposures were 10 and 12 s on the first night when the apparent speed reached 26 arcsec/min, but with the speed reaching 1700 arcsec/min on the second night exposures of 0.6, reducing to 0.4 s were utilised. 2023 BU trailed no more than 11 arcsecs, allowing all the images on both nights to be measured with a standard aperture in *Astrometrica*. The telescope needed repositioning 7 times on the first night and 16 times on the second. The reduction in *MPO Canopus* from 501 measurements on the first night reveals a dominant period of 77.69 s but with large systematic trends, the best fit lightcurve here labelled PAR for Jan 26.0 UTC.

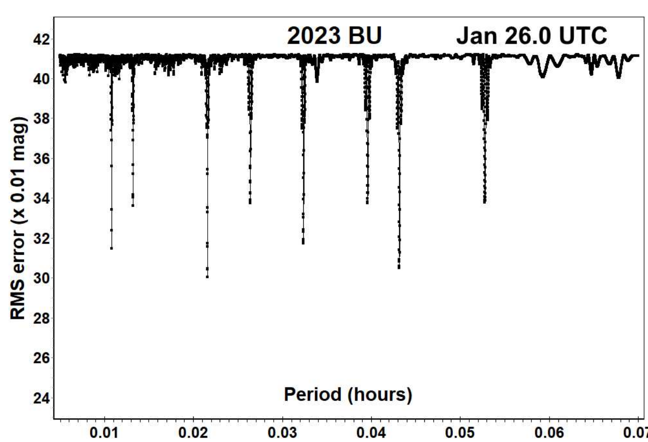

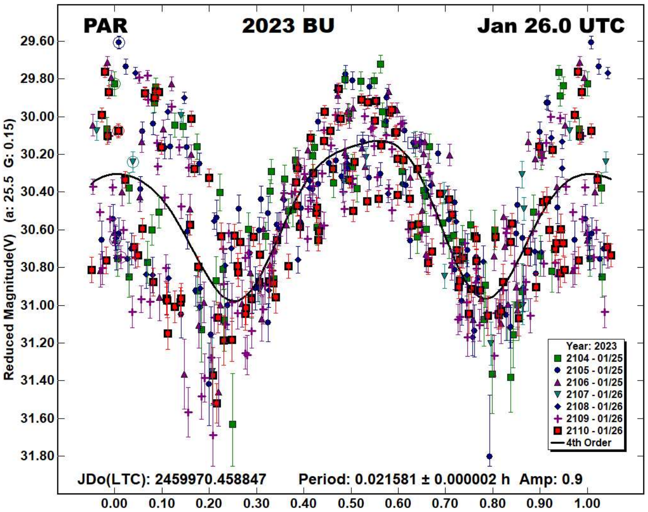


This curve is strongly suggestive of tumbling or non-principal axis (NPA) rotation and a period spectrum covering solutions from 18 - 252 s and labelled Jan 26.0 UTC shows two sets of linearly spaced minima, in multiples of 38.85 and 47.51 s. The *MPO Canopus* Dual Period Analysis function was used to try and resolve periods due to the effects of NPA rotation and the resulting best fit periods are a bimodal period of 77.70 s (= 2 × 38.85) of amplitude 0.9 and a monomodal period of 47.50 s with amplitude 0.7. These lightcurves are labelled P1 and P2 for Jan 26.0 UTC.

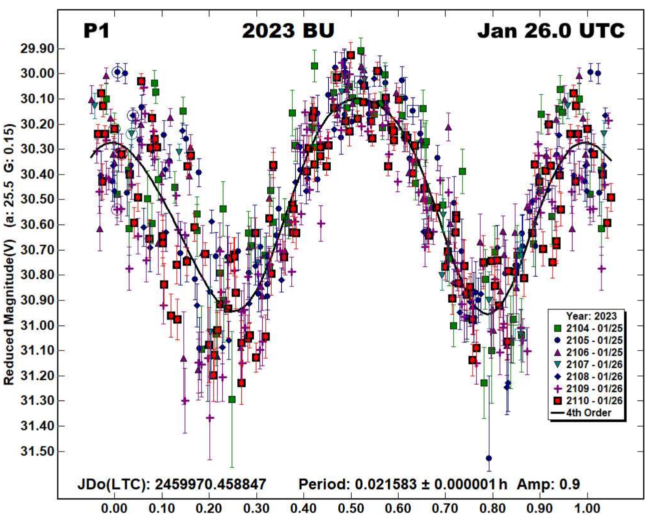


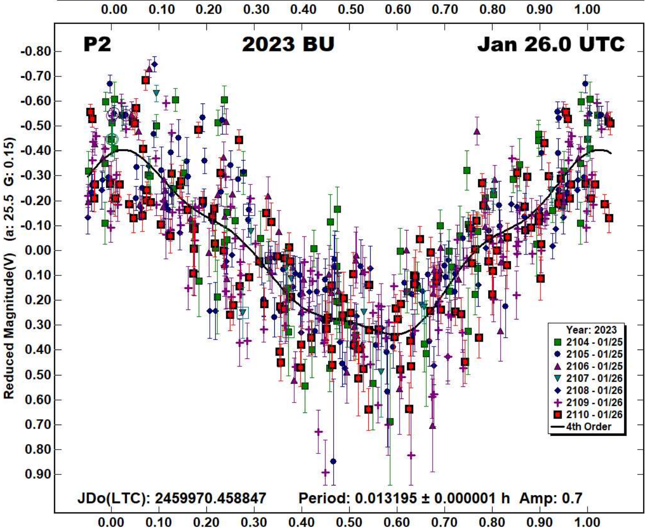


It is noted that the longest exposures used, of 12 s duration are 0.154 P1 and 0.253 P2. Lightcurve smoothing needs to be considered, where the optimal exposure length to maximise signal strength with minimal smoothing for a bimodal lightcurve of period P is determined to be 0.185 P and where exposures longer than 0.185 P would start to smooth and distort the lightcurve (Pravec et al., 2000). The factor of 0.154 for the P1 curve is safely below the optimal value and is estimated to reduce the amplitude of the P1 curve to ~85% of its actual value. The value of 0.253 for the P2 period is also not expected to cause serious lightcurve smoothing, as the strength of the dominant 1st harmonic for this monomodal curve is estimated to only be reduced to ~90% of its actual value, less affected by lightcurve smoothing than the P1 curve.

The analysis of 281 measurements from the second night, during the close approach, was not straightforward. In the 42 minutes 2023 BU was under observation the phase angle doubled from 10.1 to 20.5° as the distance reduced from 0.097 to 0.071 LD. The ephemeris magnitude, using the SBDB values of H=29.69 and G=0.15 does not represent the observed magnitude or the change in magnitude well, indeed the H/G system is not able to reproduce the observed changes. The diagram labelled Raw plots the observed magnitudes uncorrected for phase and distance (black dots), together with the SBDB magnitude formula (solid line) and also a solution assuming G = 1.0 and fitting H = 30.01 by least squares (dashed line). Neither magnitude formula represents the observed brightening well.

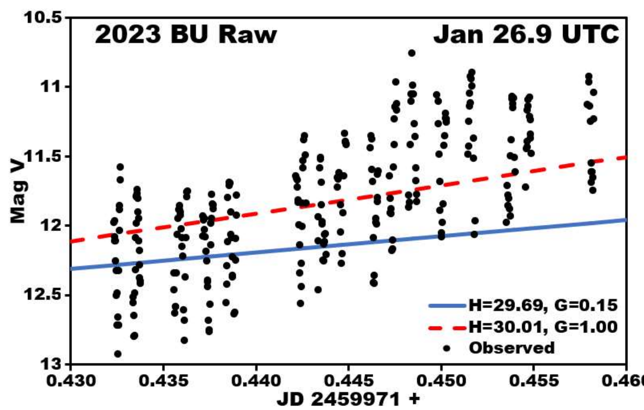


To analyse the lightcurve, the 16 separate sessions were levelled by adjusting the zero-points of each session to minimise the overall RMS fit, this lightcurve is labelled PAR for Jan 26.9 UTC and results in a period of 77.73 s with amplitude 1.0. The degree of scatter due to tumbling visible in the first night appears to be much reduced and additionally, a period spectrum from the second night, labelled PAR for Jan 26.9 UTC shows little evidence of the secondary signals detected the night before. To further investigate, the Dual Period Analysis function was again used, to subtract the effect of the dominant 77.73 s period from the second night and this produced a period spectrum labelled P1 subtracted, showing RMS minima at multiples of 23.76 s. An NPA solution for the second night produces lightcurves labelled P1 and P2 for Jan 26.9 UTC, giving the dominant period at 77.71 s with amplitude of 1.0 and a weaker secondary, bimodal lightcurve with amplitude of 0.3 and a period of 47.51 s, very similar to the 47.50 s monomodal period determined from the measurements obtained for the previous night.

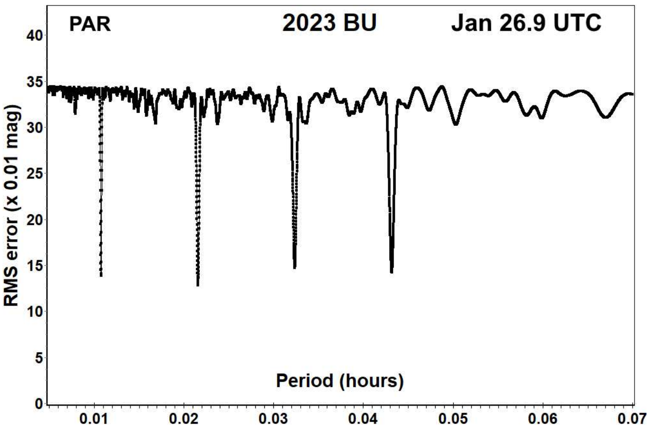


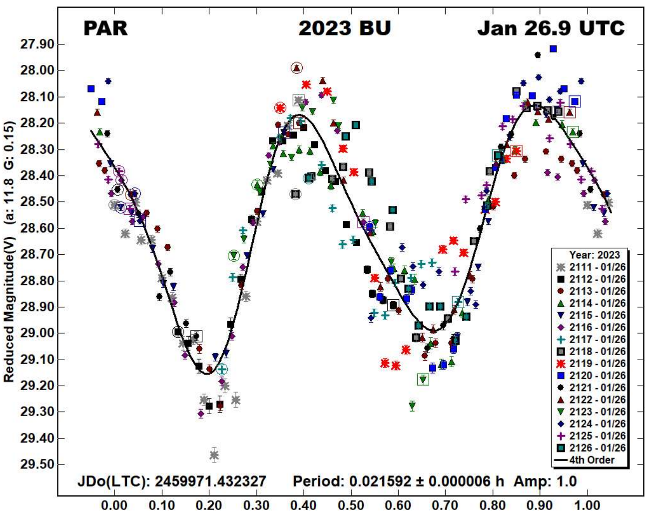


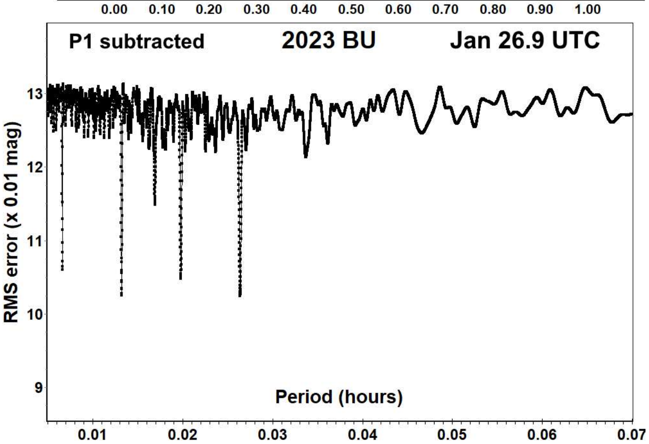


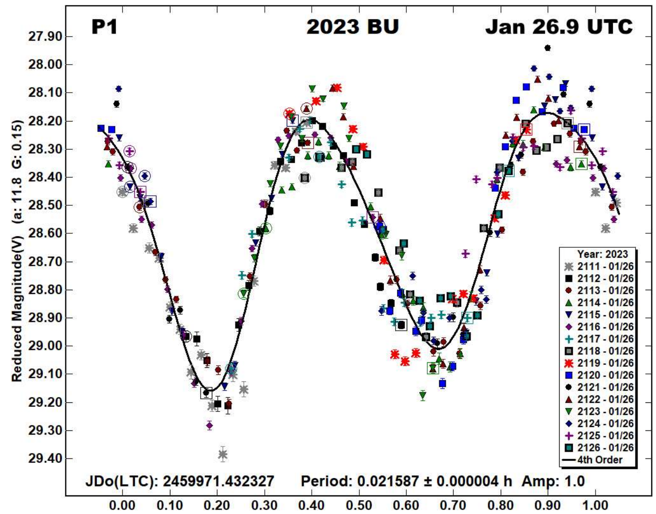


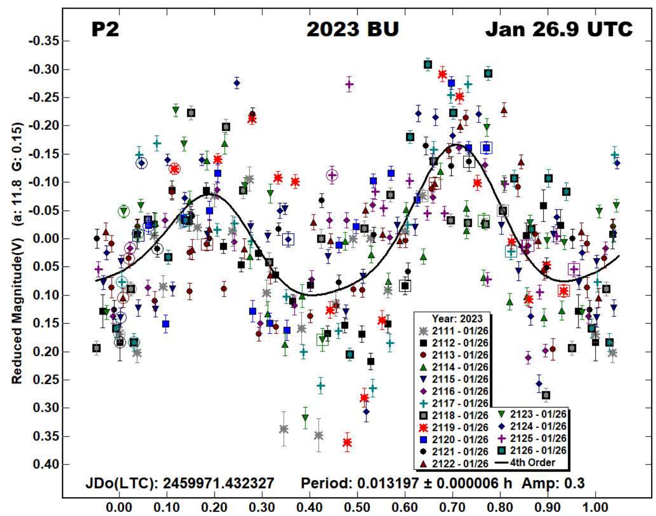


Lightcurves for 2023 BU have appeared on Twitter from San Marcello Pistoiese Observatory, IAU code 104 (Bacci, 2023web) and Northolt Branch Observatory, IAU code Z80 (Wells and Bamberger, 2023web), both from observations made around 2023 Jan 26.8 - 26.9 and both indicating principal axis rotation with a period of 0.0216 ± 0.0001 h, with 104 giving an amplitude of 0.91 and Z80 an amplitude of 0.84. These PAR results are in good agreement with the P1 NPAR results in this paper for Jan 26.0 UTC of period 0.021583 ± 0.000001 h, amplitude 0.9 and for Jan 26.9 UTC of period 0.021587 ± 0.000004 h and amplitude 1.0.

It is concluded that 2023 BU is tumbling and that the main period of 77.70 s is well established, but the other apparent period, of 47.50 s is actually one of a few possible solutions for the second period. The amplitudes of the harmonics related to the frequency 1/47.50 s change dramatically between the two nights (it is predominated by the 1st harmonic on the first night, but by the 2nd harmonic on the second night) suggests that it may be actually a linear combination of the two real frequencies rather than the other real frequency, but this is unsure without full physical modelling. However, on the scale defined in Pravec et al. (2005) it still warrants a coding of PAR = -3, i.e., “NPA rotation reliably detected with the two periods resolved. An ambiguity of the periods solution may be tolerated provided the resulting spectrum of frequencies with significant signal is the same for the different solutions.” (Petr Pravec, personal communication).

| Number | Name | Integration times | Max intg/Pd | Min a/b | Pts | Flds |
|---|---|---|---|---|---|---|
| | 2023 AQ | 14.6-14.9 | 0.119 | 1.4* | 184 | 3 |
| | 2023 BU | 0.4-12 | 0.253 | 1.9 | 782 | 23 |

Table I. Ancillary information, listing the integration times used (seconds), the fraction of the period represented by the longest integration time (Pravec et al., 2000), the calculated minimum elongation of the asteroid (Zappala et al., 1990), the number of data points used in the analysis and the number of times the telescope was repositioned to different fields. Note: * = Value uncertain, based on phase angle > 40°.

Acknowledgements

The author is indebted to Petr Pravec for his help with tumbler 2023 BU. The author also gratefully acknowledges a Gene Shoemaker NEO Grant from the Planetary Society (2005) and a Ridley Grant from the British Astronomical Association (2005), both of which facilitated upgrades to observatory equipment used in this study.

References

ADS (2023). Astrophysics Data System. *https://ui.adsabs.harvard.edu/*

Bacci, P. (2023web). @backman_B09 on Twitter. *https://twitter.com/backman_B09/status/1618762606701060098*

Harris, A.W.; Young, J.W.; Scaltriti, F.; Zappala, V. (1984). "Lightcurves and phase relations of the asteroids 82 Alkmene and 444 Gyptis." *Icarus* **57**, 251-258.

Harris, A.W.; Young, J.W.; Bowell, E.; Martin, L.J.; Millis, R.L.; Poutanen, M.; Scaltriti, F.; Zappala, V.; Schober, H.J.; Debehogne, H.; Zeigler, K. (1989). "Photoelectric Observations of Asteroids 3, 24, 60, 261, and 863." *Icarus* **77**, 171-186.

JPL (2023). Small-Body Database Lookup. *https://ssd.jpl.nasa.gov/tools/sbdb_lookup.html*

Melnikov, S.; Hoegner, C.; Ludwig, F.; Stecklum, B.; Foglia, S.; Galli, G.; Buzzi, L.; Pettarin, E.; Zoltowski, F.B.; Hogan, J.K.; Christensen, E.J.; Fay, D.; Fazekas, J.B.; Fuls, D.C.; Gibbs, A.R. and 25 colleagues (2023). "2023 AQ" MPEC 2023-A57. *https://minorplanetcenter.net/mpec/K23/K23A57.html*

Pravec, P.; Hergenrother, C.; Whiteley, R.; Sarounova, L.; Kusnirak, P.; Wolf, M. (2000). "Fast Rotating Asteroids 1999 TY2, 1999 SF10, and 1998 WB2" *Icarus* **147**, 477-486.

Pravec, P.; Harris, A.W.; Scheirich, P.; Kušnirák, P.; Šarounová, L.; Hergenrother, C.W.; Mottola, S.; Hicks, M.D.; Masi, G.; Krugly, Yu.N.; Shevchenko, V.G.; Nolan, M.C.; Howell, E.S.; Kaasalainen, M.; Galád, A. and 5 colleagues. (2005). "Tumbling Asteroids." *Icarus* **173**, 108-131.

Raab, H. (2018). Astrometrica software, version 4.12.0.448, *http://www.astrometrica.at/*

Warner, B.D.; Harris, A.W.; Pravec, P. (2009). "The Asteroid Lightcurve Database." *Icarus* **202**, 134-146. Updated 2023 Feb. *https://www.minorplanet.info/php/lcdb.php*

Warner, B.D. (2022). MPO Software, Canopus version 10.8.6.12, Bdw Publishing, Colorado Springs, CO.

Wells, G.; Bamberger, D. (2023web). @NBObservatories on Twitter. *https://twitter.com/NBObservatories/status/1618988658056654848*

Zacharias, N.; Finch, C.T.; Girard, T.M.; Henden, A.; Bartlett, J.L.; Monet, D.G.; Zacharias, M.I. (2013). "The Fourth US Naval Observatory CCD Astrograph Catalog (UCAC4)." *The Astronomical Journal* **145**, 44-57.

Zappala, V.; Cellini, A.; Barucci, A.M.; Fulchignoni, M.; Lupishko, D.E. (1990). "An analysis of the amplitude-phase relationship among asteroids." *Astron. Astrophys.* **231**, 548-560.

Zoltowski, F.B.; Helou, G.; Prince, T.A.; Venkataramani, K.; Ye, Q.-Z.; Collaboration, Z.T.F.; Duev, D.A.; Lin, H.-W.; Mahabal, A.A.; Masci, F.J.; Losse, F.; Birtwhistle, P.; Borisov, G.; Mastaler, R.A.; Brucker, M.J. and 18 colleagues (2023). "2023 BU" MPEC 2023-B72. *https://minorplanetcenter.net/mpec/K23/K23B72.html*

| Number | Name | 2023 mm/ dd | Phase | $L_{PAB}$ | $B_{PAB}$ | Period(h) | P.E. | Amp | A.E | PAR | H |
|---|---|---|---|---|---|---|---|---|---|---|---|
| | 2023 AQ | 01/15 | 42.8-43.6 | 136 | -8 | 0.034636 | 0.000009 | 0.9 | 0.2 | | 22.8 |
| | 2023 BU | 01/25-01/26 | *25.5-24.6 | 123 | 3 | 0.021583 | 0.000001 | 0.9 | 0.2 | -3 | 29.7 |
| | | | | | | 0.013195 | 0.000001 | 0.7 | 0.2 | | |

Table II. Observing circumstances and results. The phase angle is given for the first and last date. If preceded by an asterisk, the phase angle reached an extrema during the period. $L_{PAB}$ and $B_{PAB}$ are the approximate phase angle bisector longitude/latitude at mid-date range (see Harris et al., 1984). Amplitude error (A.E.) is calculated as √2 × (lightcurve RMS residual). PAR is the expected Principal Axis Rotation quality detection code (Pravec et al., 2005) and H is the absolute magnitude at 1 au from Sun and Earth taken from the Small-Body Database Lookup (JPL, 2023).

# LIGHTCURVE ANALYSIS OF TWO NEAR-EARTH ASTEROIDS

Paolo Bacci, Martina Maestripieri
GAMP - San Marcello Pistoiese (104), Pistoia, ITALY
b09.backman@gmail.com

(Received: 2023 April 6)

We report photometric analysis of two near-Earth asteroids observed during close approaches in 2023 March. For 2023 EY we found P=0.0281 ± 0.0001 h, amplitude of 0.59 mag; Results for 2023 DZ2 are P=0.1050 ± 0.0001 h, amplitude of 0.48 mag.

The CCD observations were made in 2023 March using the instrumentation described in the Table I. Lightcurve analysis was performed with *MPO Canopus* (Warner, 2016). All the images were calibrated with dark and flat frames and converted to R magnitudes using solar colored field stars from CMC15 catalogue distributed with *MPO Canopus*. Table II shows the observing circumstances and results.

No previously reported results have been found in the Asteroid Lightcurve Database (LCDB) (Warner et al., 2009), The size estimates are calculated using H values from the Small-Body Database Lookup (JPL, 2023a). Both asteroids are small in size and have a rotation period below the spin-barrier, they are probably monolithic objects.

2023 EY is an Apollo orbit class, discovered by ATLAS South Africa, Sutherland in 2023 March 13 (Cromer et al., 2023), with H = 26.81 and a Minimum Orbit Intersection Distance (MOID) from Earth of 0.00167 au. It was observed for 47 minutes starting at 2023 March 16, 22:56 UT when it was at magnitude 15.4 and motion 121 arcsec/min, at range 0.0028 au. We found a synodic period of P = 0.0281 ± 0.0001 h with amplitude A = 0.59 ± 0.10 mag. and ratio a/b=1.7±0.1 based on the amplitude, for an assumed triaxial ellipsoid viewed equatorially (Zappala et al. 1990).

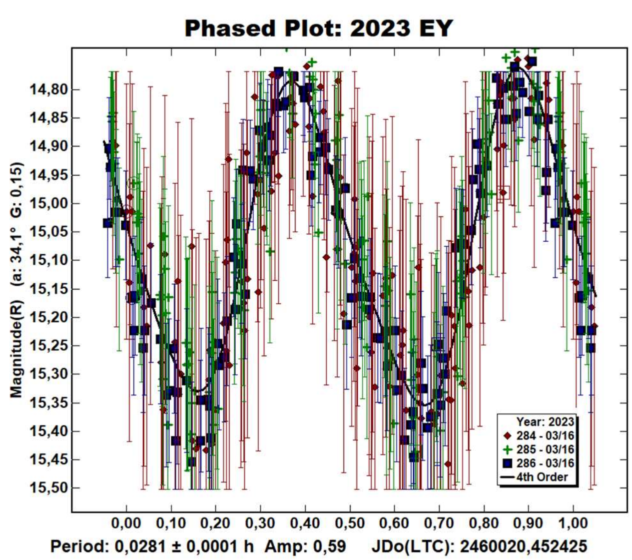


2023 DZ2 is an Apollo asteroid, discovered 2023 February 27 at La Palma (Vaduvescu et al., 2023b), with H = 24.23 and a Minimum Orbit Intersection Distance (MOID) from Earth of 4.776E-5 au. It was originally listed as a Virtual Impactor with a 1/621 probability of hitting Earth on March 27, 2026. Subsequently with a 66-day observation span, it was removed from the Sentry Risk Table (JLP, 2023b) on March 21, 2023. It was observed for 96 minutes starting at 2023 March 22, 19:55 UT, when it was at magnitude 17.0 and motion 2.45 arcsec/min, at range 0.013 au, with unfiltered exposures 120 second. A second observation starting at 2023 March 23 20:18 UT, of 90 minutes, when it was at magnitude 16.1 and motion 7.06 arcsec/min, at range 0.0086 au, with exposures 120 second, using alternating photometric filters V-Rc. We found a synodic period of P = 0.1050 ± 0.0001 h with amplitude A = 0.48 ± 0.10 mag. and ratio a/b=1.6±0.1 based on the amplitude, for an assumed triaxial ellipsoid viewed equatorially (Zappala et al., 1990). We found the color index (V-R) = 0.42 ± 0.03, consistent with a M-type asteroid (Shevchenko and Lupishko, 1998). The period and spectral class are close to the previously published results Goldstone Radar Observations of Asteroid 2023 DZ2 (Benner, 2023).

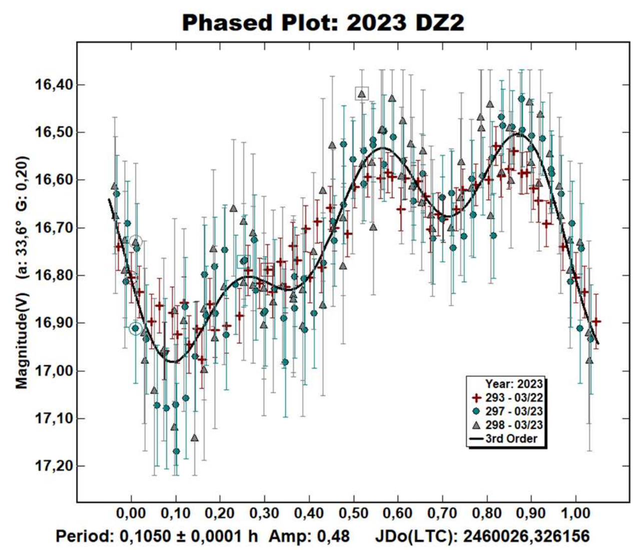


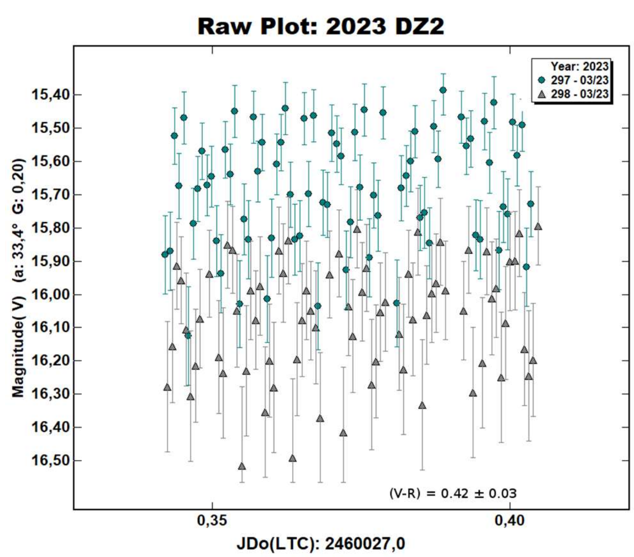

| Observatory (MPC code) | Telescope | CCD | Filter | Observed asteroid |
|---|---|---|---|---|
| GAMP(104) | 0.60-m NRT f/4.0 | Apogee Alta | C, V, Rc | 2023 EY, 2023 DZ2 |

Table I. Observing Instrumentations. CDK: Corrected Dall-Kirkham, MCT: Maksutov-Cassegrain, NRT: Newtonian Reflector, RCT: RitcheyChretien, SCT: Schmidt-Cassegrain.

| Number | Name | 2023 mm/dd | Phase | $L_{PAB}$ | $B_{PAB}$ | Period(h) | P.E. | Amp | A.E. | H |
|---|---|---|---|---|---|---|---|---|---|---|
| | 2023 EY | 16/03 | 34.1 | 157 | 7.5 | 0.0281 | 0.0001 | 0.59 | 0.1 | 26.81 |
| | 2023 DZ2 | 22-23/03 | 33.6/33.4 | 150/152 | -0.5/-0.6 | 0.1050 | 0.0001 | 0.48 | 0.1 | 24.23 |

Table II. Observing circumstances and results. The phase angle is given for the first and last date. If preceded by an asterisk, the phase angle reached an extrema during the period. $L_{PAB}$ and $B_{PAB}$ are the approximate phase angle bisector longitude/latitude at mid-date range (see Harris et al., 1984). Grp is the asteroid family/group (Warner et al., 2009). H is the absolute magnitude at 1 au from Sun and Earth taken from the Small-Body Database Lookup (JPL, 2022).


## Acknowledgements

We thank Luciano Tesi, Honorary President of GAMP - Gruppo Astrofili Montagna Pistoiese, for his fundamental contribution to the study of minor bodies after more than 40 years of presidency and leadership. The observational work of the Pistoiese Mountain Astronomical Observatory is generously supported by Gene Shoemaker NEO Grants awarded by the Planetary Society in 2019.


## References


Benner, L.A.M. (2023). Goldstone Radar Observations Planning: 2023 DZ2. *https://echo.jpl.nasa.gov/asteroids/2023DZ2/2023DZ2.2023.goldstone.planning.html*

Cromer, D.; Hug, G.; Goodin, D.;Valentine, R.; and 8 colleagues (2023).“2023 EY” MPEC 2023-E78. *https://www.minorplanetcenter.net/mpec/K23/K23E78.html*

Harris, A.W.; Young, J.W.; Scaltriti, F.; Zappala, V. (1984). “Lightcurves and phase relations of asteroids 82 Alkmene and 444 Gyptis.” *Icarus* **57**, 251-258.

JPL (2023a). Small-Body Database Lookup. *https://ssd.jpl.nasa.gov/tools/sbdb_lookup.html*

JPL (2023b). Sentry: Earth Impact Monitoring. *https://cneos.jpl.nasa.gov/sentry/*

Shevchenko, V.G.; Lupishko, D.F. (1998). “Optical properties of Asteroids from Photometric Data.” *Solar System Research* **32**, 220-232.

Vaduvescu, O.; Barwell, F.; Jhass, K.; Popescu, M.; de la Fuente, M.C.; de la Fuente, M.R. (2022b). “2023 DZ2” MPEC 2023-F12. *https://www.minorplanetcenter.net/mpec/K22/K22UE5.html*

Warner, B.D.; Harris, A.W.; Pravec, P. (2009). “The Asteroid Lightcurve Database.” *Icarus* **202**, 134-146. Updated 2016 Sep. *http://www.minorplanet.info/lightcurvedatabase.html*

Warner, B.D. (2016). MPO Software, *MPO Canopus* version 10.8.6.9. Bdw Publishing, Eaton, CO.

Zappala, V.; Cellini, A.; Barucci, A.M.; Fulchignoni, M.; Lupishko, D.E. (1990). “An analysis of the amplitude-phase relationship among asteroids.” *Astron. Astrophys.* **231**, 548-560.

# ASTEROID PHOTOMETRY AND LIGHTCURVE ANALYSIS OF 1037 DAVIDWEILLA, 1369 OSTANINA, 1718 NAMIBIA, 4221 PICASSO, 4368 PILLMORE, 4901 O'BRIAIN, 6223-DAHL, AND 7353 KAZUYA

Rafael González Farfán (Z55)
Observatorio Uraniborg
Écija (Sevilla, SPAIN)
uraniborg16@gmail.com

Faustino García de la Cuesta (J38)
La Vara, Valdés
(Asturias, SPAIN)

Javier Ruiz Fernández (J96)
Aroa del Mar Matos Pinto
Observatorio de Cantabria
(Cantabria, SPAIN)

Esteban Fernández Mañanes (Y90)
Noelia Graciá Ribes
Observatorio Estelia
Ladines, (Asturias, SPAIN)

Juan-Luis González Carballo (I84)
Observatorio Cerro del Viento
(Badajoz, SPAIN)

Javier De Elías Cantalapiedra (L46)
Observatorio en Majadahonda
(Madrid, SPAIN)

Jesús Delgado Casal (Z73)
Observatorio Nuevos Horizontes
Camas (Sevilla, SPAIN)

E. Díez Alonso
Instituto Universitario de Ciencias y Tecnologías
Espaciales de Asturias
C/ Independencia, 13, 33004
Oviedo, SPAIN

(Received: 2023 Feb 9)

Lightcurves for eight asteroids were measured from 2022 May to August, except for 6223 Dahal, which was observed in 2021 November. Subsequent analysis found periods of: 1037 Davidweilla (4.508 h); 1369 Ostanina (8.392 h); 1718 Namibia (8.594 h); 4221 Picasso (3.111 h); 4368 Pillmore (3.605 h); 4901 O'Briain (2.650 h); 6223 Dahl (3.334 h); and 7353 Kazuya (6.387 h).

All observations reported here were unfiltered. The images were calibrated using bias, dark, and flat frames. Images were measured and periods analysis were done using *FotoDif* (2021) and *Períodos* (2020) packages. All data were light-time corrected. The results are summarized below. Individual lightcurve plots along additional with comments as required are also presented. In some cases, we wanted to update the data of these asteroids, but in others, we did not find any recent photometric data, or models, for them.

1037 Davidweilla. Discovered by Benjamin Jekhowsky in 1924 October at Argelia, we could find no lightcurve or rotational period previously published. Our data were taken from 2022 July 29 to August 8, with phase angles of 24.1º and 20.5º respectively. We found $P = 4.508 \pm 0.007$ h and $A = 0.34 \pm 0.01$ mag. There were insufficient data to model the asteroid's spin axis.

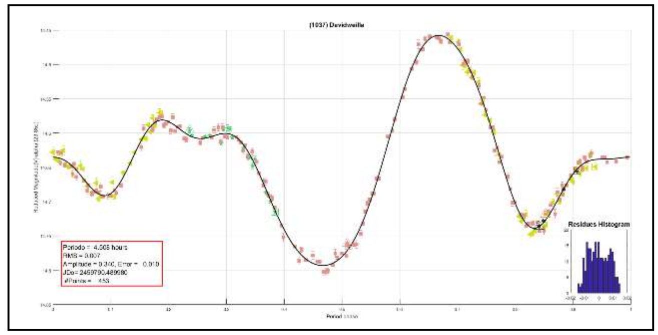


1369 Ostanina. There is a model of 1369 Ostanina in the DAMIT database (Durech, 2022) that was made in 2019. The last published lightcurve was by Behrend (2016web). We observed Ostatina from 2022 June 24-28. Our results are very similar to previous work: $P = 8.392 \pm 0.009$ h, $A = 1.110 \pm 0.013$.

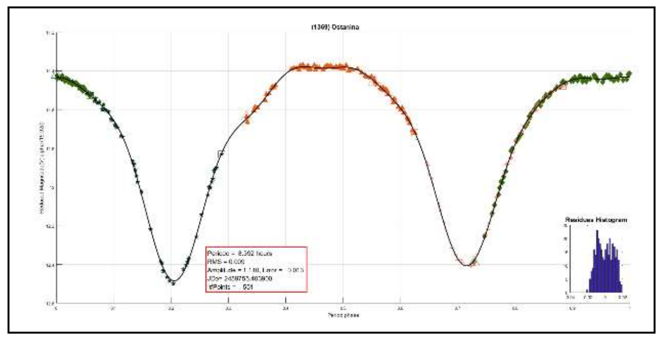


1718 Namibia. We found only one lightcurve reported for 1718 Namibia (Ferrero, 2011; 8.61 h) but no model in DAMIT. We took data between 2022 August 17-25. The phase angle decreased from 13.7º to 9.9º during that time. Our results are in excellent agreement with the Ferrero's: $P = 8.594 \pm 0.008$ h, $A = 0.17 \pm 0.01$ mag. All our data have been uploaded to the ALCDEF database.

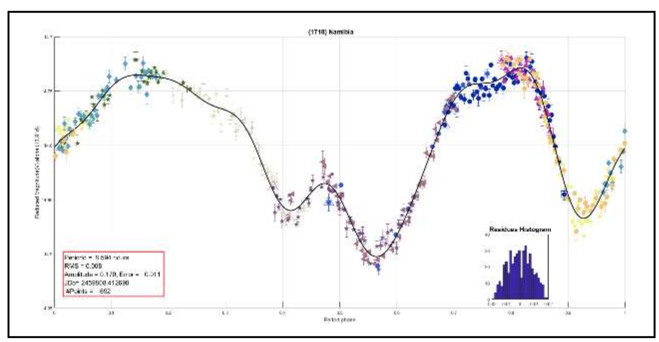


In addition, we obtained a very preliminary model for this asteroid. The only dense lightcurves available in the ALCDEF database are from this work. Regardless, it's possible to estimate a preliminary 3-D model when combining dense data obtained in just one season with sparse dat. As has been shown (Ďurech et al, 2020; Hanuš et al., 2021), models can be found using sparse data alone.

We combined our dense lightcurves with sparse data from ASAS-SN (Shappee et al., 2014), aplying the lightcurve inversion method (Kaasalainen and Torppa, 2001) implemented in the *MPO LCInvert* package (BDW Publishing, 2016). We obtained a preliminary spin axis of $\lambda = 150$, $\beta = +53$. We emphasize that this is a preliminary result and additional dense lightcurves from different seasons are necessary to obtain a more robust solution.

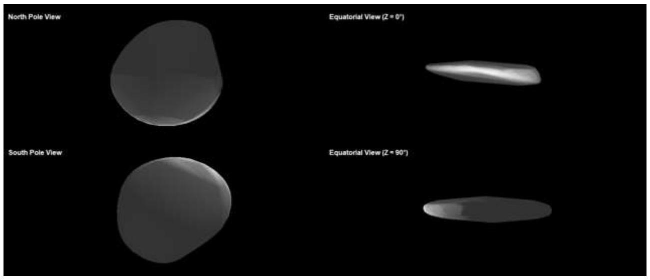


4221 Picasso was discovered by Jeffrey Thomas Alu in 1988 March at the Mount Palomar Observatory. It belongs to the main belt of asteroids. Percy (2018) reported $P$ = 3.11 h and $A$ = 0.31 mag. Our data were taken from 2022 May 27 (phase angle = 20.2º) to June 1 (phase angle = 21.6º). Our results are in good agreement with those from Percy: $P$ = 3.111 ± 0.012 h and $A$ = 0.30 ± 0.02 mag. However, the lightcurve shape is a little bit strange; it seems that there might be two signals in it. There is no model of Picasso in DAMIT.

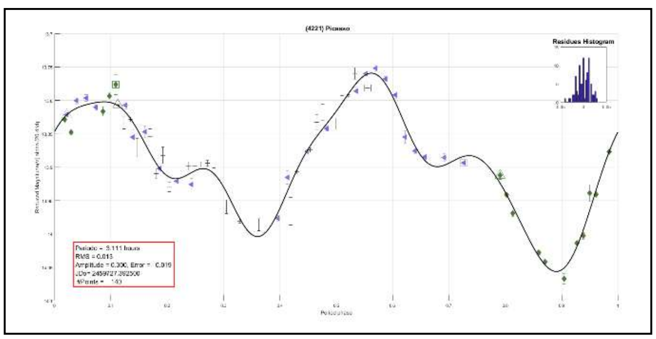


4368-Pillmore. There is a lightcurve of Pillmore reported by Warner (2006). We thought that the rotation period might need a revision, so we observed it between 2022 July 10 (phase = 12.9 º) and July 28 (phase = 10.2 º). Our results were very similar to Warner (2006): $P$ = 3.605 ± 0.014 h and $A$ = 0.28 ± 0.02. We conclude there has not been any significant change in the period over recent years.

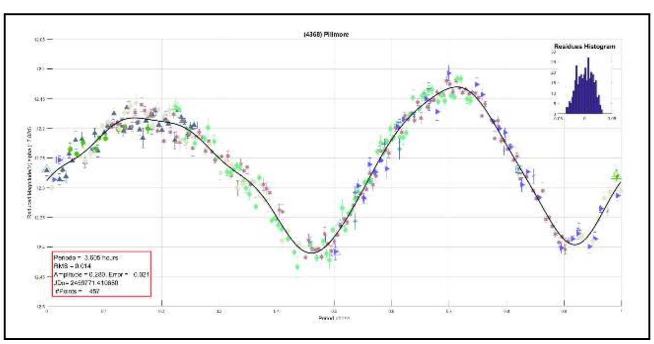


4901 O'Briain (1988 VJ) belongs to the main belt. It was discovered in 1988 November by Masaru Arai and Hiroshi Mori at the Yorii Observatory in Japan. We did not find any photometric data model or published lightcurve for O'Briain. We worked on it from 2022 July 1 (phase angle = 28.5 º) to July 10 (phase angle = 26.2 º). Our results are $P$ = 2.650 ± 0.011 h and $A$ = 0.14 ± 0.02 mag.

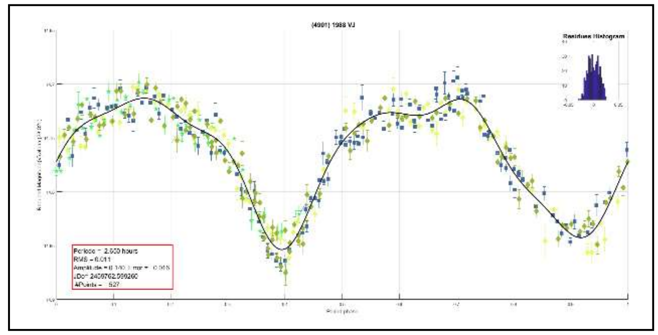


6223 Dahl (1980 RD). We found a lightcurve of Dahl reported by Waller (2013). His results are in agreement with ours. We started our observations on 2021 November 6 (phase angle = 12.8 º) and finished on November 10. Our analysis found $P$ = 3.334 ± 0.024 h, $A$ = 0.42 ± 0.03 mag.

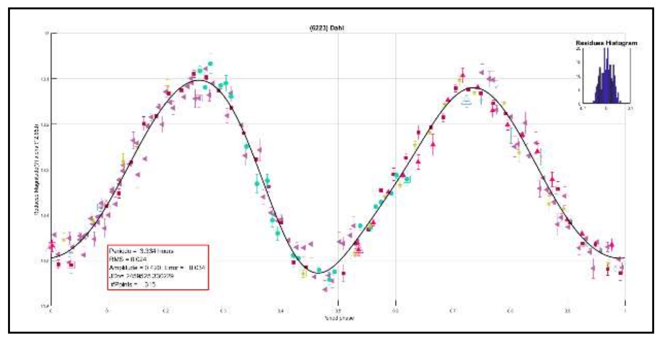


7353-Kazuya. It seems, Kazuya is not a very popular asteroid to observe: we found no photometric data, lightcurve, or model for it. Our observations started on 2022 August 12th (phase = 26.8 º) and finished on August 27th (phase = 24.6 º). Our measurement showed us a very clear light curve, and $P$ = 6.387 ± 0.009 h, $A$ = 0.24 ± 0.01 mag. Kazuya was discovered in 1995 January by M. Hirasawa and S. Suzuki at the Monte Nyukasa Observatory, in Japan.

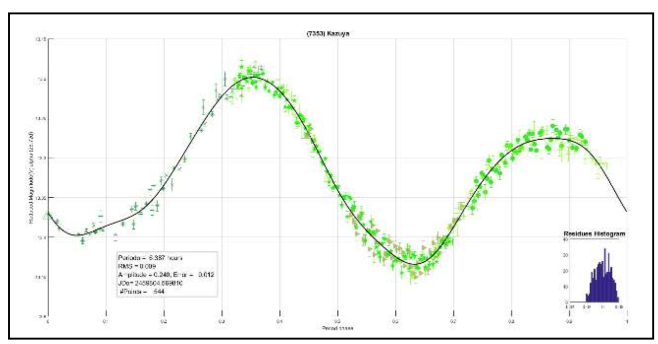

| Number | Asteroid | 20yy mm/dd | Phase | Period(h) | P.E. | Amp | A.E. |
|---|---|---|---|---|---|---|---|
| 1037 | Davidweilla | 22/07/29-22/08/08 | 24.1-20.5 | 4.508 | 0.007 | 0.340 | 0.010 |
| 1369 | Ostanina | 22/06/24-22/06/28 | 15.8-16.8 | 8.392 | 0.009 | 1.110 | 0.013 |
| 1718 | Namibia | 22/08/17-22/08/25 | 13.7-09.9 | 8.594 | 0.008 | 0.170 | 0.011 |
| 4221 | Picasso | 22/05/27-22/06/01 | 20.2-21.6 | 3.111 | 0.013 | 0.300 | 0.019 |
| 4368 | Pillmore | 22/07/10-22/07/28 | 12.9-10.2 | 3.605 | 0.014 | 0.280 | 0.021 |
| 4901 | O'Briain | 22/07/01-22/07/10 | 28.5-26.2 | 2.650 | 0.011 | 0.140 | 0.016 |
| 6223 | Dahl | 21/11/06-21/11/11 | 12.8-14.7 | 3.334 | 0.024 | 0.420 | 0.034 |
| 7353 | Kazuya | 22/08/12-22/08/27 | 26.8-24.6 | 6.387 | 0.009 | 0.240 | 0.012 |

Table I. Observing circumstances and results. Phase is the solar phase angle given at the start and end of the date range. If preceded by an asterisk, the phase angle reached an extrema during the period.

References

ALCDEF (2022). Asteroid Photometry Database. *http://alcdef.org/*

BDW Publishing (2016). *http://www.minorplanetobserver.com/MPOsoftware/MPOLCInvert.htm*

Behrend, R. (2016web). Observatoire de Geneve web site. *https://obswww.unige.ch/~behrend/*

Durech, J. (2022). DAMIT database. *https:/astro.troja.mff.cuni.cz/projects/damit/*

Ďurech, J.; Tonry, J.; Erasmus, N.; Denneau, L.; Heinze, A.N.; Flewelling, H.; Vančo, R. (2020). "Asteroid models reconstructed from ATLAS photometry." *Astronomy & Astrophysics* **643**, A59.

Ferrero, A. (2012). "Lightcurve Determination at the Bigmuskie Observatory from 2011 July - December." *Minor Planet Bulletin* **39**, 65-66.

*FotoDif* (2021). *http://astrosurf.com/orodeno/fotodif/index.htm*

Hanuš, J.; Pejcha, O.; Shappee, B.J.; Kochanek, C.S.; Stanek, K.Z.; Holoien, T.S. (2021). "V-band photometry of asteroids from ASAS-SN-Finding asteroids with slow spin." *Astronomy & Astrophysics* **654**, A48.

Kaasalainen, M.; Torppa, J. (2001). "Optimization methods for asteroid lightcurve inversion: I. shape determination." *Icarus* **153**, 24-36.

Percy, S.C. (2018). "Rotation Period for 4221 Picasso." *Minor Planet Bulletin* **45**, 326-328.

*Períodos* (2020). *http://www.astrosurf.com/salvador/Programas.html*

Shappee, B.; Prieto, J.; Stanek, K.Z.; Kochanek, C.S.; Holoien, T.; Jencson, J.; Basu, U.; Beacom, J.F.; Szczygiel, D.; Pojmanski, G.; Brimacombe, J.; Dubberley, M.; Elphick, M.; Foale, S.; Hawkins, E.; Mullins, D.; Rosing, W.; Ross, R.; Walker, Z. (2014). "All Sky Automated Survey for SuperNovae (ASAS-SN or "Assassin")." in *American Astronomical Society Meeting Abstracts* **223**, id. 236.03.

Solar System Objects (Small-Body Database Lookup). *https://ssd.jpl.nasa.gov/*

Waller, E.B. (2013). "Lightcurve Photometry and Rotational Periods of 2890 Vilyujsk and 6223 Dahl." *Minor Planet Bulletin* **40**, 109-110.

Warner, B.D. (2006). "Asteroid lightcurve analysis at the Palmer Divide Observatory: July - September 2005." *Minor Planet Bulletin* **33,** 35-39.

# LIGHTCURVES FOR TEN MINOR PLANETS

Tom Polakis
Command Module Observatory
121 W. Alameda Dr.
Tempe, AZ 85282
tpolakis@cox.net

(Received: 2023 March 30)

Photometric measurements were made for 10 main-belt asteroids, based on CCD observations made from 2023 January through 2023 February. Phased lightcurves were created for seven asteroids, while three did not yield period solutions. All the data have been submitted to the ALCDEF database.

CCD photometric observations of 10 main-belt asteroids were performed at Command Module Observatory (MPC V02) in Tempe, AZ. Images were taken using a 0.32-m f/6.7 Modified Dall-Kirkham telescope, SBIG STXL-6303 CCD camera, and a 'clear' glass filter. Exposure time for all the images was 2 minutes. The image scale after 2×2 binning was 1.76 arcsec/pixel. Table I shows the observing circumstances and results. All of the images for these asteroids were obtained between 2023 January and 2023 February.

Images were calibrated using a dozen bias, dark, and flat frames. Flat-field images were made using an electroluminescent panel. Image calibration and alignment was performed using MaxIm DL software.

The data reduction and period analysis were done using *MPO Canopus* (Warner, 2023). The 45′×30′ field of the CCD typically enables the use of the same field center for three consecutive nights. In these fields, the asteroid and three to five comparison stars were measured. Comparison stars were selected with colors within the range of 0.5 < B-V < 0.95 to correspond with color ranges of asteroids. In order to reduce the internal scatter in the data, the brightest stars of appropriate color that had peak ADU counts below the range where chip response becomes nonlinear were selected. *MPO Canopus* plots instrumental vs. catalog magnitudes for solar-colored stars, which is useful for selecting comp stars of suitable color and brightness.

Since the sensitivity of the KAF-6303 chip peaks in the red, the clear-filtered images were reduced to Sloan r´ to minimize error with respect to a color term. Comparison star magnitudes were obtained from the ATLAS catalog (Tonry et al., 2018), which is incorporated directly into *MPO Canopus*. The ATLAS catalog derives Sloan *griz* magnitudes using a number of available catalogs. The consistency of the ATLAS comp star magnitudes and color-indices allowed the separate nightly runs to be linked often with no zero-point offset required or shifts of only a few hundredths of a magnitude in a series.

A 9-pixel (16 arcsec) diameter measuring aperture was used for asteroids and comp stars. It was typically necessary to employ star subtraction to remove contamination by field stars. For the asteroids described here, I note the RMS scatter on the phased lightcurves, which gives an indication of the overall data quality including errors from the calibration of the frames, measurement of the comp stars, the asteroid itself, and the period-fit. Period determination was done using the *MPO Canopus* Fourier-type FALC fitting method (cf. Harris et al., 1989). Phased lightcurves show the maximum at phase zero. Magnitudes in these plots are apparent and scaled by *MPO Canopus* to the first night. In cases where rotation periods could not be determined, raw lightcurves are presented, with "RAW" appearing in the upper right-hand corner of the plots.

Asteroids were selected from the CALL website (Warner, 2011), either for having uncertain periods or for needing more lightcurves for shape modeling. In this set of observations, 2 of the 10 asteroids had U = 1, 6 were rated as U=2, and 2 had U = 3. The Asteroid Lightcurve Database (LCDB; Warner et al.,2009) was consulted to locate previously published results. All the new data for these asteroids can be found in the ALCDEF database.

814 Tauris was discovered in 1916 by Grigory Neujmin at Simeis in 1883. It lies in a highly eccentric and inclined orbit. Recent published rotation periods include Alkema (2013), 35.8 ± 0.1 h; Behrend (2020web), 18.030 ± 0.002 h; and Colazo et al. (2022a), 36.081 ± 0.008 h. During five nights, 573 data points were gathered to determine a period of 35.87 ± 0.06 h, agreeing with previous values. The amplitude of the lightcurve is 0.17 ± 0.015 mag.

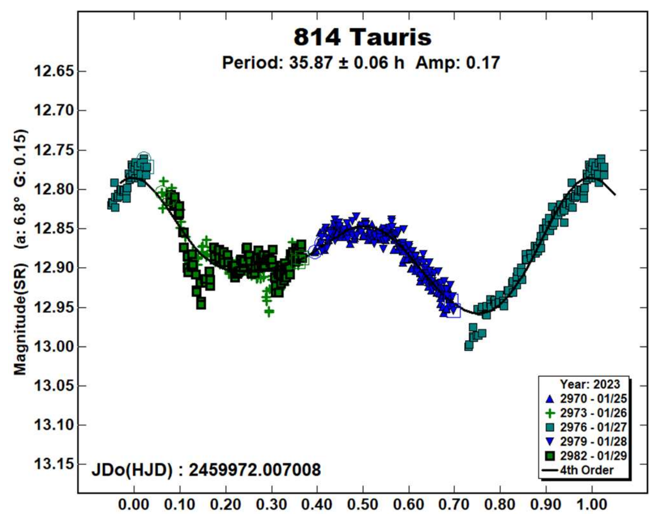


858 El Djezair is an outer main-belt asteroid, discovered by Frédéric Sy in 1916 at Algiers. Several disparate periods have been published. They include Warner (2005), 22.31 ± 0.2 h; Polakis (2019), 14.830 ± 0.015 h; Colazo et al. (2021), 33.525 ± 0.013 h; and Dose (2022), 29.639 ± 0.003 h. A total of 271 images were taken in four nights, producing a period of 31.16 ± 0.25 h, in rough agreement with Colazo's and Dose's results. The amplitude is 0.20 ± 0.032 mag.

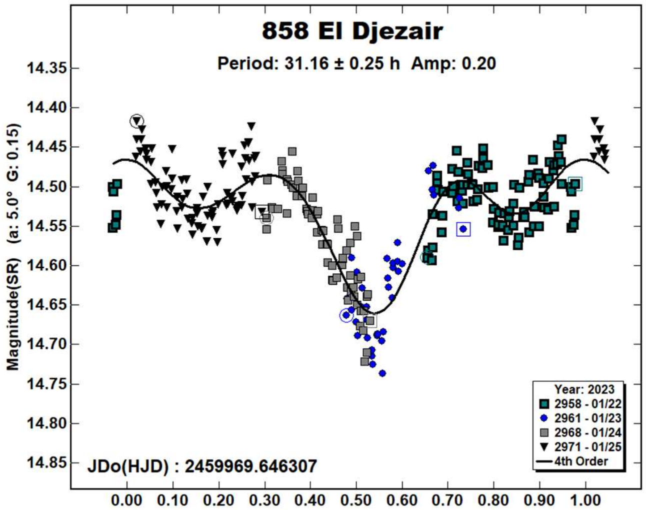


957 Camelia was discovered by Karl Reinmuth in 1921 from Heidelberg. Again, there is no consensus on the period. Warner (2001) shows a period of 5.391 ± 0.02 h, while Polakis (2022) computed 85.05 ± 0.11 h. During six nights, 380 images were taken, but no period solution was obtained. The raw lightcurve is presented.

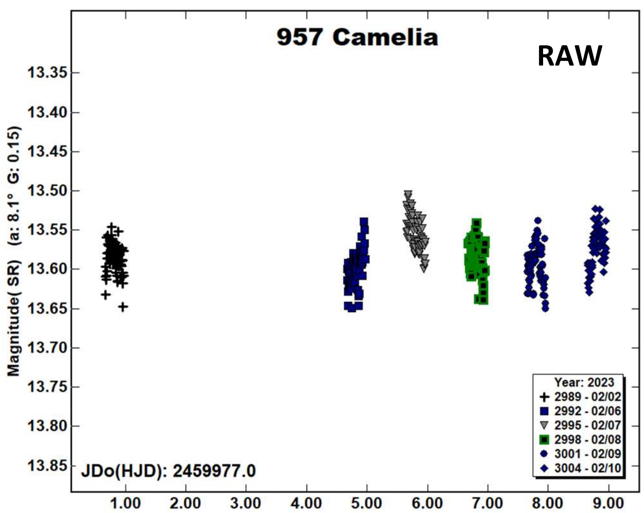


995 Sternberga was discovered by Sergey Belyavskij at Simeis in 1923. Several period solutions appear in the literature. Stephens (2013) obtained 14.612 ± 0.001h, Marciniak et al. (2018) shows 11.198 ± 0.002 h, and Colazo et al. (2022b) published a period of 22.392 ± 0.006 h. A total of 319 images were gathered in five nights. As shown, the raw lightcurve was flat, so no further imaging was done, as a period solution could not be determined.

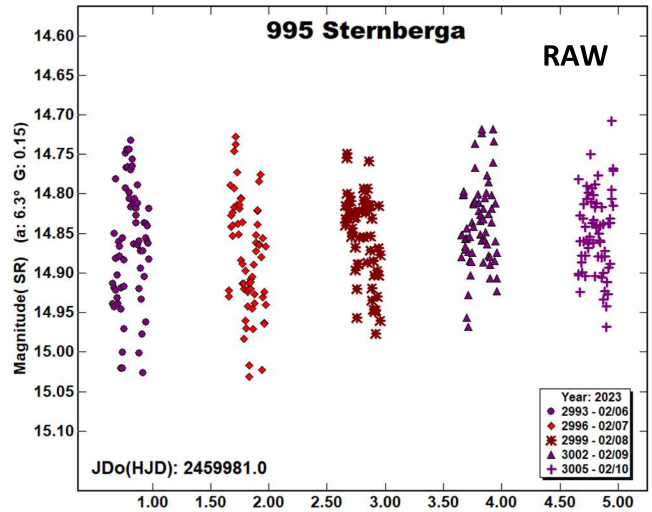


1007 Pawlowia is an outer main-belt asteroid, discovered by Vladimir Albitzkij in 1923 at Simeis. Clark (2006) computed a period of 8.23 h, while Fauerbach and Nelson (2019) published a value of 121 ± 3 h. The slow rotation of the target required 13 nights of observation, during which 435 images were obtained. The rotation period of 384.8 ± 6.8 h disagrees with previous assessments. The amplitude is 0.49 mag, with an RMS error of 0.045 mag.

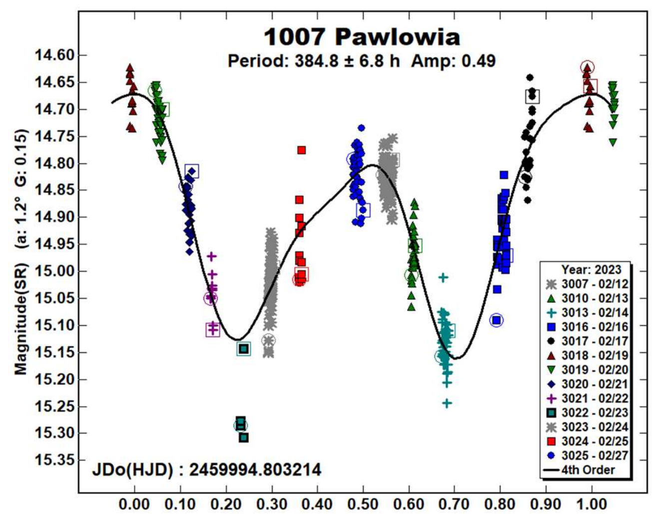


1243 Pamela. This minor planet was discovered by Cyril Jackson at Johannesburg in 1932. There is good agreement in the period solutions in the LCDB. Garceran et al. (2016) computed 26.00 ± 0.01 h and Polakis (2022) shows 26.01 ± 0.02 h. A total of 517 images were taken during 10 nights, and a rotation period of 25.96 ± 0.02 h was computed. The amplitude of the lightcurve is 0.49 ± 0.038 mag.

| Number | Name | yy/mm/dd | Phase | $L_{PAB}$ | $B_{PAB}$ | Period(h) | P.E. | Amp | A.E. | Grp |
|---|---|---|---|---|---|---|---|---|---|---|
| 814 | Tauris | 23/01/25-01/29 | 6.8,7.9 | 113 | 13 | 35.87 | 0.06 | 0.17 | 0.02 | MB-O |
| 858 | El Djezair | 23/01/22-01/25 | 5.0,5.9 | 112 | 8 | 31.16 | 0.25 | 0.20 | 0.03 | MB-O |
| 957 | Camelia | 23/02/02-02/10 | 8.1,8.4 | 135 | -19 | -- | -- | -- | -- | MB-O |
| 995 | Sternberga | 23/02/06-02/10 | 6.3,6.6 | 135 | -16 | -- | -- | -- | -- | MB-M |
| 1007 | Pawlowia | 23/02/12-02/27 | 1.2,7.4 | 140 | -1 | 384.8 | 6.8 | 0.49 | 0.05 | MB-O |
| 1243 | Pamela | 23/01/22-02/01 | 8.1,10.9 | 100 | -10 | 25.96 | 0.02 | 0.49 | 0.04 | MB-O |
| 1478 | Vihuri | 23/01/22-01/23 | 5.3,5.8 | 113 | 4 | -- | -- | -- | -- | MB-I |
| 2089 | Cetacea | 23/01/26-02/10 | 5.3,8.7 | 125 | 9 | 206.6 | 0.2 | 0.79 | 0.05 | MB-I |
| 2545 | Verbiest | 23/02/12-02/14 | 2.3,1.1 | 147 | -1 | 10.064 | 0.027 | 0.13 | 0.03 | FLOR |
| 8548 | Sumizihara | 23/02/12-02/14 | 3.1,1.9 | 147 | 1 | 3.195 | 0.004 | 0.17 | 0.05 | MB-I |

Table I. Observing circumstances and results. The phase angle is given for the first and last date. If preceded by an asterisk, the phase angle reached an extrema during the period. $L_{PAB}$ and $B_{PAB}$ are the approximate phase angle bisector longitude/latitude at mid-date range (see Harris et al., 1984). Grp is the asteroid family/group (Warner et al., 2009).

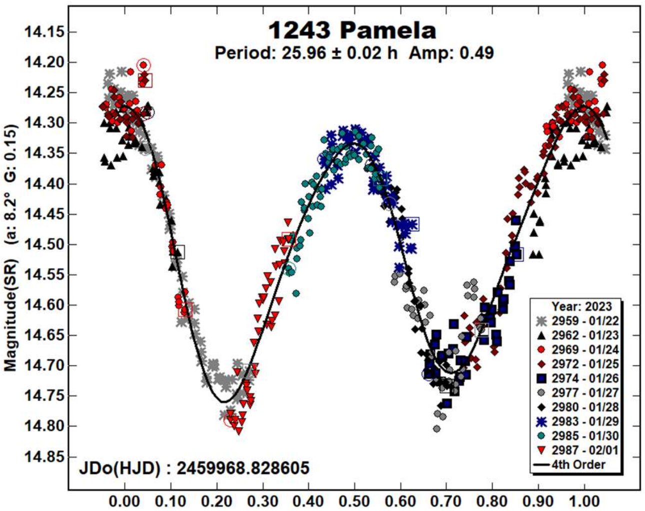


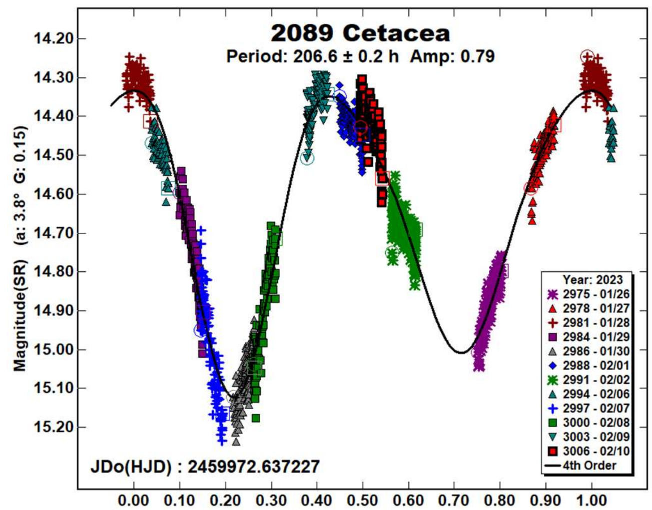


1478 Vihuri is an inner main-belt asteroid, discovered at Turku in in 1938 by Yrjö Väisälä. The only period solution in the LCDB is that of Binzel (1987), who published a value of 19.5 h. During two nights, 160 data points appeared too flat to produce a period solution. The raw lightcurve is provided.

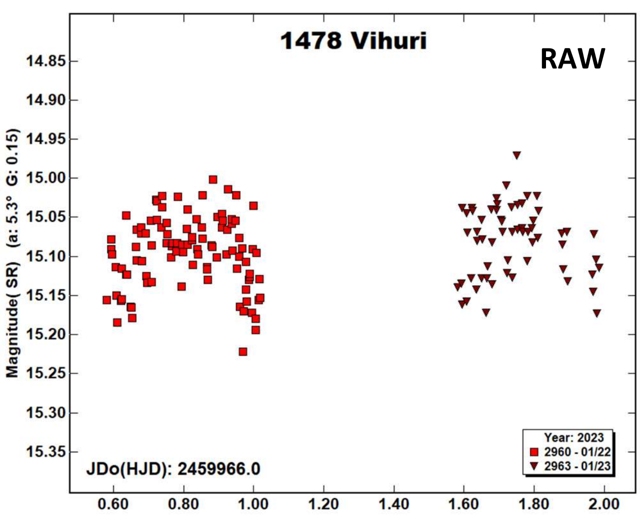


2089 Cetacea was discovered in 1977 by Norm Thomas at Flagstaff. Bembrick et al. (2006) published a period of 39.120 ± 0.093 h. During 12 nights, 1452 images were gathered, producing a unique period solution of 206.6 ± 0.2 h. The lightcurve has an amplitude of 0.79 mag, with an RMS error of 0.048 mag.

2545 Verbiest is a Flora-family asteroid. It was discovered by Eugène Delporte in 1935 at Uccle. The only period solution in the LCDB is that of Behrend (2008web), who computed 10 h. The asteroid was observed on three nights, and 142 images were obtained, yielding a synodic period of 10.064 ± 0.027 h. The lightcurve has an amplitude of 0.13 ± 0.030 mag.

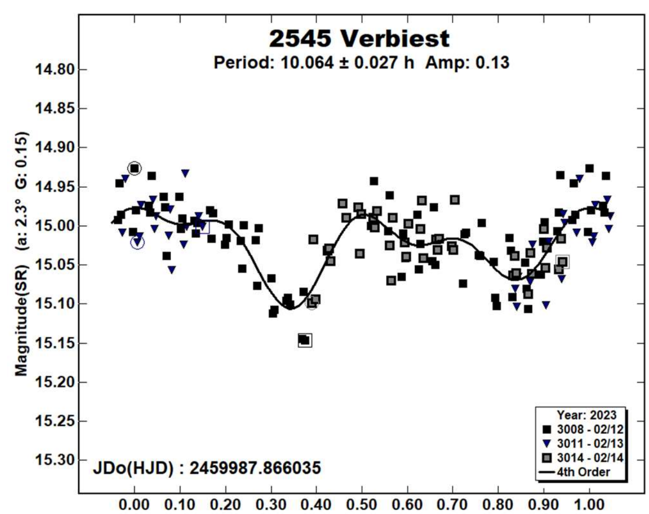

8548 Sumizihara. This inner-belt asteroid was discovered by Kin Endate and Kazuro Watanabe in 1994 at Kitame. The target is in a highly eccentric orbit, and its 2023 opposition was near favorably placed near perihelion. Waszczak et al. (2015) published a period of 3.192 ± 0.0006 h. During three nights, 124 images were used to calculate a synodic period of 3.195 ± 0.004 h, in agreement with the previous solution. The amplitude of the lightcurve is 0.17 mag, with an RMS error of 0.045 mag.

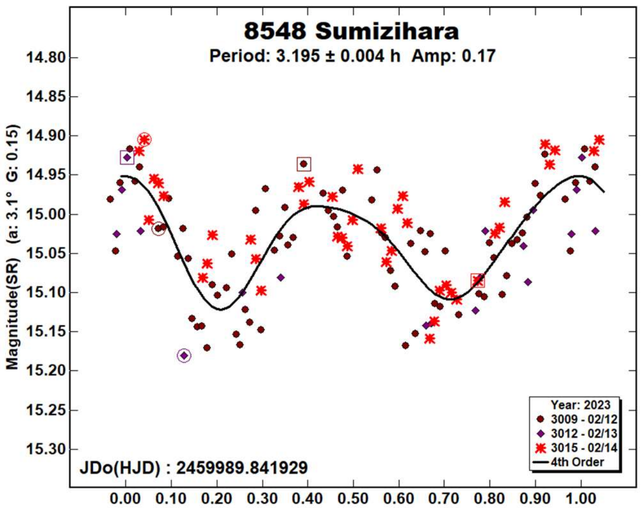


Acknowledgements

The author would like to express his gratitude to Brian Skiff for his indispensable mentoring in data acquisition and reduction. Thanks also go out to Brian Warner for support of his *MPO Canopus* software package.

References

Alkema, M.S. (2013). "Asteroid Lightcurve Analysis at Elephant Head Observatory: 2013 April - July." *Minor Planet Bull*. **40**, 215-216.

Behrend, R. (2008web, 2020web). Observatoire de Geneve web site. *http://obswww.unige.ch/~behrend/page_cou.html*

Bembrick, C.S.; Allen, B.; Richards, T. (2006). "Lightcurves from two oppositions of 227 Philosophia and 2089 Cetacea." *Minor Planet Bull*. **33**, 42-43.

Binzel, R.P. (1987). "A photoelectric survey of 130 asteroids." *Icarus* **72**, 135-208.

Clark, M. (2006). "Lightcurve results for 383 Janina, 899 Jokaste, 1825 Klare, 2525 O'Steen 5064 Tanchozuru, and (17939) 1999 HH8." *Minor Planet Bull*. **33**, 53-56.

Colazo, M. and 19 co-authors (2021). "Asteroid Photometry and Lightcurve Analysis at GORA'S Observatories Part IV." *Minor Planet Bull*. **48**, 140-143.

Colazo, M. and 19 co-authors (2022a). "Photometry and Light Curve Analysis of Six Asteroids by GORA'S Observatories." *Minor Planet Bull*. **49**, 125-127.

Colazo, M. and 19 co-authors (2022b). "Asteroid Photometry and Lightcurve Results for Seven Asteroids." *Minor Planet Bull*. **49**, 189-192.

Dose, E. (2022). "Lightcurves of Seventeen Asteroids." *Minor Planet Bull*. **49**, 141-148.

Fauerbach, M.; Nelson, K.M. (2019). "Photometric Observations of 1007 Pawlowia, 1774 Kulikov, 2764 Moeller, 5110 Belgirate, (8505) 1990 YK, and (34459) 2000 SC91." *Minor Planet Bull*. **46**, 21-23.

Garceran, A.C.; Aznar, A.; Mansego, E.A.; Rodriguez, P.B.; de Haro, J.L.; Silva, A.F.; Silva, G.F.; Martinez, V.M.; Chiner, O.R. (2016). "Nineteen Asteroids Lightcurves at Asteroids Observers (OBAS) - MPPD: 2015 April - September." *Minor Planet Bull*. **43**, 92-97.

Harris, A.W.; Young, J.W.; Scaltriti, F.; Zappala, V. (1984). "Lightcurves and phase relations of asteroids 82 Alkmene and 444 Gyptis." *Icarus* **57**, 251-258.

Harris, A.W.; Young, J.W.; Bowell, E.; Martin, L.J.; Millis, R.L.; Poutanen, M.; Scaltriti, F.; Zappala, V.; Schober, H.J.; Debehogne, H.; Zeigler, K.W. (1989). "Photoelectric Observations of Asteroids 3, 24, 60, 261, and 863." *Icarus* **77**, 171-186.

Marciniak, A.; Bartczak, P.; Müller, T.; Sanabria, J.J.; and 39 co-authors (2018). "Photometric survey, modelling, and scaling of long-period and low-amplitude asteroids." *Astron. Astrophys*. **610**, A7.

Polakis, T. (2019). "Lightcurves of Twelve Main-Belt Minor Planets." *Minor Planet Bull*. **46**, 287-292.

Polakis, T. (2022). "Lightcurves for Thirteen Minor Planets." *Minor Planet Bull*. **43**, 131-135.

Stephens, R.D. (2013). "Asteroids Observed from Santana and CS3 Observatories: 2012 July - September." *Minor Planet Bull*. **40**, 34-35.

Tonry, J.L.; Denneau, L.; Flewelling, H.; Heinze, A.N.; Onken, C.A.; Smartt, S.J.; Stalder, B.; Weiland, H.J.; Wolf, C. (2018). "The ATLAS All-Sky Stellar Reference Catalog." *Astrophys. J.* **867**, 105.

Warner, B.D. (2001). "Asteroid Photometry at the Palmer Divide Observatory: Results for 706 Hirundo, 957 Camelia, and 1719 Jens." *Minor Planet Bull*. **28**, 4-5.

Warner, B.D. (2005). "Asteroid lightcurve analysis at the Palmer Divide Observatory - Spring 2005." *Minor Planet Bull*. **32**, 90-92.

Warner, B.D.; Harris, A.W.; Pravec, P. (2009). "The Asteroid Lightcurve Database." *Icarus* **202**, 134-146. Updated 2023 Feb. *http:// minorplanet.info/lightcurvedatabase.html www*

Warner, B.D. (2011). Collaborative Asteroid Lightcurve Link website. *http://www.minorplanet.info/call.html*

Warner, B.D. (2023). *MPO Canopus* software. *http://bdwpublishing.com*

Waszczak, A.; Chang, C.-K.; Ofek, E.O.; Laher, R.; Masci, F.; Levitan, D.; Surace, J.; Cheng, Y.-C.; Ip, W.-H.; Kinoshita, D.; Helou, G.; Prince, T.A.; Kulkarni, S. (2015). "Asteroid Light Curves from the Palomar Transient Factory Survey: Rotation Periods and Phase Functions from Sparse Photometry." *Astron. J.* **150**, A75.

# LIGHTCURVE ANALYSIS FOR FOUR MAIN BELT ASTEROIDS

Giovanni Battista Casalnuovo
Filzi School Observatory D12
Laives, ITALY
gb.minorplanet@gmail.com

(Received: 2023 April 4)

Photometric observations of four main-belt asteroids, 2384 Schulhof, 7468 Anfimov, (42790) 1998 XS93, and (53090) 1998 YS7, were made at the Filzi School Observatory (Laives - Italy) MPC code D12.

CCD photometric observations, were made at the Filzi School Observatory, all are with no filter (clear). All images were obtained with a 0.35-m reflector telescope reduced to *f*/8.0, a QHY9 CCD camera, and then calibrated with dark and flat-field frames. The pixel scale was 1.56 arcsec when binned at 4×4 pixels. All exposures were 120 seconds. The computer clock was synchronized with an Internet time server before each session. Differential photometry and period analysis were done using *MPO Canopus* version 10.8.1.1 (Warner, 2019). Solar type stars from CMC15 catalog in R band were used as comparison stars.

2384 Schulhof. This main-belt asteroid was reported as a lightcurve photometry opportunity for 2023 March on the MinorPlanet.info web site (*https://www.minorplanet.info/php/callopplcdbquery.php*; hereafter referenced as MPI). It was discovered on March 2nd, 1943, by French astronomer Marguerite Laugier at Nice Observatory in France. The asteroid is dedicated to the Hungarian astronomer Lipót Schulhof. It is a main-belt asteroid with a semi-major axis of 2.61 AU, eccentricity 0.12, inclination 13.52 deg, and orbital period of 4.22 yr. Its absolute magnitude is H = 11.95 mag. It was observed for three nights (March 2023). The derived synodic period was P = 3.2935 ± 0.0001 h with an amplitude of A = 0.39 ± 0.05 mag. Images were taken with V and R photometric filters. The V and R band frames were acquired in sequence changing alternatively the filters (VR-VR-VR). This allowed us to find the color index of V-R = 0.44 ± 0.03 mag (mean of 30 values). The lightcurve is symmetric bimodal. The result presented here is in very close agreement with the results reported by several other observers in the LCDB (Warner et al., 2009).

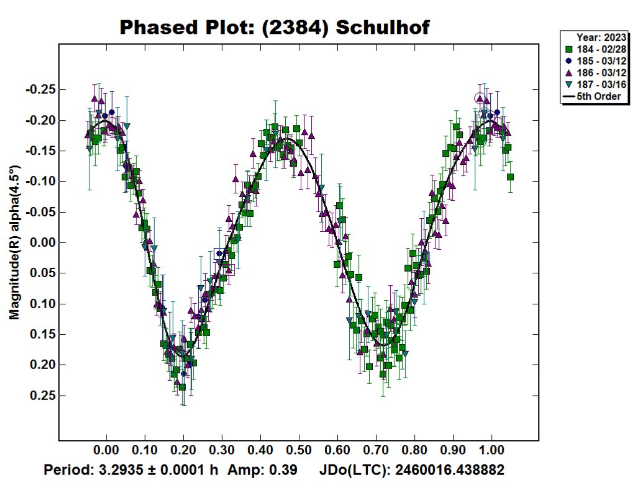


7468 Anfimov. This main-belt asteroid was reported as a lightcurve photometry opportunity for 2022 December on the MPI. Discovered on 1990 Oct. 17 by L.I. Chernykh at the Crimean Astrophysical Observatory, dedicated to Nikolaj Apollonovich Anfimov, a well-known scientist in space technology and the theory of heat mass exchange. It is a main-belt asteroid with a semi-major axis of 3.04 AU, eccentricity 0.12, inclination 4.37 deg, and orbital period of 5.30 yr. Its absolute magnitude is H = 12.40 mag. It was observed for four nights. The derived synodic period was P = 6.40 ± 0.01 h with an amplitude of A = 0.67 ± 0.05 mag. For this asteroid. Durech (2020) reports a period of 5.65126 h. The period spectrum, in this work, from 4 measurement groups spanning all four nights, shows the most significant RMS minima in 6.40 ± 0.01 h.

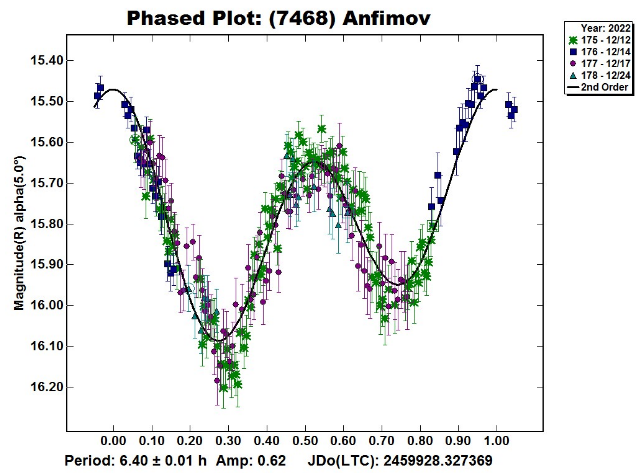


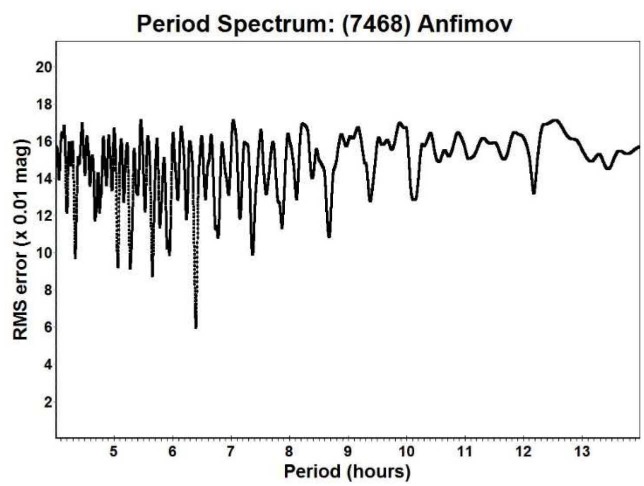


(42790) 1998 XS93. This main-belt asteroid was reported as a lightcurve photometry opportunity for 2022 November on the MinorPlanet.info. It was discovered in 1998-12-15 by LINEAR at Socorro. It is a main-belt asteroid with a semi-major axis of 2.55 AU, eccentricity 0.13, inclination 14.09 deg, orbital period of 4.07 year, and absolute magnitude of H = 13.33. It was observed for four nights (November 2022). The derived synodic period was P = 3.549 ± 0.001 h with amplitude of A = 0.58 ± 0.05 mag. There were no entries in the LCDB (Warner et al., 2009) for this asteroid.

| Number | Name | yyyy mm/dd | Phase | | $L_{PAB}$ | $B_{PAB}$ | Period(h) | P.E. | Amp | A.E. | Grp |
|---|---|---|---|---|---|---|---|---|---|---|---|
| 2384 | Schulhof | 2023 02/28-03/16 | 4.6 | 7.1 | 162.7 | 7.6 | 3.2935 | 0.0001 | 0.39 | 0.05 | MB |
| 7468 | Anfimov | 2022 12/12-12/24 | 4.5 | 9.3 | 69.1 | 1.3 | 6.40 | 0.01 | 0.67 | 0.05 | MB |
| 42790 | 1998 XS93 | 2022 11/12-11/20 | 3.0 | 7.1 | 43.9 | 1.0 | 3.549 | 0.001 | 0.58 | 0.05 | MB |
| 53090 | 1998 YS7 | 2022 09/04-09/22 | 5.7 | 13.4 | 343.1 | 10.1 | 2.843 | 0.001 | 0.20 | 0.05 | MB |

Table I. Observing circumstances and results. The phase angle is given for the first and last date. If preceded by an asterisk, the phase angle reached an extrema during the period. $L_{PAB}$ and $B_{PAB}$ are the approximate phase angle bisector longitude/latitude at mid-date range (see Harris et al., 1984). Grp is the asteroid family/group (Warner et al., 2009).

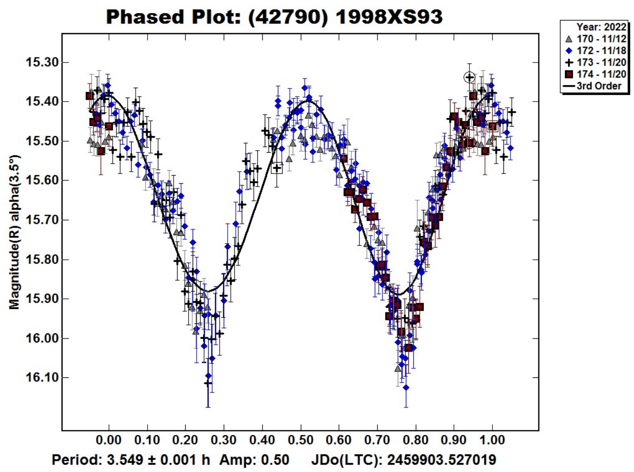


(53090) 1998 YS7. This main-belt asteroid was reported as a lightcurve photometry opportunity for 2022 September on the MinorPlanet.info. It was discovered in 1998-12-24 by CSS at Catalina. It is a main-belt asteroid with a semi-major axis of 2.29 AU, eccentricity 0.26, inclination 23.19 deg, orbital period of 3.48 year, and absolute magnitude of H = 13.91 mag. It was observed for five nights (September 2022). The derived synodic period was P = 2.843 ± 0.001 h with amplitude of A = 0.20 ± 0.05 mag. There were no entries in the LCDB (Warner et al., 2009) for this asteroid.

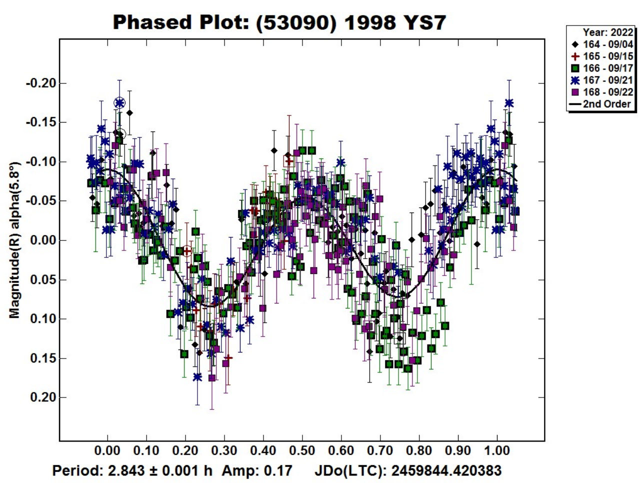


Acknowledgements

We thank student of “Fabio Filzi” School, in Laives (Italy): Ciatto, E.; Debiasi, V.; Fernandez, V.; Pergher, D.; Dotta, C.; Turra, G.; Montes, E.; Pellegrini, G.; Tripodi, G.; Stranieri, E.; Spadoni, D.; Tomasi, E. The students were supported by Prof. Casalnuovo, G.B.; Chinaglia, R.; Volani, S. The students illustrated lightcurve (2384) Sculhof, in the Science Day “Subzero” at “Eurac Research” in Bolzano (Italy)

References

Durech, J.; Tonry, J.; Erasmus, N.; Denneeau, L.; Heinze, A.N.; Flewelling, H.; Vanco, R. (2020). “Asteroid model reconstructed from ATLAS photometry.” *A&A* **643**, A59.

Harris, A.W.; Young, J.W.; Scaltriti, F.; Zappala, V. (1984). “Lightcurves and phase relations of the asteroids 82 Alkmene and 444 Gyptis.” *Icarus* **57**, 251-258.

Minor Planet Call. *http://www.minorplanet.info/PHP*

Minorplanet.Info
*http://www.minorplanet.info/lightcurvedatabase.html*

Warner, B.D.; Harris, A.W.; Pravec, P. (2009). “The Asteroid Lightcurve Database.” *Icarus* **202**, 134-146. Updated 2018 June. *https://www.minorplanet.info/php/lcdb.php*

Warner, B.D. (2019). MPO Software. *MPO Canopus*, version 10.8.1.1. *Bdw Publishing. http://minorplanetobserver.com*

# ASTEROID LIGHTCURVE ANALYSIS AT THE CENTER FOR SOLAR SYSTEM STUDIES PALMER DIVIDE STATION: 2023 JANUARY-FEBRUARY

Brian D. Warner
Center for Solar System Studies (CS3)
446 Sycamore Ave.
Eaton, CO 80615 USA
brian@MinPlanObs.org

(Received: 2023 April 10)

CCD photometric observations of twelve asteroids were made at the Center for Solar System Studies Palmer Divide Station during 2023 January and February. Data analysis found a weak to moderate secondary period for the Hilda asteroids 1268 Libya and 2312 Duboshin, both possibly as sign of (unexpected) tumbling, the NEA (68359) 2001 IZ13 presents an unusual lightcurve with a very large amplitude of ~1.8 mag, and that NEA (98943) 2001 CC21 is a probable tumbler.

CCD photometric observations of twelve asteroids were carried out at the Center for Solar System Studies Palmer Divide Station (CS3-PDS) during 2023 January and February as part of an ongoing general study of asteroid rotation periods with a concentration on near-Earth, Hungaria, and Hilda group/family asteroids.

| Telescope | Camera |
|---|---|
| 0.30-m *f*/6.3 SCT | SBIG STL-1001E |
| 0.35-m *f*/9.1 SCT (x3) | FLI Microline 1001E |
| 0.50-m *f*/8.1 Ritchey-Chrétien | FLI Proline 1001E |

Table I. List of available telescopes and CCD cameras at CS3-PDS. The exact combination for each telescope/camera pair can vary due to maintenance or specific needs.

Table I lists the five telescope/CCD cameras pairs used at CS3-PDS. All the cameras use CCD chips from the KAF 1001 blue-enhanced family and so have essentially the same response. The pixel scales ranged from 1.24-1.60 arcsec/pixel. All lightcurve observations were made with no or a clear filter. The exposures varied depending on the asteroid's brightness.

To reduce the number of times and amounts of adjusting nightly zero-points, the ATLAS catalog r´ (SR) magnitudes (Tonry et al., 2018) are used. Those adjustments are usually ≤ ±0.03 mag. The rare greater corrections may have been related in part to using unfiltered observations, poor centroiding of the reference stars, and not correcting for second-order extinction. Another cause may be selecting what appears to be a single star but is actually an unresolved pair.

The Y-axis values are ATLAS SR "sky" (catalog) magnitudes. The values in the parentheses give the phase angle(s), *a*, along with the value of *G* used to normalize the data to the comparison stars used in the earliest session. This, in effect, adjusts all the observations so that they seem to have been made at a single fixed date/time and phase angle. Presumably, any remaining variations are due only to the asteroid's rotation and/or albedo changes.

There can be up to three phase angles If two, the values are for the first and last night of observations. If three, the middle value is the extrema (maximum or minimum) reached between the first and last observing runs. The X-axis shows rotational phase from -0.05 to 1.05. If the plot includes the amplitude, e.g., "Amp: 0.65," this is the amplitude of the Fourier model curve and *not necessarily the adopted amplitude for the lightcurve*.

For brevity, only some of the previous results are referenced. A more complete listing is in the asteroid lightcurve database (Warner et al, 2009; "LCDB" from here on).

<u>1268 Libya</u>. Dahlgren et al. (1998) reported a period of 14.05 h, which is in reasonable agreement with the 2023 CS3-PDS result of 14.11 h. That's the good news. Warner and Stephens (2020) found what seems to be a reliable solution of 17.572 h based on data from 2019 September. The period spectrum for the 2023 data shows a weaker solution near the longer period. Trying to force the data from each year to the solution for the other year produced a lightcurve too unusual and large of RMS to be acceptable.

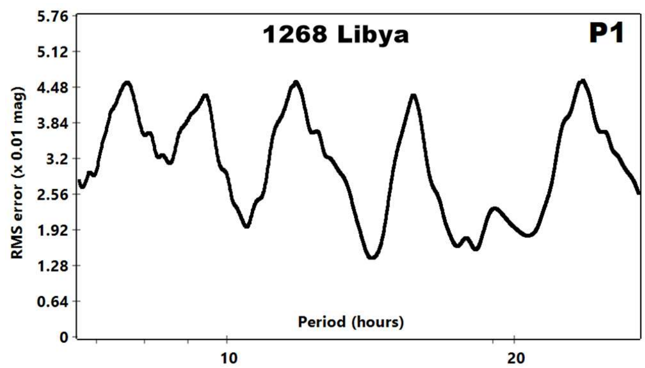


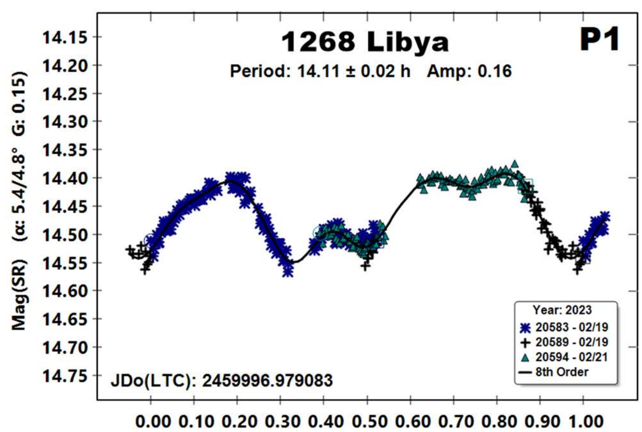


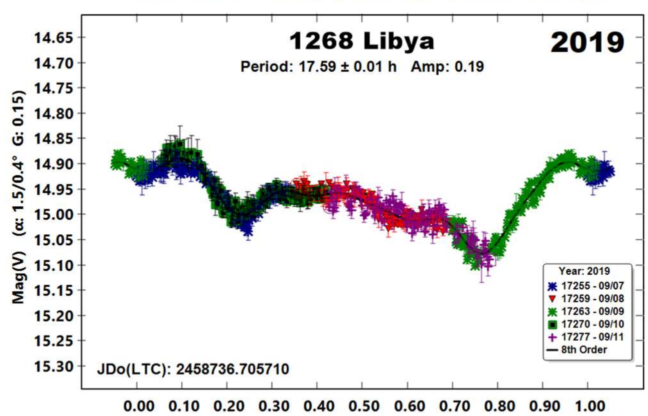

The 2023 data also led to finding a secondary period that significantly improved the fit of the data to $P_1$. It stands out enough in the period spectrum to dismiss it entirely even though the resulting lightcurve has $A_2$ = 0.08 mag.

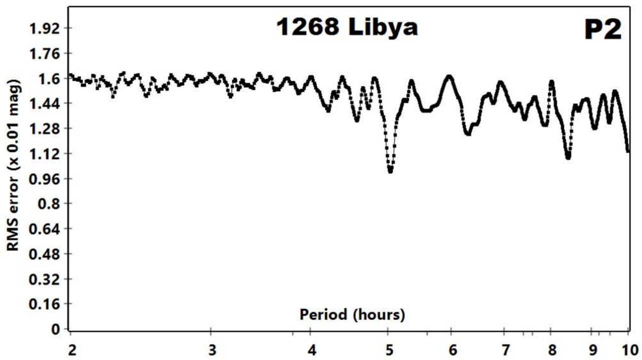


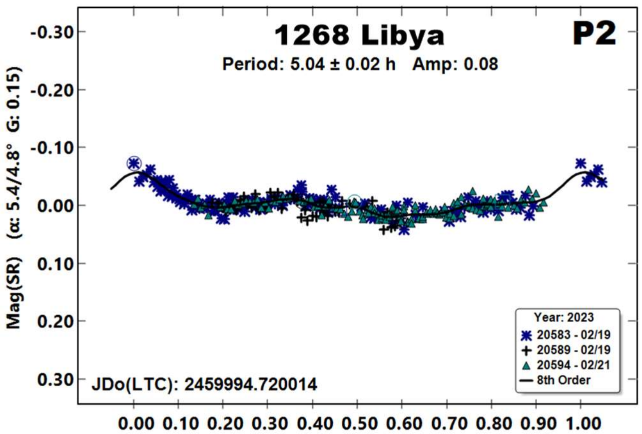


Based on the rules of thumb from Pravec et al. (2005; 2014), the asteroid is a poor candidate for tumbling. Additional observations in the future may help resolve the conundrum.

<u>2312 Duboshin</u>. Stephens (2016) found a period of 50.78 h based on data obtained in 2016. This is in reasonable agreement with the period of 51.72 h derived from the 2023 data. As seen in the $P_1$ period spectrum, that solution is hardly unique and less than fully reliable especially given the shape of the lightcurve.

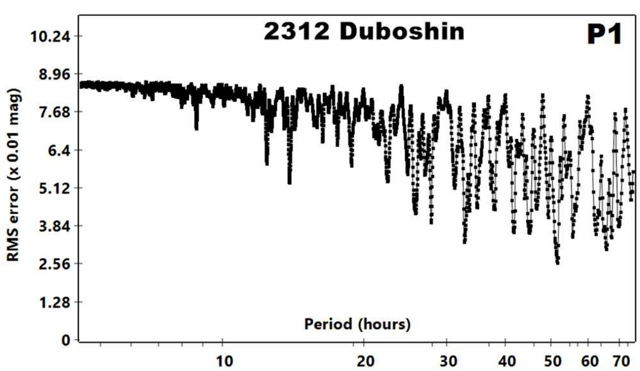


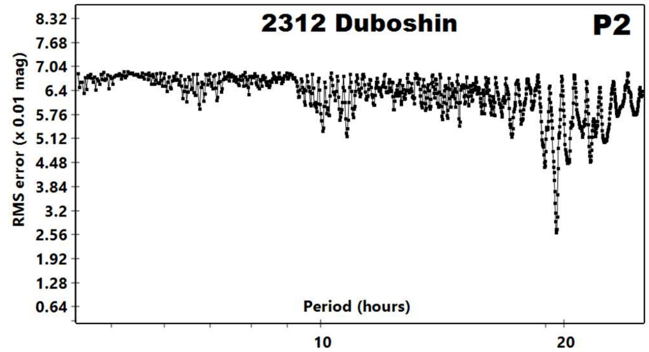


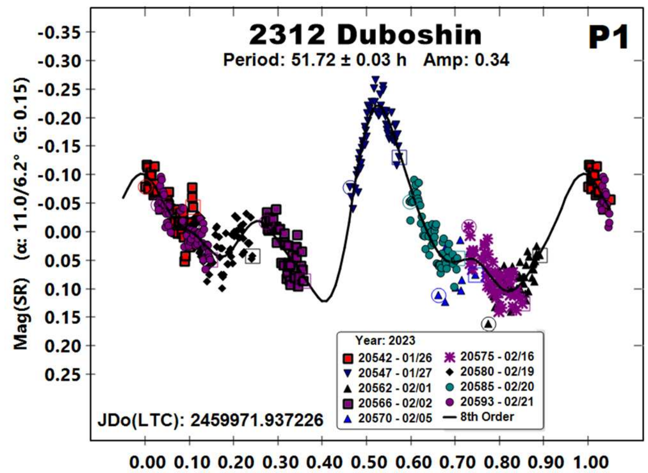


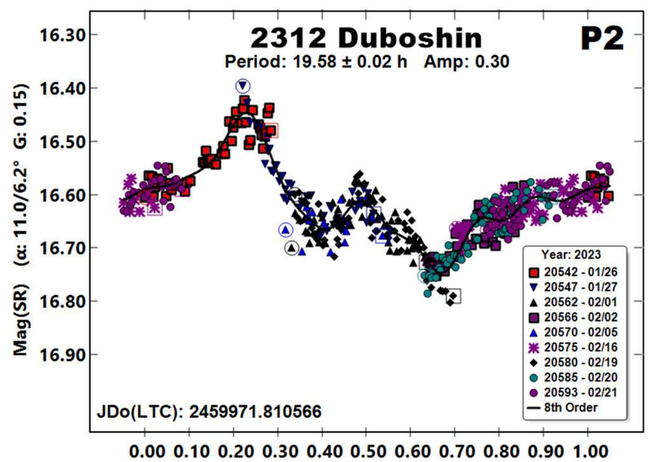


Again, the rules of thumb from Pravec et al. (2005; 2014) for tumbling makes this a very unlikely candidate for tumbling and yet there is undoubtedly a strong solution for a secondary period of 19.58 h. More probable is that $P_2$ is a harmonic artifact of the analysis since ($P1$ * 3) is very close to ($P_2$ * 8).

<u>2760 Kacha</u>. There were three previous solutions in the LCDB: Dahlgren et al. (1998; 13.0 h), Durech and Hanus (2018; 53.040 h sidereal), and Warner and Stephens (2021; 26.247 h). The most recent CS3-PDS result of 26.53 h is in good agreement with the last of the three. It's worth noting that the sidereal period from Durech and Hanus (2018) is almost exactly twice the result from 2023. Trying to fit those data to the doubled period produced large gaps in the lightcurve and some sessions not following the shape of the Fourier curve.

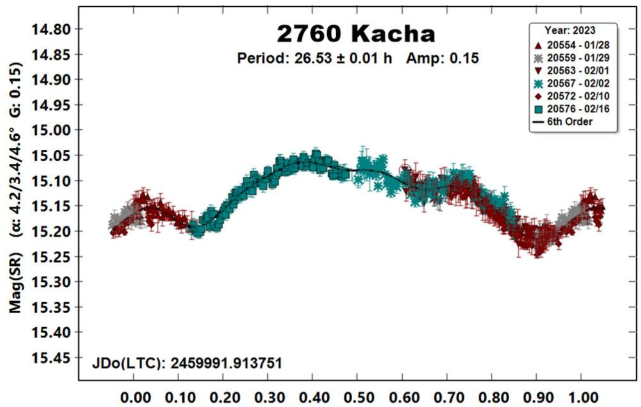


3122 Florence. In addition to numerous solutions found in the LCDB for this NEA, Benner et al. (2017), using the Arecibo radar, discovered that this a three-body system. The two satellites are between 100 to 300 m in size, making them about 5% the size of the asteroid and so should not contribute much to the lightcurve of the asteroid as a whole. Even so, a weak secondary period of $P_2$ = 18.8 h was found. Subtracting its lightcurve from the analysis improved the $P_1$ fit considerably.

Benner et al. (2017) estimated the orbits of the inner and outer satellites to be about 8 h and 24 h, respectively. It may be that the secondary period reported here is the result of finding harmonics of one or both of those orbital periods.

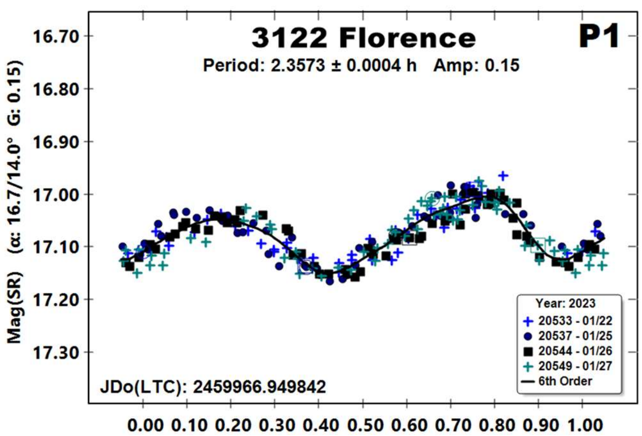


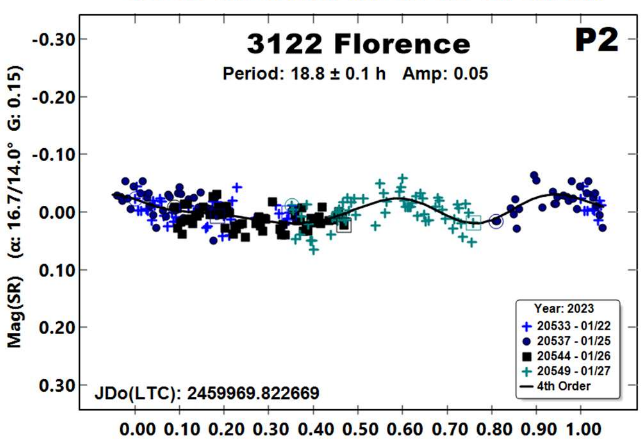


4486 Mithra. Brozovic et al. (2010) used radar to estimate a rotation period about 67.5 h for this contact binary asteroid.

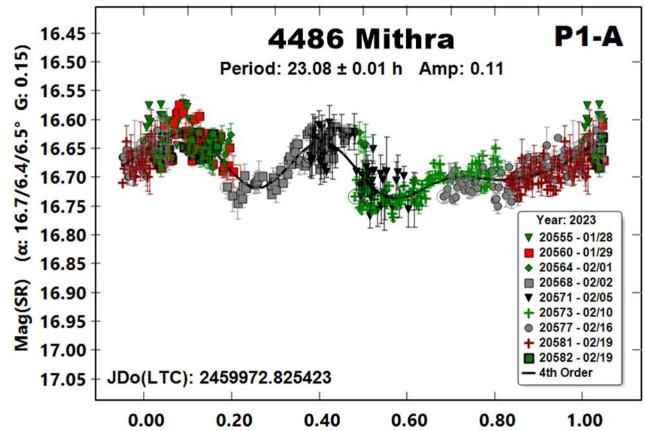


It's hard to argue against radar results, so it's hard to explain the period of 23.08 h found from the 2023 observations as CS3-PDS. Trying to force the solution to something near the radar period produced a multimodal lightcurve with large gaps. "More data!" needs to echo over the years with the hope that the new data will lead to a reliable solution.

14669 Beletic. This appears to be the first rotation period reported for this 27-km Hilda group member. Given the amplitude and low phase angles, the solution is reliable (Harris et al., 2014).

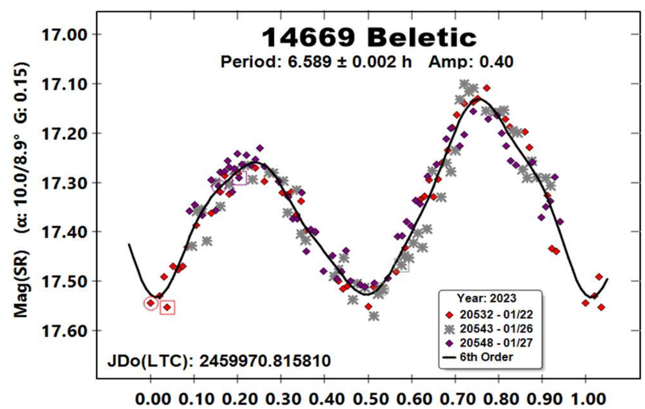


(68359) 2001 OZ13. The period spectrum showed a few possible solutions between 15 and 22 h. The lightcurves for the two more favorable, based on RMS fit to the Fourier curve, are given here.

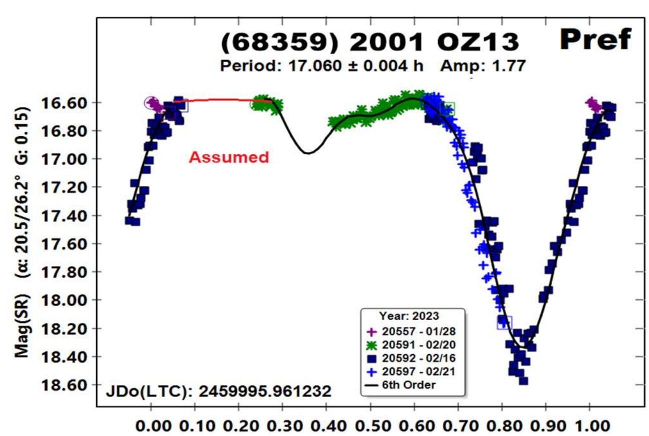

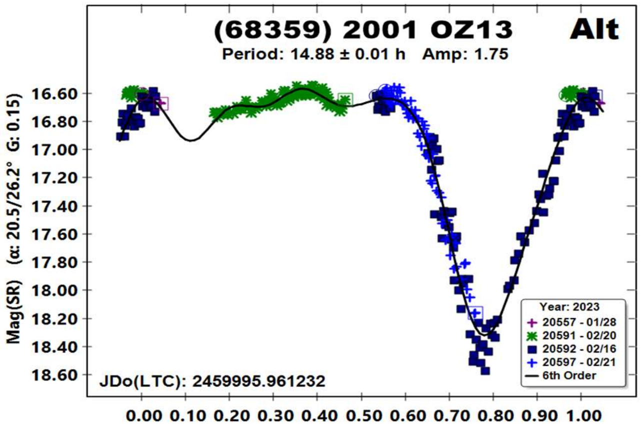


The only previous result in the LCDC was 2.91031 h from Pal et al. (2020) using dense TESS data. The CS3-PDS data seem to reject that solution outright. The preferred solution of 17.060 h is more symmetrical in that the two minimums are closer to 0.5 rotation apart than in the alternate solution. However, both meet a general criterium that the estimated width of the deep attenuation be close to 0.5 rotation phase. Many other solutions were tried and rejected based on this requirement, let alone that they led to multimodal lightcurves.

The problem is to explain the unusual shape of either lightcurve, i.e., to imagine a body, or bodies, that would produce such a lightcurve. Unfortunately, there is seemingly no simple solution.

(98943) 2001 CC21. Pravec et al. (2002web) found a reliable solution of 5.017 h and then, two decades later, a period of 5.0247 h (Pravec et al., 2022web). Analysis of the CS3-PDS data found 5.0159 h, which is in good agreement. *However*, the reasonably clean fit in the "P1" plot was possible *only* by subtracting two other periods.

The three may be harmonically related:

$$5.0159/24 \cong ((15.82 - 11.26) /24)$$

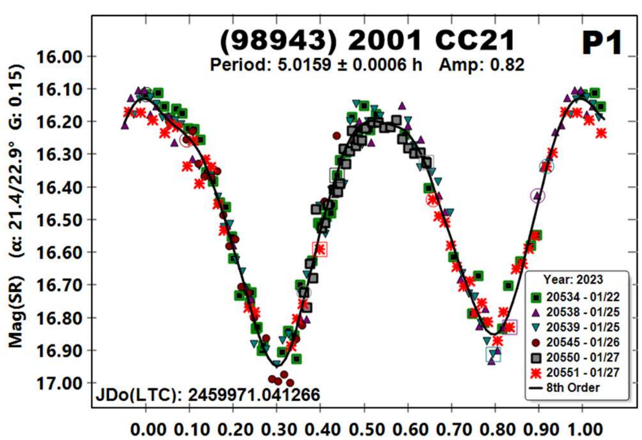


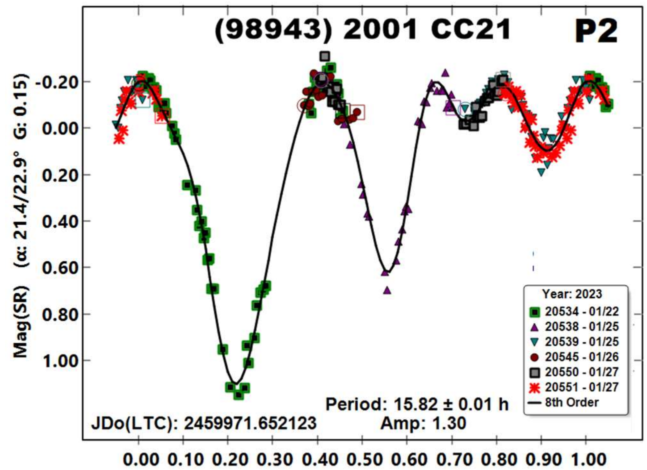


Were the two secondary period amplitudes of low amplitude, it would be easier to accept that they are artifacts of the Fourier analysis. The large amplitude of $P_2$ seems to argue against that. Since the phase angles were not severe during the period of observations and there was little change in the phase angle bisector, deep shadowing leading to the unusual solution also seems improbable. No explanation is offered at this time and, once again, a call for additional observations at future apparitions is made.

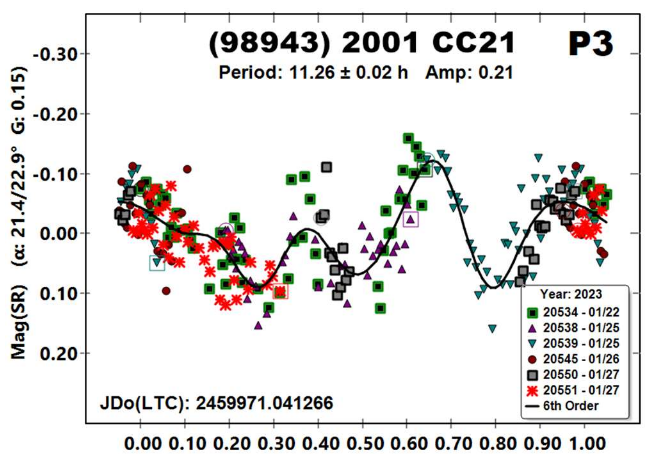


(199145) 2005 YY128. There were no previous entries of any kind in the LCDB for this 650-m NEA.

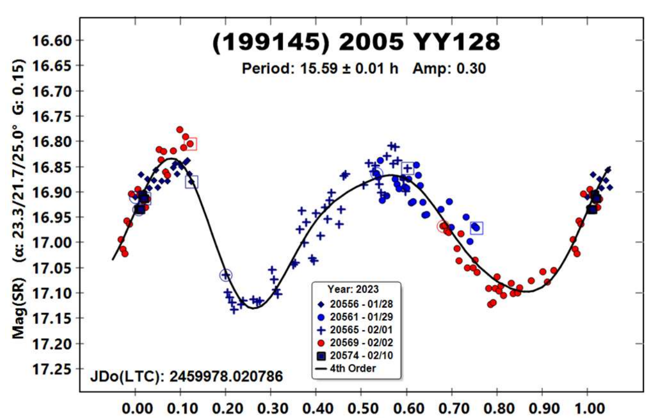

| Number | Name | 2023/mm/dd | Phase | $L_{PAB}$ | $B_{PAB}$ | Period(h) | P.E. | Amp | A.E. | Grp |
|---|---|---|---|---|---|---|---|---|---|---|
| 1268 | Libya | 02/19-02/21 | 5.4,4.8 | 168 | 0 | $^{D}$14.11 | 0.01 | 0.11 | 0.02 | HIL |
| | | | | | | 5.04 | 0.02 | 0.08 | 0.01 | |
| 1268 | Libya | 2019/09/07-09/11 | 1.5,0.4 | 350 | 0 | 17.59 | 0.01 | 0.19 | 0.02 | HIL |
| 2312 | Duboshin | 01/26-02/21 | 11.0,6.2 | 176 | 5 | $^{D}$51.72 | 0.03 | 0.34 | 0.03 | HIL |
| | | | | | | 19.58 | 0.02 | 0.30 | 0.03 | |
| 2760 | Kacha | 01/28-02/16 | *4.2,4.6 | 136 | 10 | 26.53 | 0.01 | 0.15 | 0.02 | HIL |
| 3122 | Florence | 01/22-01/27 | 16.7,14.0 | 150 | 7 | $^{P}$2.3573 | 0.0004 | 0.15 | 0.02 | NEA |
| | | | | | | 18.8 | 0.1 | 0.05 | 0.01 | |
| 4486 | Mithra | 01/28-02/19 | *16.7,6.4 | 148 | 5 | $^{A}$23.08 | 0.04 | 0.11 | 0.02 | NEA |
| | | | | | | 42.33 | 0.04 | 0.14 | 0.02 | |
| 14669 | Beletic | 01/22-01/27 | 10.0,8.9 | 158 | -4 | 6.589 | 0.002 | 0.40 | 0.03 | HIL |
| 68359 | 2001 OZ13 | 01/29-02/21 | *20.4,26.2 | 170 | 15 | $^{A}$17.06 | 0.004 | 1.77 | 0.08 | NEA |
| | | | | | | 14.88 | 0.01 | 1.86 | 0.08 | |
| 98943 | 2001 CC21 | 01/22-01/27 | 21.3,22.8 | 127 | 14 | $^{D}$5.0159 | 0.0006 | 0.82 | 0.04 | NEA |
| | | | | | | 15.82 | 0.01 | 1.30 | 0.03 | |
| | | | | | | 11.26 | 0.02 | 0.21 | 0.05 | |
| 199145 | 2005 YY128 | 02/01-02/10 | *22.0,25.1 | 149 | -6 | 15.59 | 0.01 | 0.30 | 0.03 | NEA |
| | 2004 BE86 | 02/16-02/21 | 7.4,9.9 | 145 | -2 | 16.09 | 0.02 | 0.63 | 0.04 | NEA |
| | 2006 BE55 | 02/20-02/21 | 19.3,20.8 | 158 | 9 | 5.61 | 0.02 | 0.60 | 0.03 | NEA |
| | 2015 RD2 | 01/22-01/27 | 18.8,15.6 | 135 | 6 | 18.493 | 0.008 | 1.19 | 9.03 | NEA |

Table II. Observing circumstances and results. $^{A}$Preferred period of an ambiguous solution. $^{P}$Period of primary with one or more satellites. $^{D}$Dominant period of a multi-period solution. Unless flagged as ambiguous, subsequent lines are additional, not alternate, periods. The phase angle is given for the first and last date. If preceded by an asterisk, the phase angle reached an extremum during the period. LPAB and BPAB are the approximate phase angle bisector longitude/latitude at mid-date range (see Harris et al., 1984).

2004 BE86. Hergenrother and Whiteley (2011) reported a period of 2.422 h with an amplitude of 0.68 mag based on data from 2004. The data from 2023 don't seem to support this, leading instead to a period of 16.09 h. These two periods are not unusual for a binary asteroid, with 2.4 h being the rotation of the primary and 16 h the orbital period of a satellite.

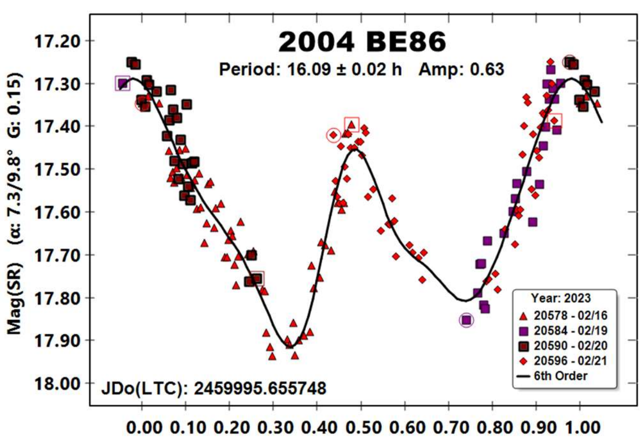


Hergenrother and Whiteley (2011) observed on only two consecutive nights. On the off chance that their data set didn't pick up on a longer period, a dual-period analysis of the 2023 data was done, forcing the short period to 2-3 h. This did find one of 2.4 h; however, it was hard to see a valid lightcurve in the noisy data set.

2006 BE55. There were no previous entries of any kind in the LCDB for this 120-m NEA.

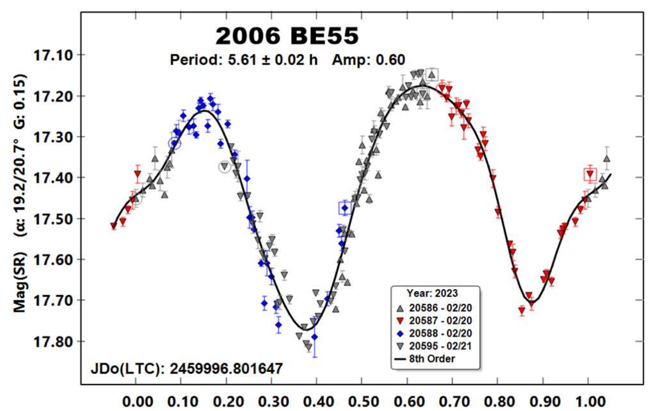


2015 RD2. Mainzer et al. (2019), using data from the WISE mission, found the albedo for this NEA to be near 0.1, about half the usually assumed value for NEAs, which leads to a diameter of about 3.5 km.

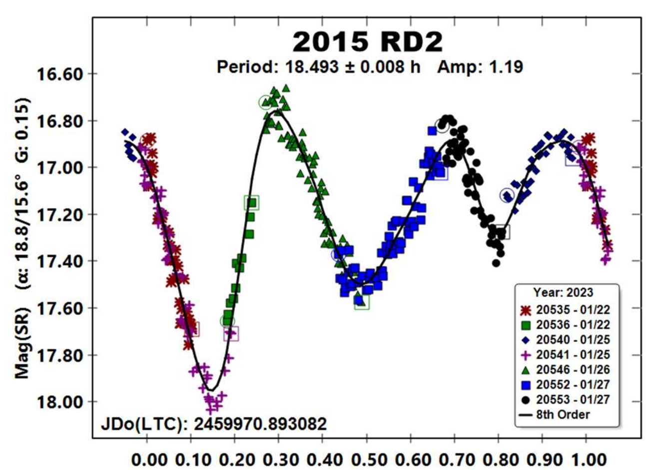

Analysis of the 2023 photometry data showed a trimodal lightcurve with a maximum amplitude of 1.19 mag that is too asymmetrical to be an alias of a shorter period. All attempts to extract one or more additional periods to produce a more typical dominant bimodal lightcurve were fruitless. For now, it appears that this is an unusually-shaped asteroid, or that it is indeed tumbling and that *MPO Canopus* could not handle the data set properly. The possibility of tumbling is likely according to Pravec et al. (2005; 2014).

Acknowledgements

This work includes data from the Asteroid Terrestrial-impact Last Alert System (ATLAS) project. ATLAS is primarily funded to search for near earth asteroids through NASA grants NN12AR55G, 80NSSC18K0284, and 80NSSC18K1575; byproducts of the NEO search include images and catalogs from the survey area. The ATLAS science products have been made possible through the contributions of the University of Hawaii Institute for Astronomy, the Queen's University Belfast, the Space Telescope Science Institute, and the South African Astronomical Observatory. The author gratefully acknowledges a Shoemaker NEO Grants from the Planetary Society (2007). This was used to purchase some of the equipment used in this research.

References

Benner, L.A.M.; Naidu, S.; Brozovic, M.; Chodas, P. (2017). "Radar Reveals Two Moons Orbiting Asteroid Florence." *https://cneos.jpl.nasa.gov/news/news199.html*

Brozovic, M.; Benner, L.A.M.; Magri, C.; Ostro, S.J.; Scheeres, D.J.; Giorgini, J.D.; Nolan, M.C.; Margot, J.-L.; Jurgens, R.F.; Rose, R. (2010). "Radar observations and a physical model of contact binary Asteroid 4486 Mithra." *Icarus* **208**, 207-220.

Dahlgren, M.; Lahulla, J.F.; Lagerkvist, C.-I.; Lagerros, J.; Mottola, S.; Erikson, A.; Gonano-Beurer, M.; Di Martino, M. (1998). "A Study of Hilda Asteroids. V. Lightcurves of 47 Hilda Asteroids." *Icarus* **133**, 247-285.

Durech, J.; Hanus, J. (2018). "Reconstruction of asteroid spin states from Gaia DR2." *Astron. Astrophys*. **620**, A91.

Harris, A.W.; Young, J.W.; Scaltriti, F.; Zappala, V. (1984). "Lightcurves and phase relations of the asteroids 82 Alkmene and 444 Gyptis." *Icarus* **57**, 251-258.

Harris, A.W.; Pravec, P.; Galad, A.; Skiff, B.A.; Warner, B.D.; Vilagi, J.; Gajdos, S.; Carbognani, A.; Hornoch, K.; Kusnirak, P.; Cooney, W.R.; Gross, J.; Terrell, D.; Higgins, D.; Bowell, E.; Koehn, B.W. (2014). "On the maximum amplitude of harmonics on an asteroid lightcurve." *Icarus* **235**, 55-59.

Hergenrother, C.W.; Whiteley, R.J. (2011). "A survey of small fast rotating asteroids among the near-Earth asteroid population." *Icarus* **214**, 194-209.

Mainzer, A.; Bauer, J.; Cutri, R.; Grav, T.; Kramer, E.; Masiero, J.; Sonnett, S.; Wright, E., Eds. (2019). "NEOWISE Diameters and Albedos V2.0." NASA Planetary Data System. urn:nasa:pds:neowise_diameters_albedos::2.0. *https://doi.org/10.26033/18S3-2Z54*

Pal, A.; Szakáts, R.; Kiss, C.; Bódi, A.; Bognár, Z.; Kalup, C.; Kiss, L.L.; Marton, G.; Molnár, L.; Plachy, E.; Sárneczky, K.; Szabó, G.M.; Szabó, R. (2020). "Solar System Objects Observed with TESS - First Data Release: Bright Main-belt and Trojan Asteroids from the Southern Survey." *Ap. J. Suppl Ser*. **247**, id. 26.

Pravec, P.; Wolf, M.; Sarounova, L. (2002web; 2022web) *http://www.asu.cas.cz/~ppravec/neo.htm*

Pravec, P.; Harris, A.W.; Scheirich, P.; Kušnirák, P.; Šarounová, L.; Hergenrother, C.W.; Mottola, S.; Hicks, M.D.; Masi, G.; Krugly, Yu.N.; Shevchenko, V.G.; Nolan, M.C.; Howell, E.S.; Kaasalainen, M.; Galád, A.; Brown, P.; Degraff, D.R.; Lambert, J.V.; Cooney, W.R.; Foglia, S. (2005). "Tumbling asteroids." *Icarus* **173**, 108-131.

Pravec, P.; Scheirich, P.; Durech, J.; Pollock, J.; Kusnirak, P.; Hornoch, K.; Galad, A.; Vokrouhlicky, D.; Harris, A.W.; Jehin, E.; Manfroid, J.; Opitom, C.; Gillon, M.; Colas, F.; Oey, J.; Vrastil, J.; Reichart, D.; Ivarsen, K.; Haislip, J.; LaCluyze, A. (2014). "The tumbling state of (99942) Apophis." *Icarus* **233**, 48-60.

Stephens, R.D. (2016). "Asteroids Observed from CS3: 2016 April-June." *Minor Planet Bull*. **43**, 336-339.

Tonry, J.L.; Denneau, L.; Flewelling, H.; Heinze, A.N.; Onken, C.A.; Smartt, S.J.; Stalder, B.; Weiland, H.J.; Wolf, C. (2018). "The ATLAS All-Sky Stellar Reference Catalog." *Astrophys. J.* **867**, A105.

Warner, B.D.; Harris, A.W.; Pravec, P. (2009). "The Asteroid Lightcurve Database." *Icarus* **202**, 134-146. Updated 2023 March. *http://www.minorplanet.info/lightcurvedatabase.html*

Warner, B.D; Stephens, R.D. (2020). "Lightcurve Analysis of Hilda Asteroids at the Center for Solar System Studies: 2018 September - 2019 September." *Minor Planet Bull.* **47**, 37-41.

Warner, B.D.; Stephens, R.D. (2021). "Lightcurve Analysis of Hilda Asteroids at the Center for Solar System Studies: 2020 August-September." *Minor Planet Bull*. **48**, 17-19.

# LIGHTCURVES OF NINE ASTEROIDS

Eric V. Dose
3167 San Mateo Blvd NE #329
Albuquerque, NM 87110
mp@ericdose.com

(Received: 2023 April 12)

We present lightcurves and synodic rotation periods for nine asteroids. A trimodal interpretation is proposed for the lightcurve of Hungaria-family 4142 Dersu-Uzala.

We present asteroid lightcurves obtained via the workflow process described by Dose (2020) and later improved (Dose, 2021). This workflow applies to each image an ensemble of typically 15-60 nearby comparison ("comp") stars selected from the ATLAS refcat2 catalog (Tonry et al., 2018). Custom diagnostic plots and the abundance of comp stars allow for rapid identification and removal of outlier, variable, and poorly measured comp stars.

The product of this custom workflow is one night's time series of absolute magnitudes, on Sloan r' (SR) catalog basis, for one target asteroid. These magnitudes are corrected for instrument transforms, sky extinction, and image-to-image ("cirrus") fluctuations and thus represent magnitudes at the top of earth's atmosphere. These magnitudes are imported directly into *MPO Canopus* software (Warner, 2021) where they are adjusted for distances and phase-angle dependence, fit by Fourier analysis including identifying and ruling out of aliases, and plotted.

Phase-angle dependence is corrected with a H-G model, using the G value minimizing best-fit RMS error across all nights' data; when we cannot estimate an asteroid's G value, usually due to a campaign's narrow range of phase angles, we apply the Minor Planet Center's default value of 0.15. No nightly zero-point adjustments (Delta Comps in *MPO Canopus* terminology) were made to any session herein, other than by estimating G, which practice we note introduces only one new fitting term vs many more terms (number of nights - 1) when applying non-zero Delta Comps.

## Lightcurve Results

Nine asteroids were observed from New Mexico Skies observatory at 2310 meters elevation in southern New Mexico. Images were acquired with a 0.35-meter SCT reduced to f/7.7; a SBIG STXL-6303E camera cooled to -35 C and fitted with an Exoplanet/Blue Blocker (BB) filter (Astrodon); and a PlaneWave L-500 mount. The equipment was operated remotely via *ACP software* (DC-3 Dreams, version 8.3), running plan files generated for each night by the author's python scripts (Dose, 2020). Exposures were autoguided, and exposure times targeted 2-5 millimagnitudes uncertainty in asteroid instrumental magnitude, subject to a minimum exposure of 150 seconds to ensure suitable comp-star photometry, and to a maximum of 900 seconds.

FITS images were plate-solved by *PinPoint* (DC-3 Dreams) or *TheSkyX* (Software Bisque) and were calibrated using temperature-matched, median-averaged dark images and recent flat images of a flux-adjustable flat panel. Every photometric image was visually inspected; the author excluded images with poor tracking, obvious interference by cloud or moon, or having stars, satellite tracks, cosmic ray artifacts, or other apparent light sources within 12 arcseconds of the target asteroid's signal centroid. Images passing these screens were submitted to the workflow.

The BB filter, a yellow filter with relatively sharp wavelength cut-off, requires only a modest first-order transform to the standard Sloan r' passband. In our hands, using this filter rather than a clear filter or no filter improves night-to-night reproducibility to a degree outweighing loss of signal-to-noise ratio from loss of flux.

Comparison stars from the ATLAS refcat2 catalog were selected if they had: distance from image boundaries and other catalogued flux sources of at least 15 arcseconds, no catalog VARIABLE flag, Sloan r' magnitude within [-2, +1] of the target asteroid's r' magnitude on that night (except that very faint asteroids used comp stars with magnitudes in the range 14 to 16), Sloan r'-i' color value within [0.10, 0.34], and absence of variability as seen in session plots of each comp star's instrumental magnitude vs time.

In this work, "period" refers to an asteroid's synodic rotation period, "SR" denotes the Sloan r' passband, and "mmag" denotes millimagnitudes (0.001 magnitude).

<u>383 Janina</u>. Our synodic period estimate of 6.426 ± 0.002 h for this Themis-family asteroid confirms all previous estimates (6.4 h, Tedesco, 1979; 6.42943 h, Ďurech et al., 2020; 6.429 h, Erasmus et al., 2020; 6.4298 h, Pilcher, 2021) but one (4.636 h, Clark, 2006).

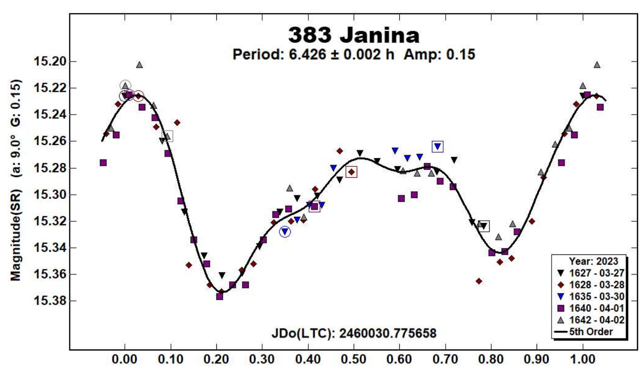


| Number | Name | yyyy mm/dd | Phase | $L_{PAB}$ | $B_{PAB}$ | Period(h) | P.E. | Amp | A.E. | Grp |
|---|---|---|---|---|---|---|---|---|---|---|
| 383 | Janina | 2023 03/27-04/02 | 9.1,7.5 | 215 | 3 | 6.426 | 0.002 | 0.15 | 0.02 | THEM |
| 784 | Pickeringia | 2022-3 12/08-01/21 | 16.4,8.5 | 141 | 12 | 13.171 | 0.001 | 0.26 | 0.03 | MB-O |
| 845 | Naema | 2023 02/05-03/14 | 18.3,18.8 | 76 | 9 | 13.378 | 0.002 | 0.13 | 0.04 | NAEM |
| 1493 | Sigrid | 2022-3 11/07-02/07 | *20.0,15.9 | 96 | 3 | 43.193 | 0.005 | 0.69 | 0.10 | MB-O |
| 1558 | Jarnefelt | 2023 01/21-01/28 | *2.2,1.4 | 125 | 3 | 6.257 | 0.001 | 0.24 | 0.04 | MB-O |
| 1639 | Bower | 2023 01/07-04/12 | *18.7,19.7 | 150 | -1 | 22.165 | 0.001 | 0.32 | 0.05 | MB-I |
| 2301 | Whitford | 2023 02/03-03/26 | *13.2,9.4 | 166 | 15 | 14.302 | 0.001 | 0.42 | 0.05 | MB-O |
| 4142 | Dersu-Uzala | 2023 01/08-04/07 | *30.7,33.6 | 142 | 36 | 411.22 | 0.28 | 0.85 | 0.15 | HUNG |
| 4635 | Rimbaud | 2023 01/12-03/14 | *5.6,24.3 | 121 | 7 | 118.510 | 0.045 | 1.38 | 0.12 | MB-I |

Table I. Observing circumstances and results. The phase angle is given for the first and last date. If preceded by an asterisk, the phase angle reached an extrema during the period. $L_{PAB}$ and $B_{PAB}$ are the approximate phase angle bisector longitude/latitude at mid-date range (see Harris et al.,1984). Grp is the asteroid family/group (Warner, 2009a).

The lightcurve shape for 383 Janina is clearly bimodal. Our Fourier fit RMS error is 12 mmag; given our narrow phase angle range, we applied the Minor Planet Center's default G value of 0.15. Our period spectrum supports the consensus period.

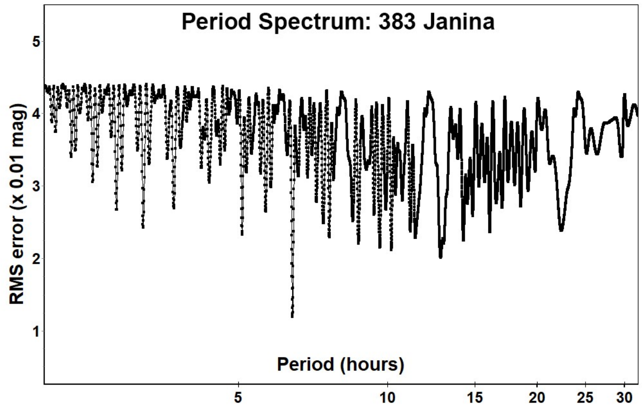


784 Pickeringia. For this outer main-belt asteroid, we estimate the period as 13.171 ± 0.001 h, in agreement with known previous estimates (13 h, Hainaut-Rouelle et al., 1995; 13.17 h, Behrend, 2004web; 13.1699 h, Hanuš et al., 2011; 13.16995 h, Ďurech et al., 2016; 13.16998 h, Hanuš et al., 2016; 13.16999 h, Martikainen et al., 2021; 13.144 h, Mas et al., 2018; 13.169 h, Pilcher, 2022). Our Fourier fit RMS error is 9 mmag, and the lightcurve shape is clearly bimodal. Given our narrow range of phase angles, we applied G value of 0.15.

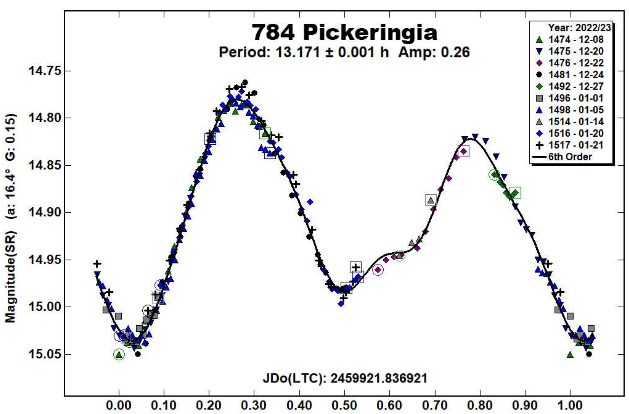


845 Naema. Our period estimate for this primary asteroid of the Naema family is 13.378 ± 0.002 h, at variance from both known published estimates (20.892 h, Bembrick et al., 2008; 12.1 h, Behrend, 2017web). Our lightcurve is bimodal.

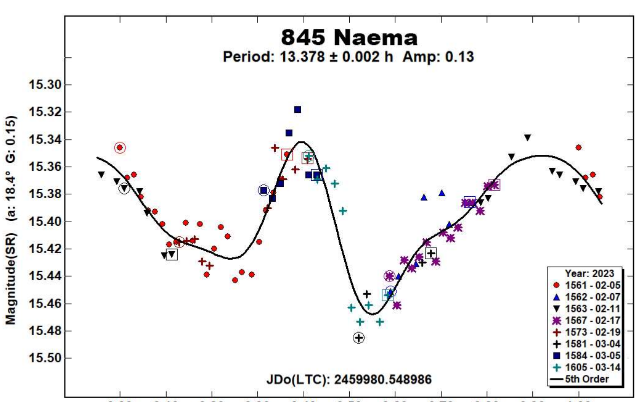


Our Fourier fit RMS error is 14 mmag; given our very narrow phase angle range, we applied G value of 0.15. Our period spectrum disfavors both previously published period estimates. We cannot explain differences in these estimates from ours either by multiples of half-period or by sidereal aliases.

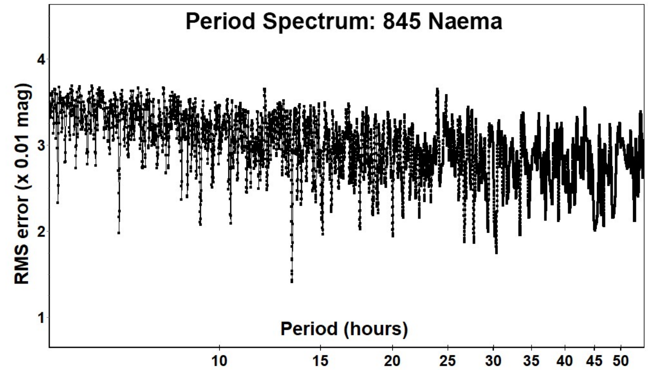


1493 Sigrid. Our period estimate of 43.193 ± 0.005 h for this Nysa-Polana family asteroid agrees with most (43.296 h, Bembrick and Byron, 2007; 43.179 h, Hanuš et al, 2013; 43.1795 h, Ďurech et al., 2016) but not all (22.68 h, Behrend, 2010web) published estimates. The Behrend estimate appears to be a monomodal interpretation, but the other estimates and the lightcurve offered here suggest a bimodal interpretation. While our phase coverage is incomplete, the difference in brightness between the two minima is significant and leaves little doubt that a bimodal interpretation is superior to monomodal. Our Fourier fit RMS error is 29 mmag; G of 0.23 minimized the fit error, though the improvement over a value of 0.15 was marginal.

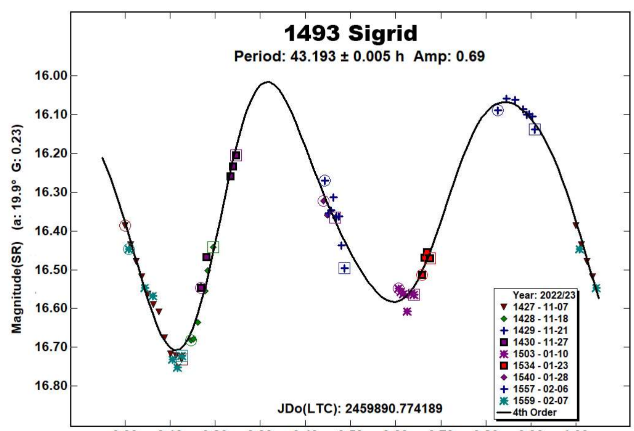


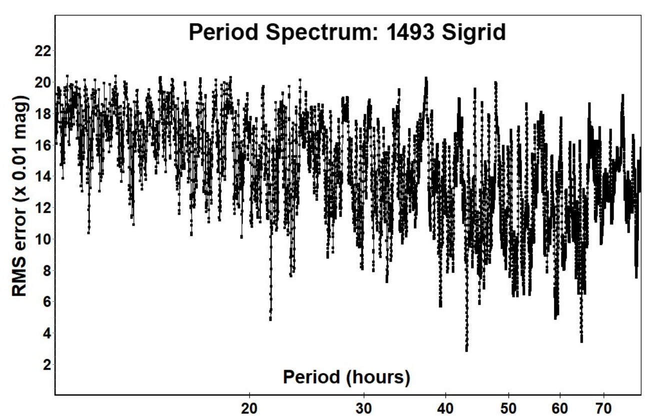

1558 Jarnefelt. For this outer main-belt asteroid, we find a synodic period of 6.257 ± 0.001 h, agreeing with two published estimates (6.252 h, Polakis, 2019; 6.255 h, Polakis, 2022) but differing from one other (18.22 h, Hawkins and Ditteon, 2008). The latter lightcurve suffered incomplete coverage as phased to 18.22 h; phased lightcurves of 2019 and 2022 were heavily covered with over 200 data points each and were more clearly bimodal in shape.

Our lightcurve benefited from three sessions each covering more than one period. Our Fourier fit RMS error is 10 mmag; a G value near 0.25 strongly minimized the fit error. We suggest that a bimodal-basis period near 6.25 h appears secure.

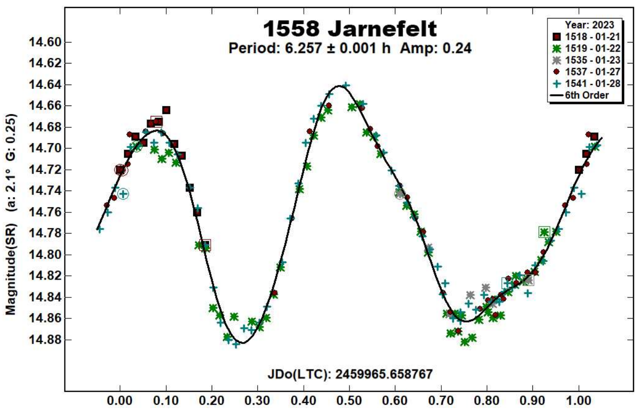


1639 Bower. We confirm most previously reported period estimates (22.4 h, Behrend, 2005web; 12.5 h, Robinson, 2011web; 22.181 h, Polakis, 2018a; 22.1759 h, Ďurech et al, 2019) with our estimate of 22.165 ± 0.001 h for this inner main-belt asteroid. Our Fourier fit RMS error is 16 mmag; G value of 0.03 reduced fit error by about half relative to fitting with MPC's default value of 0.15.

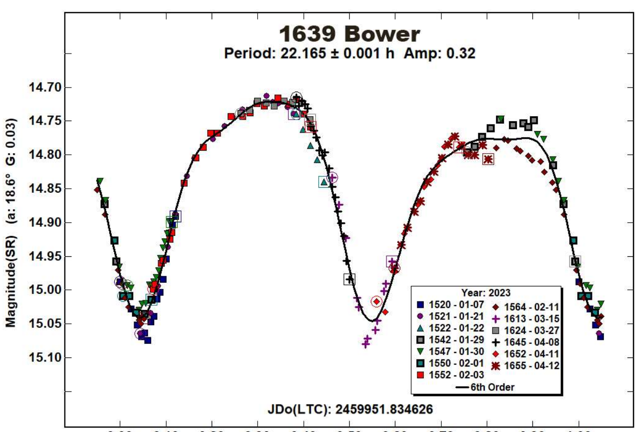


2301 Whitford. We estimate the period for this outer main-belt asteroid to be 14.302 ± 0.001 h, disagreeing with one published report (27.1 h, Aznar, 2011web) but agreeing with three others (14.275 h, Waszczak et al., 2015; 14.30151 h, Ďurech et al., 2020; 14.319 h, Polakis, 2022). Our Fourier fit RMS error is 17 mmag; a G value of 0.30 markedly reduced fit error relative to a value of 0.15.

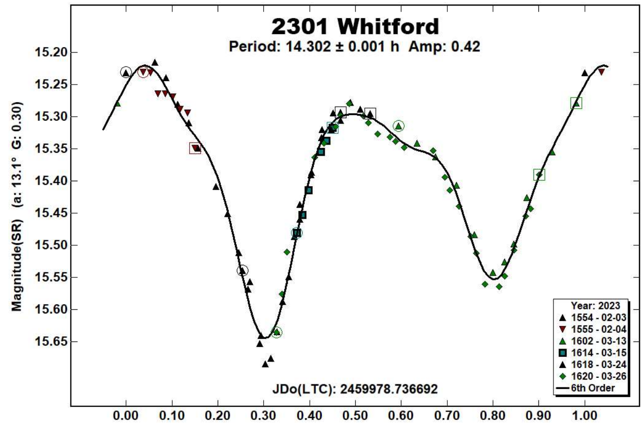


4142 Dersu-Uzala. The rotation period for this Hungaria-family asteroid has proven difficult to establish with confidence, despite its lightcurve having substantial amplitude. The early-2023 apparition during which we observed was not especially favorable in magnitude, but it was extraordinarily favorable in declination (ca. +60°) for Northern Hemisphere observers, both in the number of months that it remained near maximum brightness and in allowing for observations during full moons.

From our extended lightcurve campaign and data captured from 26 nights over 13 weeks, we report a period of 411.22 ± 0.28 h. The lightcurve shape retained its trimodal shape through our observations which extended over more than 5 periods. Our Fourier fit RMS error is 39 mmag; a G value of -0.05 modestly reduced the fit error relative to 0.15 and is an uncertain estimate. Unfortunately, we had no clear night at the major brightness minimum (near our phase 0.93), so that our amplitude estimate of 0.85 magnitudes is somewhat uncertain.

Our period result differs from all known previous reports (71.2 h, Warner, 2007; 71 h, Warner, 2015; 140 h, Warner et al., 2009b; 276 h, Polakis, 2018b). We suggest that the 140 h and 276 h estimates represent monomodal and bimodal interpretations, where our interpretation is trimodal. Though we saw no strong evidence of precession ("tumbling") effect, our data do not rule out a minor effect.

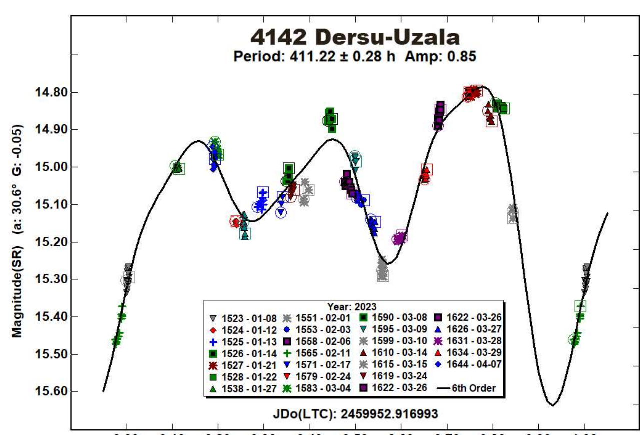

Our period spectrum favors our proposed period over periods near 276, 140, and 71 h.

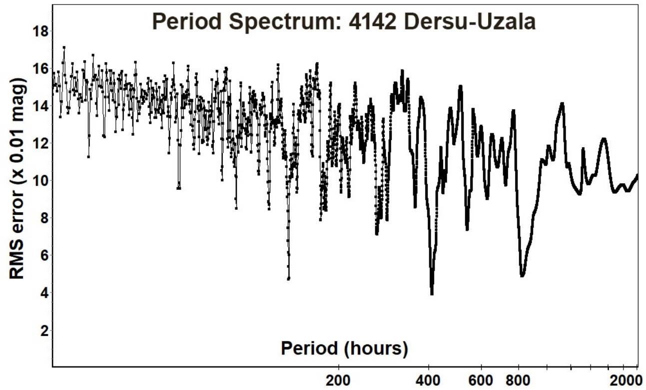


4635 Rimbaud. For this very high-amplitude, inner main-belt asteroid, we report a period of 118.510 ± 0.045 h, in agreement with one previous report (117.91 h, Stephens and Warner, 2019) and in approximate agreement with one other (125 h, Podlewska-Gaca et al., 2021). Our Fourier fit RMS error is 34 mmag; G value of 0.54 strongly reduced fit error relative to MPC's default of 0.15.

Though our campaign continued for 15 nights over 9 weeks, our phase coverage remains incomplete. Even so, our lightcurve shape is clearly bimodal, especially in the difference between the two brightness minima.

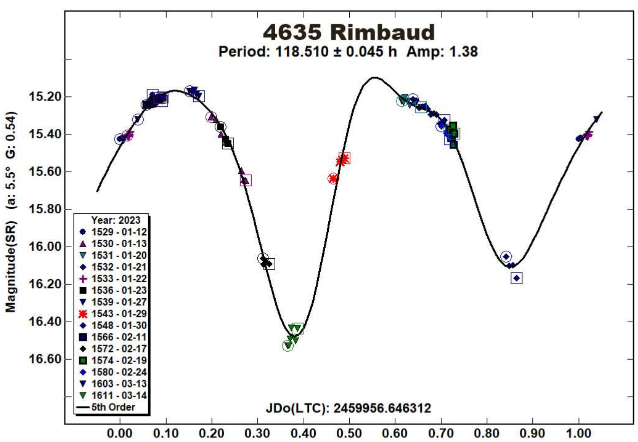


Our period spectrum favors only period estimates of multiples of one-half of our own estimate.

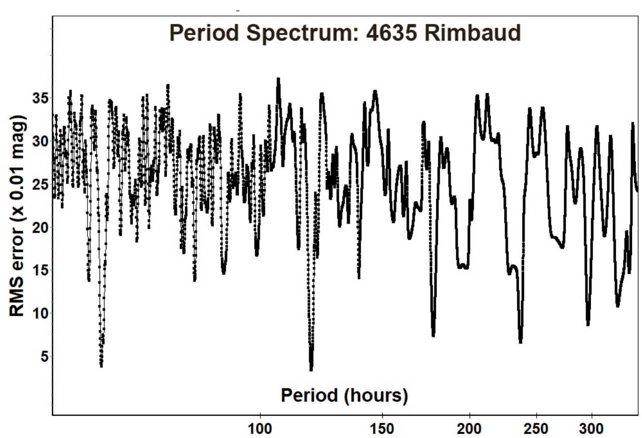


Acknowledgements

The author thanks the authors of and contributors to the ATLAS paper (Tonry et al., 2018) for providing openly and without cost the ATLAS refcat2 catalog release. This current work also makes extensive use of the python language interpreter and of several supporting packages (notably: astropy, ccdproc, ephem, matplotlib, pandas, photutils, requests, skyfield, and statsmodels), all made available openly and without cost.

References

Aznar, A. (2011). Web reference, as cited in LCDB. Inaccessible directly on 2023-04-10. *http://www.apt.com.es/*

Behrend, R. (2004web, 2005web, 2010web, 2017web). Observatoire de Genève web site. *http://obswww.unige.ch/~behrend/page_cou.html*

Bembrick, C.; Byron, J. (2007). "A Rotation Period for 1493 Sigrid." *Minor Planet Bull*. **34**, 1.

Bembrick, C.; Allen, B.; Bolt, G. (2008). "The Rotation Periods of 845 Naëma, 1607 Mavis, and (30105) 2000 FO3." *Minor Planet Bull*. **35**, 74-75.

Clark, M. (2006). "Lightcurve Results for 383 Janina, 899 Jokaste, 1825 Klare, 2525 O'Steen, 5064 Tanchozuru, and (17939) 1999 HH8." *Minor Planet Bull*. **33**, 53-56.

Dose, E. (2020). "A New Photometric Workflow and Lightcurves of Fifteen Asteroids." *Minor Planet Bull*. **47**, 324-330.

Dose, E. (2021). "Lightcurves of Nineteen Asteroids." *Minor Planet Bull*. **48**, 69-76.

Ďurech, J.; Hanuš, J.; Oszkiewicz, D.; Vančo, R. (2016). "Asteroid models from the Lowell photometric database." *Astron. Astrophys.* **587**, A48.

Ďurech, J.; Hanuš, J.; Vančo, R. (2019). "Inversion of asteroid photometry from Gaia DR2 and the Lowell Observatory photometric database." *Astron. Astrophys.* **631**, A2.

Ďurech, J.; Tonry, J.; Erasmus, N.; Denneau, L.; Heinze, A.N.; Flewelling, H.; Vančo, R. (2020). "Asteroid models reconstructed from ATLAS photometry." *Astron. Astrophys.* **643**, A59.

Erasmus, N.; Navarro-Meza, S.; McNeill, A.; Trilling, D.E.; Sickafoose, A.A.; Denneau, L.; Flewelling, H.; Heinze, A.; Tonry, J.L. (2020). "Investigating Taxonomic Diversity within Asteroid Families through ATLAS Dual-band Photometry." *Astrophys. J. Suppl. Ser.* **247**, 13.

Hainaut-Rouelle, M.-C.; Hainaut, O.R.; Detal, A. (1995). "Lightcurves of selected minor planets." *Astron. Astrophys. Suppl. Ser.* **112**, 125-142.

Hanuš, J.; Ďurech, J.; Brož, M.; Warner, B.D.; Pilcher, F.; Stephens, R.; Oey, J.; Bernasconi, L.; Casulli, S.; Behrend, R.; Polishook, D.; Henych, T.; Lehký, M.; Yoshida, F.; Ito, T. (2011). "A study of asteroid pole-latitude distribution based on an extended set of shape models derived by the lightcurve inversion method." *Astron. Astrophys.* **530**, A134.

Hanuš, J.; Brož, M.; Ďurech, J.; Warner, B.D.; Brinsfield, J.; Durkee, R.; Higgins, D.; Koff, R.A.; Oey, J.; Pilcher, F.; Stephens, R.; Strabla, L.P.; Ulisse, Q.; Girelli, R. (2013). "An anisotropic distribution of spin vectors in asteroid families." *Astron. Astrophys.* **559**, A134.

Hanuš, J. and 168 colleagues (2016). "New and updated convex shape models of asteroids based on optical data from a large collaboration network." *Astron. Astrophys.* **586**, A108.

Harris, A.W.; Young, J.W.; Scaltriti, F.; Zappala, V. (1984). "Lightcurves and phase relations of asteroids 82 Alkmene and 444 Gyptis." *Icarus* **57**, 251-258.

Hawkins, S.; Ditteon, R. (2008). "Asteroid Lightcurve Analysis at the Oakley Observatory - May 2007." *Minor Planet Bull*. **35**, 1-4.

Martikainen, J.; Muinonen, K.; Penttilä, A.; Cellino, A.; Wang, X.-B. (2021). "Asteroid absolute magnitudes and phase curve parameters from Gaia phometry." *Astron. Astrophys.* **649**, A98.

Mas, V.; Fornas, G.; Lozano, J.; Rodrigo, O.; Fornas, A.; Carreño, A.; Arce, E.; Brines, P.; Herrero, D. (2018). "Twenty-One Asteroid Lightcurves at Asteroids Observers (OBAS) - MPPD: Nov 2016 - May 2017." *Minor Planet Bull*. **45**, 76-82.

Pilcher, F. (2021). "Lightcurves and Rotation Periods of 49 Pales, 383 Janina, and 764 Gedania." *Minor Planet Bull*. **48**, 5-6.

Pilcher, F. (2022). "Lightcurves and Rotation Periods of 330 Adalberta, 494 Virtus, 530 Turandot, 784 Pickeringia, and 1009 Sirene." *Minor Planet Bull*. **49**, 122-124.

Podlewska-Gaca, E.; Poleski, R.; Bartczak, P.; McDonald, I.; Pál, A. (2021). "Determination of Rotation Periods for a Large Sample of Asteroids from the K2 Campaign 9." *Astrophys. J. Suppl. Series* **255**, 4.

Polakis, T. (2018a). "Lightcurve Analysis for Seven Main-Belt Asteroids." *Minor Planet Bull*. **45**, 112-115.

Polakis, T. (2018b). "Lightcurve Analysis for Fourteen Main-Belt Minor Planets." *Minor Planet Bull*. **45**, 347-352.

Polakis, T. (2019). "Photometric Observations of Seventeen Minor Planets." *Minor Planet Bull*. **46**, 400-406.

Polakis, T. (2022). "Lightcurves for Thirteen Minor Planets." *Minor Planet Bull*. **49**, 131-135.

Robinson, L. (2011web). Web reference accessed 2023-04-12. *http://btboar.tripod.com/lightcurves/*

Stephens, R.D.; Warner, B.D. (2019). "Main-Belt Asteroids Observed from CS3: 2018 October - December." *Minor Planet Bull*. **46**, 180-187.

Tedesco, E.F. (1979). Ph.D. Dissertation, New. Mex. State Univ., as cited in LCDB.

Tonry, J.L.; Denneau, L.; Flewelling, H.; Heinze, A.N.; Onken, C.A.; Smartt, S.J.; Stalder, B.; Weiland, H.J.; Wolf, C. (2018). "The ATLAS All-Sky Stellar Reference Catalog." *Astrophys. J.* **867**, A105.

Warner, B.D. (2007). "Asteroid Lightcurve Analysis at the Palmer Divide Observatory - September-December 2006." *Minor Planet Bull*. **34**, 32-37.

Warner, B.D.; Harris, A.W.; Pravec, P. (2009a). "The asteroid lightcurve database." *Icarus* **202**, 134-146.
*https://minplanobs.org/MPInfo/php/lcdb.php*

Warner, B.D.; Stephens, R.D.; Harris, A.W.; Pravec, P. (2009b). "A Re-examination of the Lightcurves for Seven Hungaria Asteroids." *Minor Planet Bull*. **36**, 176-179.

Warner, B.D. (2015). "Asteroid Lightcurve Analysis at CS3-Palmer Divide Station: 2015 March-June." *Minor Planet Bull*. **42**, 267-276.

Warner, B.D. (2021). *MPO Canopus* Software, version 10.8.4.11, BDW Publishing. *http://www.bdwpublishing.com*

Waszczak, A.; Chang, C.-K.; Ofek, E.O.; Laher, R.; Masci, F.; Levitan, D.; Surace, J.; Cheng, Y.-C.; Ip, W.-H.; Kinoshita, D.; Helou, G.; Prince, T.A.; Kulkarni, S. (2015). "Asteroid light curves from the Palomar Transient Factory survey: rotation periods and phase functions from sparse photometry." *Astronomical Journal* **150**, 75.

# COLLABORATIVE ASTEROID PHOTOMETRY FROM UAI: 2023 JANUARY-MARCH


Lorenzo Franco
Balzaretto Observatory (A81), Rome, ITALY
lor_franco@libero.it

Alessandro Marchini, Riccardo Papini
Astronomical Observatory, University of Siena (K54)
Via Roma 56, 53100 - Siena, ITALY

Marco Iozzi
HOB Astronomical Observatory (L63)
Capraia Fiorentina, ITALY

Giulio Scarfi
Iota Scorpii Observatory (K78), La Spezia, ITALY

Gianni Galli
GiaGa Observatory (203), Pogliano Milanese, ITALY

Paolo Fini, Guido Betti
Blessed Hermann Observatory (L73), Impruneta, ITALY

Alessandro Coffano, Wladimiro Marinello
Osservatorio Serafino Zani (130), Lumezzane (BS), ITALY

Paolo Bacci, Martina Maestripieri
GAMP - San Marcello Pistoiese (104), Pistoia, ITALY

Nello Ruocco
Osservatorio Astronomico Nastro Verde (C82), Sorrento, ITALY

Fabio Mortari, Davide Gabellini
Hypatia Observatory (L62), Rimini, ITALY

Giorgio Baj
M57 Observatory (K38), Saltrio, ITALY

Matteo Lombardo
Zen Observatory (M26), Scandicci, ITALY

Pietro Aceti, Massimo Banfi
Seveso Observatory (C24), Seveso, ITALY

Luciano Tinelli
GAV (Gruppo Astrofili Villasanta), Villasanta, ITALY


(Received: 2023 April 12)

Photometric observations of eight asteroids were made to acquire lightcurves for shape/spin axis modeling. Synodic period and lightcurve amplitude were found for 111 Ate, 197 Arete, 261 Prymno, 325 Heidelberga, 359 Georgia, 737 Arequipa, 1523 Pieksamaki, and 2023 BU. Color indices were measured for 111 Ate, 197 Arete, 261 Prymno, and 737 Arequipa. H-G parameters were found for 197 Arete, 261 Prymno, and 359 Georgia.

Collaborative asteroid photometry was done inside the Italian Amateur Astronomers Union (UAI; 2023) group. The targets were selected mainly in order to acquire lightcurves for shape/spin axis modeling. Table I shows the observing circumstances and results.

The CCD observations of eight asteroids were made in 2023 January-March using the instrumentation described in the Table II. Lightcurve analysis was performed at the Balzaretto Observatory with *MPO Canopus* (Warner, 2021). All the images were calibrated with dark and flat frames and converted to standard magnitudes using solar colored field stars from custom versions of the CMC15 and ATLAS catalogues distributed with *MPO Canopus*. For brevity, the following citations to the asteroid lightcurve database (LCDB; Warner et al., 2009) will be summarized only as "LCDB".

For H-G plots, the R band magnitudes were converted to V band adding the color index (V-R) and evaluating the half peak-to-peak magnitude using a Fourier model of the same order of the lightcurve plot (Buchheim, 2010).

111 Ate is a Ch-type (Bus and Binzel, 2002) middle main-belt asteroid. Collaborative observations were made over six nights. The period analysis shows a synodic period of $P = 22.080 \pm 0.005$ h with an amplitude $A = 0.11 \pm 0.02$ mag. The period is close to the previously published results in the LCDB. Multiband photometry was made by M. Iozzi (L63) on 2023 March 15. We found B-V = 0.66 ± 0.02 and V-R = 0.36 ± 0.02, which are consistent with a C-type asteroid (Shevchenko and Lupishko, 1998).

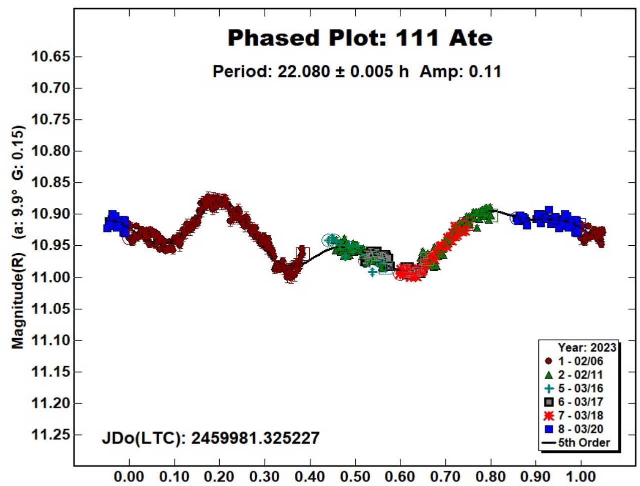


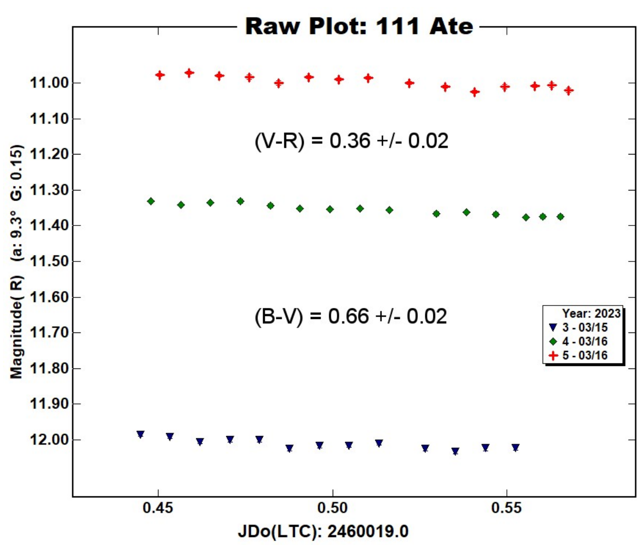

197 Arete is a S-type (Bus and Binzel, 2002) middle main-belt asteroid. Collaborative observations were made over four nights. The period analysis shows a synodic period of $P = 6.640 \pm 0.001$ h with an amplitude $A = 0.11 \pm 0.02$ mag. The period is close to the previously published results in the LCDB. Multiband photometry was done by M. Iozzi (L63) on 2023 February 14. We found the B-V = 0.80 ± 0.07 and V-R = 0.47 ± 0.04. These are close to an S-type asteroid (Shevchenko and Lupishko, 1998). We also found H-G parameters of $H = 9.44 \pm 0.06$ and $G = 0.19 \pm 0.11$.

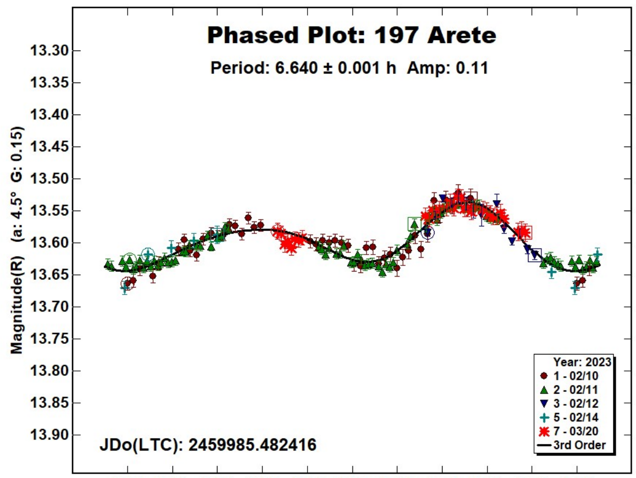


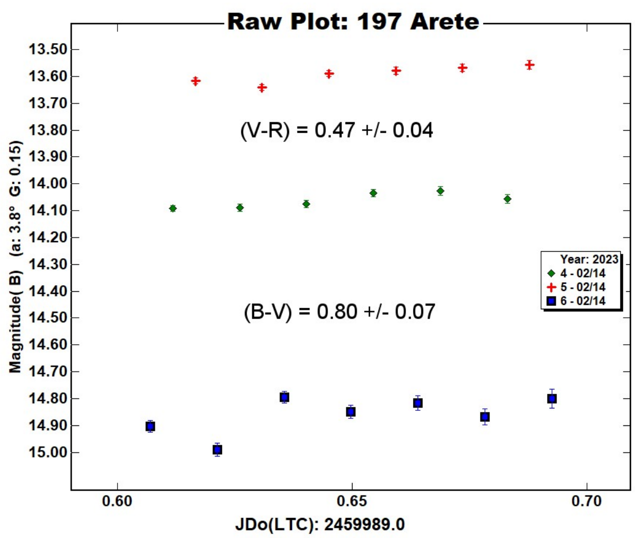


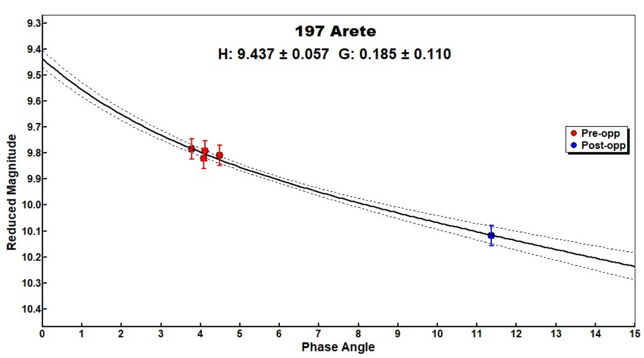


261 Prymno is an X-type (Bus and Binzel, 2002) inner main-belt asteroid. Collaborative observations were made over nine nights. The lightcurve analysis shows a synodic period of $P = 8.0016 \pm 0.0004$ h with an amplitude $A = 0.13 \pm 0.05$ mag. The period is close to the previously published results in the LCDB. Multiband photometry was done by P. Fini and G. Betti (L73) on 2023 January 29. We found V-R = 0.43 ± 0.04, which is close to an M-type asteroid (Shevchenko and Lupishko, 1998). For the H-G parameters we found $H = 9.42 \pm 0.03$ and $G = 0.12 \pm 0.05$.

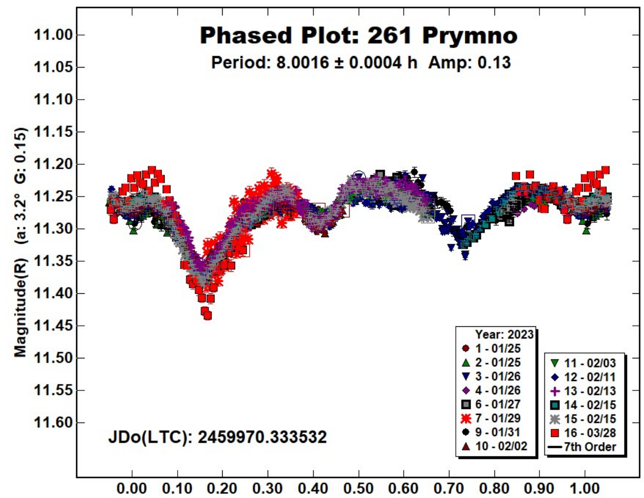


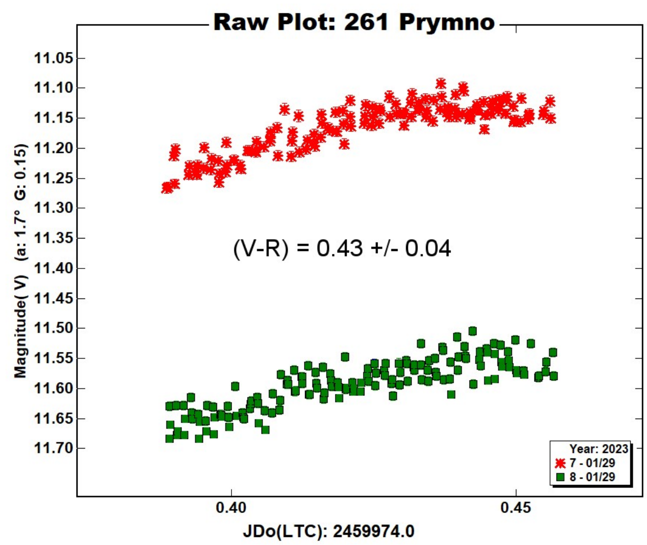


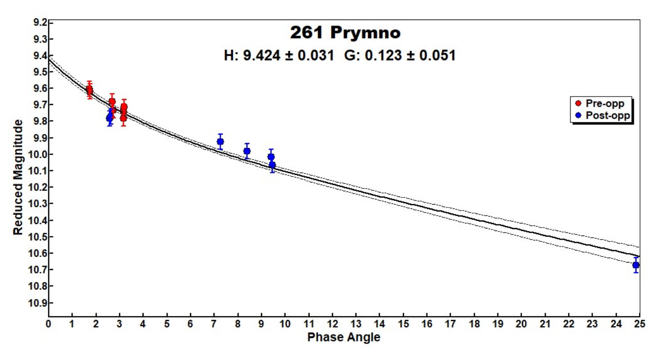

325 Heidelberga is an M-type (Tholen, 1984) outer main-belt asteroid. Observations were made over three nights by A. Marchini (K54). We found a synodic period of $P = 6.736 \pm 0.004$ h with an amplitude $A = 0.11 \pm 0.02$ mag. The period is close to the previously published results in the LCDB.

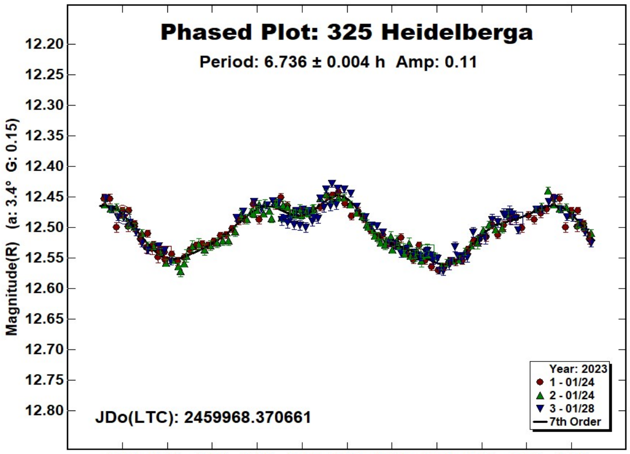


359 Georgia is an X-type (Bus and Binzel, 2002) middle main-belt asteroid. Collaborative observations were made over ten nights. Analysis shows $P = 5.5332 \pm 0.0004$ h and $A = 0.19 \pm 0.03$ mag. The period is close to the previously published results in the LCDB. Not having the color index, we assumed V-R = 0.42, which is typical for M-type asteroids (Shevchenko and Lupishko, 1998). This leads $H = 9.33 \pm 0.05$ and $G = 0.16 \pm 0.07$.

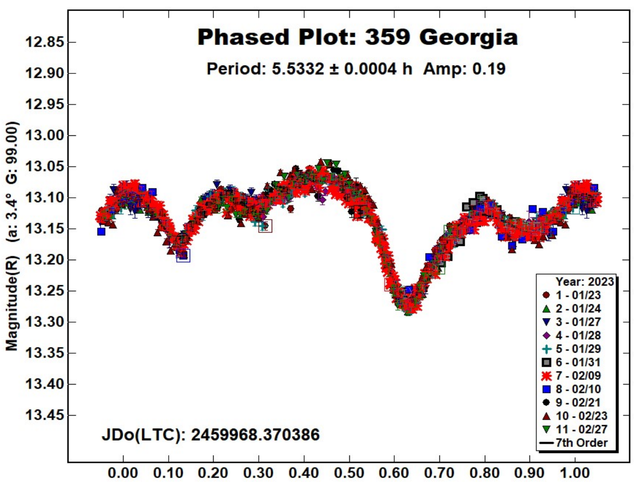


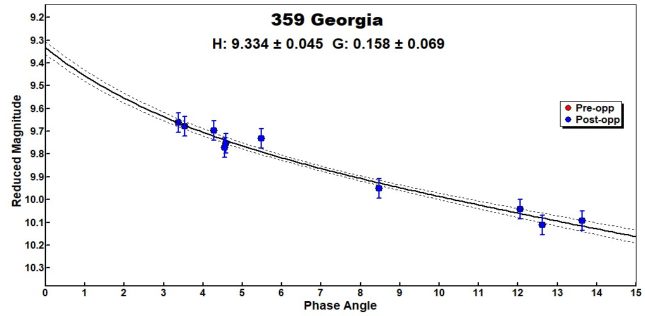


737 Arequipa is an S-type (Bus and Binzel, 2002) middle main-belt asteroid. Collaborative observations were made over six nights. We found a synodic period of $P = 7.024 \pm 0.001$ h and amplitude $A = 0.10 \pm 0.02$ mag. The period is close to the previous results in the LCDB. Multiband photometry was done by P. Bacci and M. Maestripieri (104) on 2023 March 28. We found color indices of B-V = 0.88 ± 0.04 and V-R = 0.51 ± 0.04; these are a good match to an S-type asteroid (Shevchenko and Lupishko, 1998).

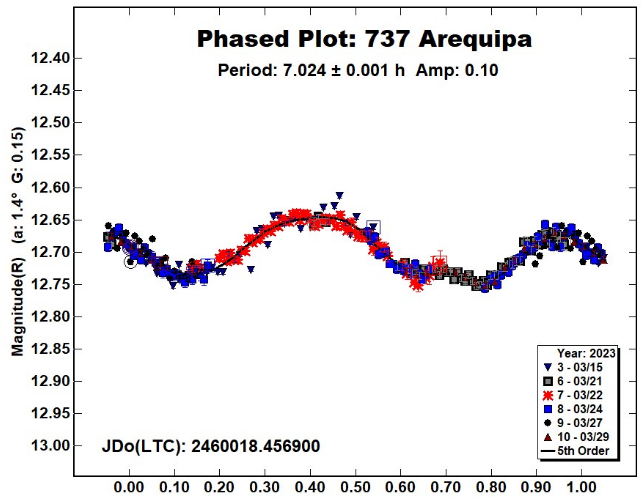


| Number | Name | 2023 mm/dd | Phase | $L_{PAB}$ | $B_{PAB}$ | Period(h) | P.E. | Amp | A.E. | Grp |
|---|---|---|---|---|---|---|---|---|---|---|
| 111 | Ate | 02/06-03/20 | *9.4, 11.4 | 156 | -3 | 22.080 | 0.005 | 0.11 | 0.02 | MB-M |
| 197 | Arete | 02/10-03/20 | *4.3, 11.3 | 148 | 10 | 6.640 | 0.001 | 0.11 | 0.02 | MB-M |
| 261 | Prymno | 01/25-03/28 | *3.2, 24.8 | 132 | 3 | 8.0016 | 0.0004 | 0.13 | 0.05 | MB-I |
| 325 | Heidelberga | 01/23-01/28 | 3.3, 4.5 | 120 | 7 | 6.736 | 0.004 | 0.11 | 0.02 | MB-O |
| 359 | Georgia | 01/23-02/27 | 3.3, 13.6 | 120 | 7 | 5.5332 | 0.0004 | 0.19 | 0.03 | MB-M |
| 737 | Arequipa | 03/14-03/28 | *1.4, 4.5 | 176 | -2 | 7.024 | 0.001 | 0.10 | 0.02 | MB-M |
| 1523 | Pieksamaki | 02/17-03/15 | *1.6, 13.6 | 152 | -1 | 5.3210 | 0.0005 | 0.45 | 0.04 | MB-I |
| | 2023 BU | 01/25-01/26 | 25.0, 22.7 | 128 | 12 | 0.021605 | 0.000005 | 0.81 | 0.35 | NEA |

Table I. Observing circumstances and results. The first line gives the results for the primary of a binary system. The second line gives the orbital period of the satellite and the maximum attenuation. The phase angle is given for the first and last date. If preceded by an asterisk, the phase angle reached an extrema during the period. $L_{PAB}$ and $B_{PAB}$ are the approximate phase angle bisector longitude/latitude at mid-date range (see Harris et al., 1984). Grp is the asteroid family/group (Warner et al., 2009).

| Observatory (MPC code) | Telescope | CCD | Filter | Asteroids Sessions |
|---|---|---|---|---|
| Astronomical Observatory University of Siena (K54) | 0.30-m MCT f/5.6 | SBIG STL-6303e (2x2) | Rc | 111(2) 197(1) 261(2) 325(3) 359(3) 737(3) |
| HOB Astronomical Observatory (L63) | 0.20-m SCT f/6.0 | ATIK 383L+ | BVRcC | 111(4) 197(2) |
| Iota Scorpii (K78) | 0.40-m RCT f/8.0 | SBIG STXL-6303e (2x2) | Rc | 197(2) 359(1) 1523(2) |
| GiaGa Observatory (203) | 0.36-m SCT f/5.8 | MORAVIAN G2-3200 | Rc | 261(1) 359(1) 1523(2) |
| Blessed Hermann Obs. (L73) | 0.30-m SCT f/6.0 | QHY 174MGPS (2x2) | VRc | 261(4) 359(1) |
| Osservatorio Serafino Zani (130) | 0.40-m RCT f/5.8 | SBIG ST8 XME (2x2) | C | 261(2) 359(1) |
| GAMP (104) | 0.60-m NRT f/4.0 | Apogee Alta | BVRcC | 737(1) 2023 BU(2) |
| Osservatorio Astronomico Nastro Verde (C82) | 0.35-m SCT f/6.3 | SBIG ST10XME (2x2) | C | 359(3) |
| Hypatia Observatory (L62) | 0.25-m RCT f/5.3 | Moravian C2-7000A | Rc | 261(3) |
| M57 (K38) | 0.35-m RCT f/5.5 | SBIG STT1603ME | Rc | 261(1) |
| Zen Observatory (M26) | 0.30-m RCT f/8.0 | SXV-H9C (2x2) | Rc | 359(1) |
| Seveso Observatory (C24) | 0.30-m SCT f/10.0 | Moravian KAF 8300 (3x3) | Rc | 737(1) |
| GAV (Gruppo Astrofili Villasanta) | 0.20-m SCT f/7.0 | SXV-H9 | Rc | 737(1) |

Table II. Observing Instrumentations. MCT: Maksutov-Cassegrain, NRT: Newtonian Reflector, RCT: Ritchey-Chretien, SCT: Schmidt-Cassegrain. The numbers in parentheses in the CCD column are the binning sizes. The Asteroids/Sessions column gives the number or designation of the asteroid(s) observed at the station while the number in parentheses immediately after is the number of observing sessions for that object.

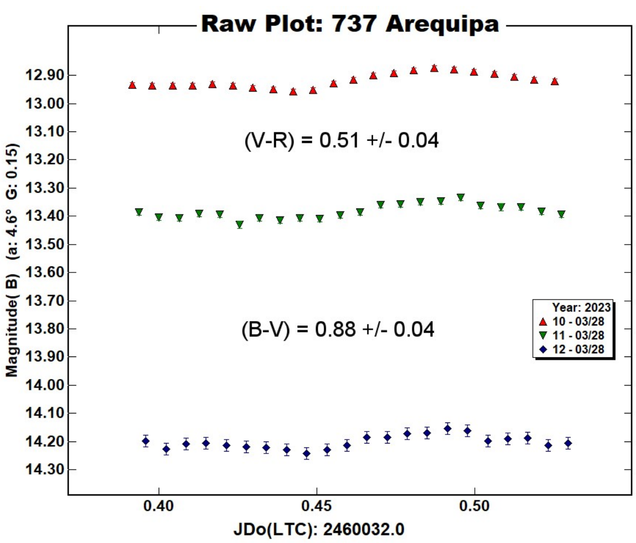


1523 Pieksamaki is a medium-albedo middle main-belt asteroid. Collaborative observations were made over three nights. We found a synodic period of $P$ = 5.3210 ± 0.0005 h and amplitude $A$ = 0.45 ± 0.04 mag. The period is close to the previously published results in the LCDB.

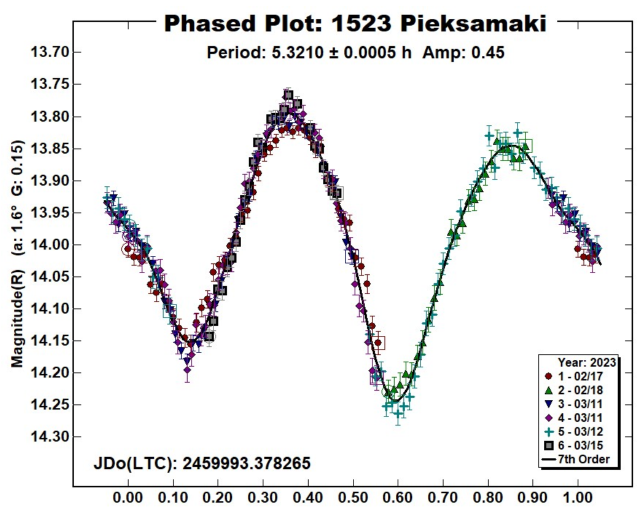


2023 BU is an Apollo Near-Earth asteroid. Observations were made over two nights by P. Bacci and M. Maestripieri (104) near the time of the asteroid's closest approach to the Earth. We found a bimodal solution with a synodic period of $P$ = 0.021605 ± 0.000005 h and an amplitude $A$ = 0.81± 0.35 mag. No previously reported periods were found in the LCDB.

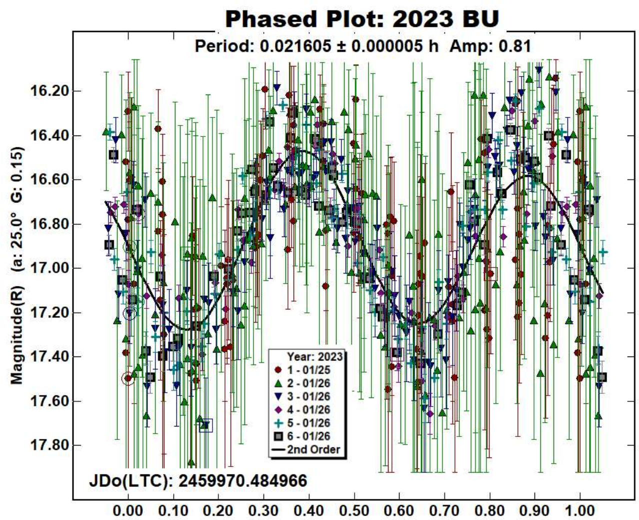


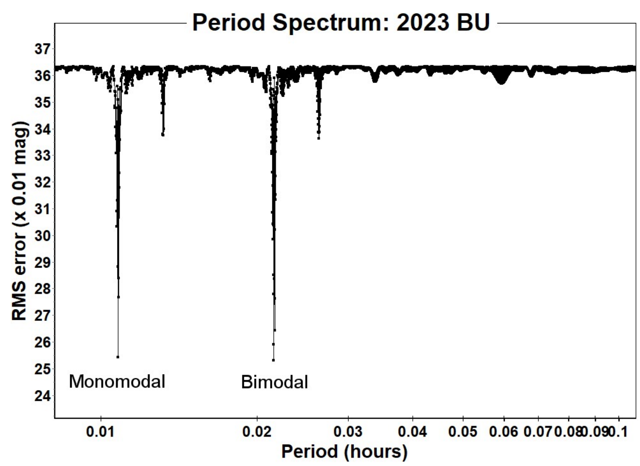



References

Buchheim, R.K. (2010). "Methods and Lessons Learned Determining the H-G Parameters of Asteroid Phase Curves." *Society for Astronomical Sciences Annual Symposium* **29**, 101-115.

Bus, S.J.; Binzel, R.P. (2002). "Phase II of the Small Main-Belt Asteroid Spectroscopic Survey - A Feature-Based Taxonomy." *Icarus* **158**, 146-177.

Harris, A.W.; Young, J.W.; Scaltriti, F.; Zappala, V. (1984). "Lightcurves and phase relations of the asteroids 82 Alkmene and 444 Gyptis." *Icarus* **57**, 251-258.

Shevchenko, V.G.; Lupishko, D.F. (1998). "Optical properties of Asteroids from Photometric Data." *Solar System Research* **32**, 220-232.

Tholen, D.J. (1984). "Asteroid taxonomy from cluster analysis of Photometry." Doctoral Thesis. University Arizona, Tucson.

UAI (2023). "Unione Astrofili Italiani" web site. *https://www.uai.it*

Warner, B.D.; Harris, A.W.; Pravec, P. (2009) "The asteroid lightcurve database." *Icarus* **202**, 134-146. Updated 2023 April 9 *https://minplanobs.org/alcdef/index.php*

Warner, B.D. (2021). MPO Software, MPO Canopus v10.8.5.0. Bdw Publishing. *http://minorplanetobserver.co*


## ROTATIONAL PERIOD AND LIGHTCURVE DETERMINATION FOR FIVE MINOR PLANETS


Mike Wiles
NAC Observatory (MPC U98)
4126 N. Twilight Cir.
Mesa, AZ 85207
mikewilesaz@gmail.com


(Received: 2023 March 3)

Photometric measurements of CMOS observations for five main-belt asteroids were made from 2022 December through 2023 February. Phased lightcurves were created for each one. Three of the asteroids have no prior published period solutions. All the data have been submitted to the ALCDEF database.

CMOS observations of five main-belt asteroids were performed at NAC Observatory (MPC U98) in Benson, AZ. Images were taken using a 0.35m *f*/7.2 Corrected Dall-Kirkham telescope, Moravian C5A-100M CMOS camera featuring a Sony IMX-461 sensor. Images were captured at a scale of 1.21"/pixel after binning 4×4. Table I shows observing circumstances and results. All images for these observations were obtained between 2022 December and 2023 February.

Data reduction and period analysis were done using *Tycho* (Parrott, 2023). The CMOS sensor provides a 58'×44' field of view, enabling the use of the same field center for three to four consecutive nights. The asteroid and five or more comparison stars were measured. Comparison stars were selected with colors within the range of 0.5 < B-V < 0.95 to correspond with color ranges of asteroids.

Comparison star magnitudes were obtained from the ATLAS catalog (Tonry et al., 2018), which is incorporated directly into *Tycho*. A 10-pixel (12.2 arcsec) diameter measuring aperture was used for asteroids and comp stars. Interference from field stars resulted in the exclusion of affected observations. Period determination was done using *Tycho*.

Asteroids were selected from the CALL website (Warner, 2011), either for having uncertain periods or no reported period at all. In this set of observations, three of the five asteroids had no previous period analysis and two had U = 1 (likely wrong). The Asteroid Lightcurve Database (LCDB; Warner et al., 2009) was consulted to locate previously published results. All new data for these asteroids have been submitted to the ALCDEF database.

1478 Vihuri was discovered in 1938 by Vaisala at Turku. A period solution published by Binzel (1987) of 19.5 hours is the only listed value in the LCDB. A total of 203 observations were made over the course of eight nights in 2023 January. These data were used to calculate a period of 19.742 h ± 0.002 h, longer than Binzel's period solution by 0.242 hours. The amplitude of the lightcurve is 0.13 ± 0.02 mag.

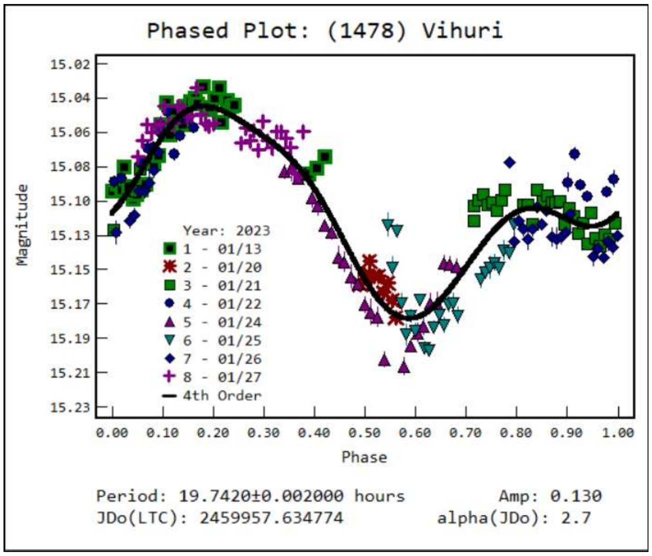


5520 Natori is an Eos family asteroid discovered at Oohira in 1990 by T. Urata. Pál et al. (2020) published a period of 3.58549 ± 0.00005 h. During a two-night interval, 232 images were obtained. Photometric measurements yield a rotation period of 3.587 ± 0.001 h, which agrees with Pal's period. The amplitude is 0.26 mag and the RMS error on the fit is 0.018 mag.

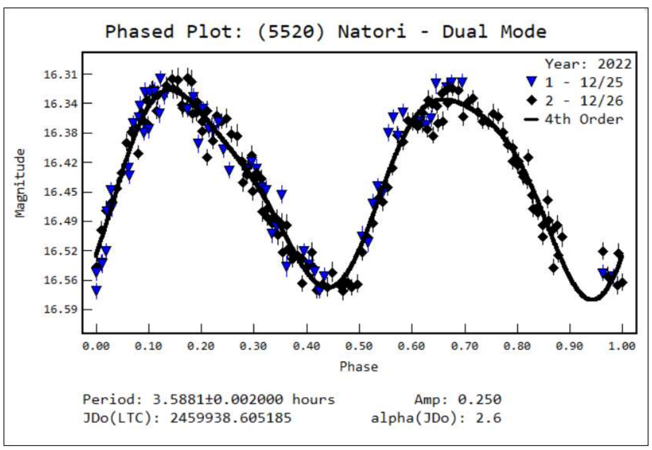


The periodogram indicates that a single mode rotational period of 1.795 ± 0.002 h, being half of the bimodal period, gives an equally good match. A split-halves plot of the shorter period shows distinct separation of multiple segments of the curve in each half, so the bimodal solution is preferred.

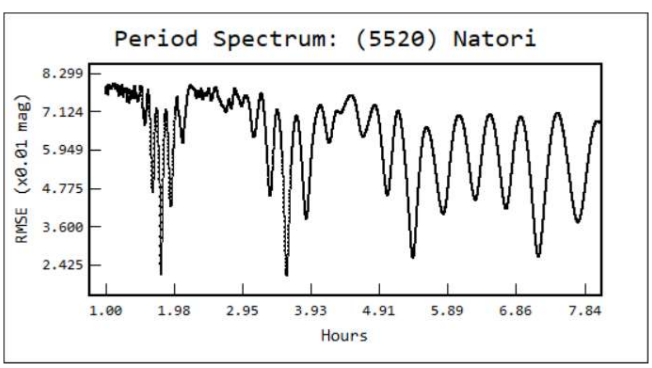


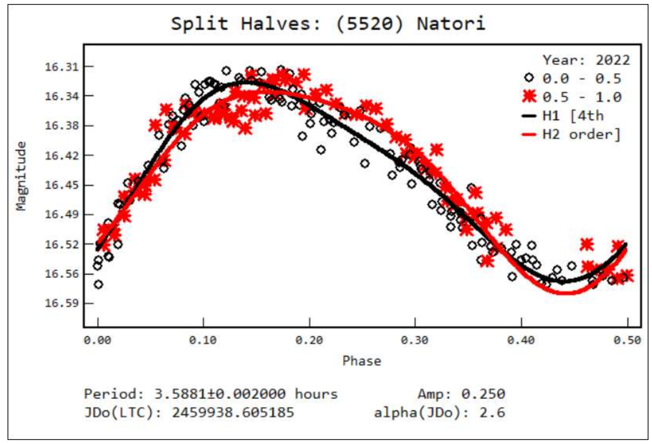


6268 Versailles is a Euterpe-family asteroid without a published period solution in the LCDB. It was discovered in 1990 by E.W. Elst at La Silla. A total of 317 observations were made over four nights in 2023 January to create an initial lightcurve. Due to interference from field stars, 62 of those observations were excluded from the final dataset. A period of 3.1304 h ± 0.001 h was calculated with the data. The amplitude is 0.17 ± 0.03 mag.

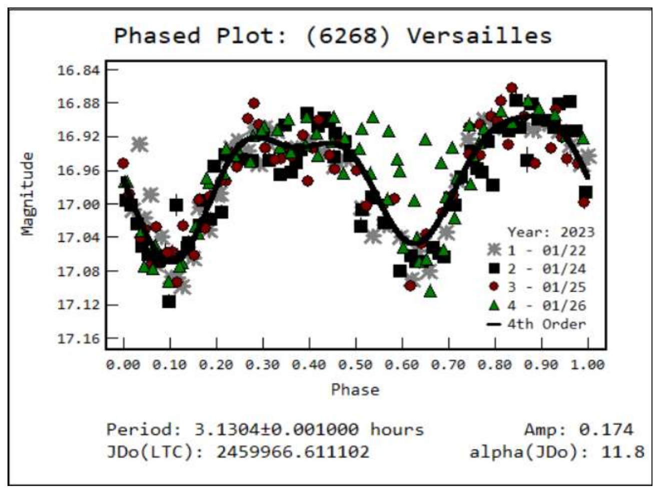


6363 Doggett is an inner main-belt asteroid discovered by E. Bowell at Flagstaff in 1981. No periods are shown in the LCDB. During two nights, 304 images were gathered, leading to a period solution of 4.298 ± 0.001 h with an amplitude of 0.25 ± 0.02 mag.

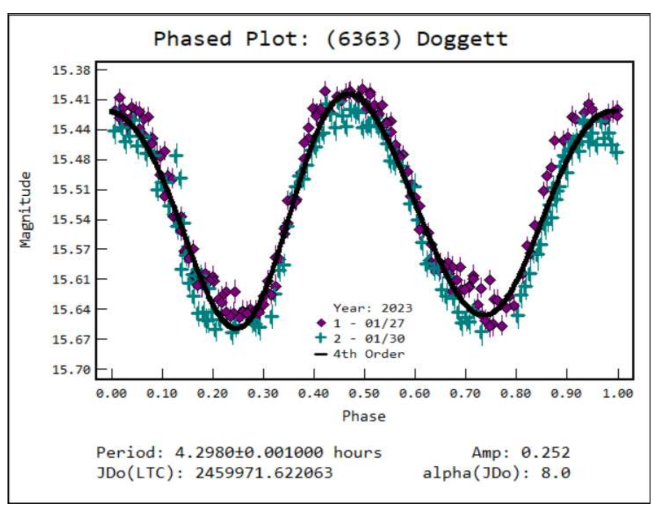

| Number | Name | yyyy mm/dd | Phase | $L_{PAB}$ | $B_{PAB}$ | Period(h) | P.E. | Amp | A.E. | Grp |
|---|---|---|---|---|---|---|---|---|---|---|
| 1478 | Vihuri | 2023 01/13-01/27 | 2.7,7.7 | 113 | 4 | 19.742 | 0.002 | 0.13 | 0.01 | MB-I |
| 5520 | Natori | 2022 12/25-12/26 | 2.6,2.9 | 88 | 4 | 3.588 | 0.002 | 0.25 | 0.02 | EOS |
| 6268 | Versailles | 2023 01/22-01/26 | 11.8,14.0 | 104 | 1 | 3.130 | 0.001 | 0.17 | 0.03 | 410 |
| 6363 | Doggett | 2023 01/27-01/30 | 8.0,9.4 | 117 | 8 | 4.298 | 0.001 | 0.25 | 0.02 | MB-I |
| 6550 | Parler | 2023 01/22-01/25 | 9.8,11.3 | 109 | 8 | 4.221 | 0.002 | 0.18 | 0.02 | MB-I |

Table I. Observing circumstances and results. The phase angle is given for the first and last date. If preceded by an asterisk, the phase angle reached an extrema during the period. $L_{PAB}$ and $B_{PAB}$ are the approximate phase angle bisector longitude/latitude at mid-date range (see Harris et al., 1984). Grp is the asteroid family/group (Warner et al., 2009).

6550 Parler is an inner main-belt asteroid discovered by A. Mrkos in the Czech Republic in 1988. No period solutions appear in the LCDB. Over a period of three nights a total of 199 images were obtained and used to calculate a rotational period of 4.221 ± 0.002 h and amplitude of 0.19 ± 0.02 mag.

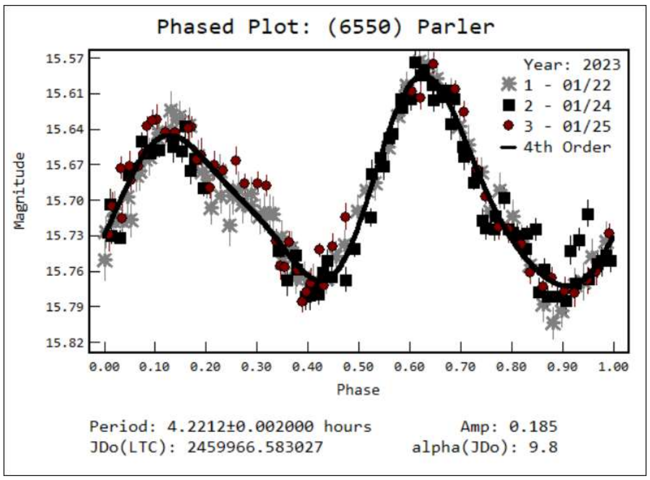


Acknowledgements

The author would like to thank Tom Polakis for his many years of encouragement and mentorship. Thanks also go out to Daniel Parrott for his responsive support of questions regarding the *Tycho* software package.

References

Binzel, R.P. (1987). "A photoelectric survey of 130 asteroids." *Icarus*. **72**, 135-208.

Harris, A.W.; Young, J.W.; Scaltriti, F.; Zappala, V. (1984). "Lightcurves and phase relations of the asteroids 82 Alkmene and 444 Gyptis." *Icarus* **57**, 251-258.

Pál, A.; Szakáts, R.; Kiss, C.; Bódi, A.; Bognár, Z.; Kalup, C.; Kiss, L.L.; Marton, G.; Molnár, L.; Plachy, E.; Sárneczky, K.; Szabó, G.M.; Szabó, R. (2020). "Solar System Objects Observed with TESS - First Data Release: Bright Main-belt and Trojan Asteroids from the Southern Survey." *Ap. J.* **247**, A26.

Parrot, D. (2023). Tycho software. *https://www.tycho-tracker.com*

Tonry, J.L.; Denneau, L.; Flewelling, H.; Heinze, A.N.; Onken, C.A.; Smartt, S.J.; Stalder, B.; Weiland, H.J.; Wolf, C. (2018). "The ATLAS All-Sky Stellar Reference Catalog." *Astrophys. J.* **867**, A105.

Warner, B.D.; Harris, A.W.; Pravec, P. (2009). "The Asteroid Lightcurve Database." *Icarus* **202**, 134-146. Updated 2023 April. *http://www.minorplanet.info/lightcurvedatabase.html*

Warner, B.D. (2011). Collaborative Asteroid Lightcurve Link website. *http://www.minorplanet.info/call.html*

# ASTEROID PHOTOMETRY AND LIGHTCURVE ANALYSIS FOR EIGHT ASTEROIDS

Milagros Colazo
Instituto de Astronomía Teórica y Experimental
(IATE-CONICET) ARGENTINA

Facultad de Matemática, Astronomía y Física
Universidad Nacional de Córdoba, ARGENTINA

Grupo de Observadores de Rotaciones de Asteroides (GORA)
ARGENTINA
*https://aoacm.com.ar/gora/index.php*
milirita.colazovinovo@gmail.com

César Fornari, Giuseppe Ciancia, Damián Scotta, Mario Morales, Raúl Melia, Aldo Wilberger, Néstor Suárez, Bruno Monteleone, Alberto García, Marcos Anzola, Francisco Santos, Aldo Mottino, Carlos Colazo
Grupo de Observadores de Rotaciones de Asteroides (GORA), ARGENTINA

Observatorio Astronómico Giordano Bruno (MPC G05)
Piconcillo (Córdoba-ESPAÑA)

Observatorio Astronómico El Gato Gris (MPC I19) – Tanti
(Córdoba-ARGENTINA)

Observatorio de Sencelles (MPC K14) - Sencelles
(Mallorca-Islas Baleares-ESPAÑA)

Osservatorio Astronomico "La Macchina del Tempo" (MPC M24)
Ardore Marina (Reggio Calabria-ITALIA)

Observatorio Los Cabezones (MPC X12) - Santa Rosa
(La Pampa-ARGENTINA)

Observatorio Galileo Galilei (MPC X31) - Oro Verde
(Entre Ríos-ARGENTINA)

Observatorio Antares (MPC X39) – Pilar
(Buenos Aires-ARGENTINA)

Observatorio Río Cofio (MPC Z03) - Robledo de Chavela
(Madrid- ESPAÑA)

Specola "Giuseppe Pustorino 3" (GORA GC3) - Palizzi Marina
(Reggio Calabria-ITALIA)

Observatorio de Damián Scotta 1 (GORA ODS) - San Carlos Centro (Santa Fe-ARGENTINA)

Observatorio de Damián Scotta 2 (GORA OD2) - San Carlos Centro (Santa Fe-ARGENTINA)

Observatorio Astronómico Vuelta por el Universo (GORA OMA)
Córdoba (Córdoba-ARGENTINA)

Observatorio de Raúl Melia Carlos Paz (GORA RMG)
Carlos Paz (Córdoba-ARGENTINA)

(Received: 2023 March 20)

Synodic rotation periods and amplitudes are reported for 244 Sita, 329 Svea, 421 Zahringia, 904 Rockefellia, 2479 Sodankyla, 4373 Crespo, (143947) 2003 YQ117, and 2015 RN35.

The periods and amplitudes of asteroid lightcurves presented here are the product of collaborative work by GORA (Grupo de Observadores de Rotaciones de Asteroides). In all the studies, we have applied relative photometry assigning V magnitudes to the calibration stars.

Image acquisition was performed without filters and with exposure times of a few minutes. All images used were corrected using dark frames and, in some cases, bias and flat-fields were also used. Photometry measurements were performed using *FotoDif* software We employed *Períodos* software (Mazzone, 2012) for analysis.

Below, we present the results for each asteroid under study. The lightcurve figures contain the following information: the estimated period and period error and the estimated amplitude and amplitude error. In the reference boxes, the columns represent, respectively, the marker, observatory MPC code, or - failing that - the GORA internal code, session date, session offset, and several data points.

Targets were selected based on the following criteria: 1) those asteroids with magnitudes accessible to the equipment of all participants, 2) those with favorable observation conditions from Argentina or Spain and Italy, i.e., with negative or positive declinations δ, respectively, and 3) objects with few periods reported in the literature and/or with Asteroid Lightcurve Database (LCDB; Warner et al., 2009) quality codes U < 3.

244 Sita was discovered in 1844 by J. Palisa. The most recent period published in the literature is $P$ = 129.06 ± 0.02 h with $A$ = 0.80 ± 0.05 mag (Vander Haagen, 2010). In this work, we provide similar results and propose $P$ = 130.218 ± 0.015 h and $A$ = 1.04 ± 0.02 mag.

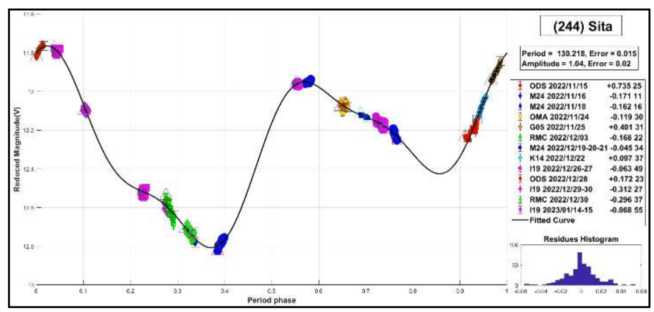


329 Svea is a C-type asteroid discovered in 1892 by M. Wolf. Several periods have been reported for this asteroid: $P$ = 15 h (Weidenschilling et al., 1990), $P$ = 15.201 ± 0.005 h (Pray, 2006), $P$ = 22.6 ± 0.01 h (Menke et al., 2008), and $P$ = 22.778 ± 0.006 h (Marciniak et al., 2015). We have determined a period of 22.778 ± 0.010 h with $A$ = 0.11 ± 0.01 mag. This is consistent with the one proposed by Marciniak et al.

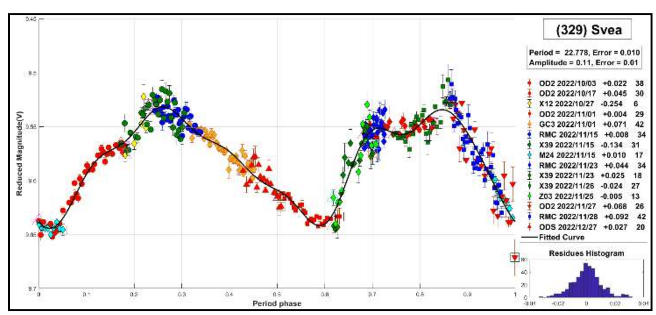

421 Zahringia is an S-type asteroid discovered in 1896 by M. Wolf. Several periods were previously measured for this asteroid: $P$ = 15.5 h ± 0.1 h (Robinson, 2002), $P$ = 17.49 ± 0.02 h (Behrend, 2005web), $P$ = 6.42 ± 0.01 h (Warner, 2010), and $P$ = 25.4891 ± 0.0376 h (Waszczak et al., 2015). The results we obtained, $P$ = 24.983 ± 0.015 h with $A$ = 0.19 ± 0.02 mag, are consistent with the longer period proposed by Waszczak et al.

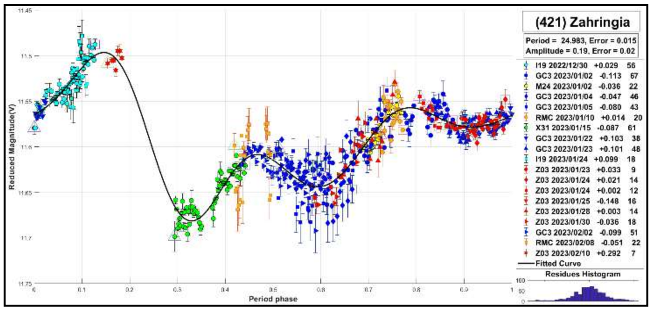


904 Rockefellia was discovered in 1918 by M. Wolf. We found in the literature three rather different periods for this object: $P$ = 4.93 h (CALL, 2011web), $P$ = 5.82 ± 0.01 h (Fauvaud and Fauvaud, 2013), and $P$ = 12.72 ± 0.05 h (Behrend, 2014web). Our analysis suggests a period that is consistent with the one proposed by Fauvaud and Fauvaud, i.e., $P$ = 6.823 ± 0.018 h and $A$ = 0.11 ± 0.03 mag.

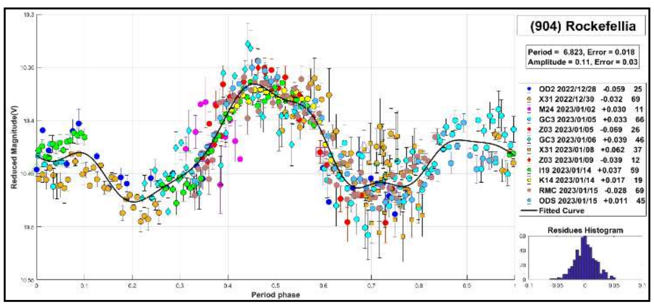


2479 Sodankyla was discovered in 1942 by Y. Vaisala. We couldn't find published periods in the literature for the asteroid. In this work, we propose a long-term period of $P$ = 26.546 ± 0.026 h with $A$ = 0.24 ± 0.04 mag.

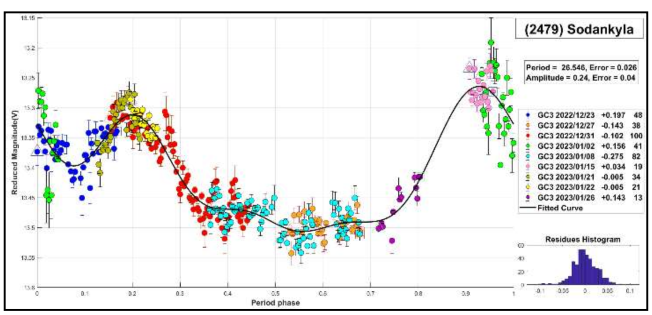


4373 Crespo was discovered in 1985 by E. Bowell. Interestingly, we couldn't find a reported period for this object in the literature. According to a thorough analysis of our observations, we propose a period of $P$ = 16.185 ± 0.022 h and $A$ = 0.14 ± 0.03 mag.

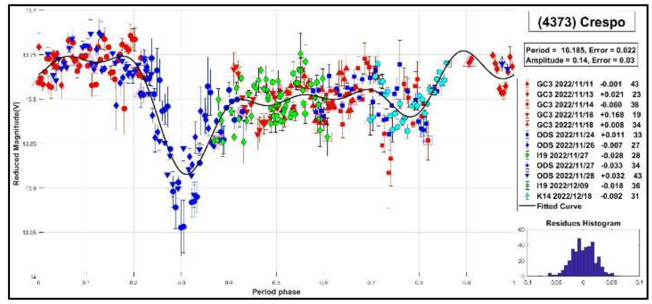


(143947) 2003 YQ117 was discovered in 2003 by NEAT. It is a poorly studied object. Here we propose a tentative period of $P$ = 36.477 ± 0.026 h with $A$ = 0.85 ± 0.04 mag.

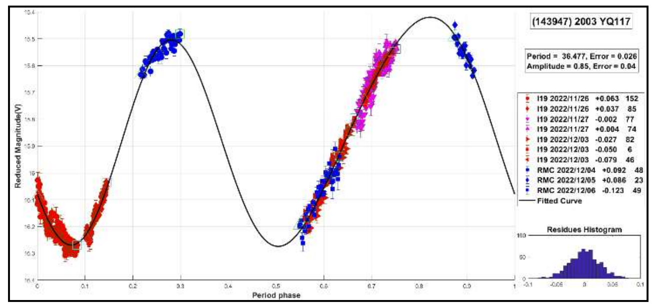


2015 RN35. This hazardous asteroid was discovered in 2015 by Pan-STARRS. A great number of probable encounters of asteroid 2015 RN35 with the Earth have been predicted (Petrov et al., 2018; Sokolov et al., 2020). We couldn't find a reported period for this object in the literature. In this paper, we present full lightcurve coverage with observations made by overlapping different nights and telescopes, thus giving confidence to our result. We measured a period of 0.478 ± 0.008 h with $A$ = 0.74 ± 0.11 mag.

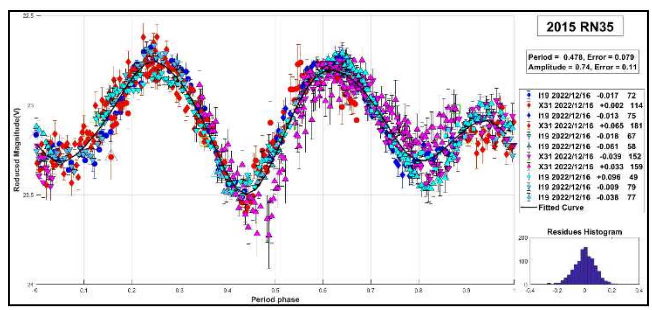


Acknowledgements

We want to thank Julio Castellano as we use his *FotoDif* program for preliminary analyses, Fernando Mazzone for his *Períodos* program, used in final analyses, and Matías Martini for his *CalculadorMDE v0.2* used for generating ephemerides used in the planning stage of the observations. This research has made use of the Small Bodies Data Ferret (*http://sbn.psi.edu/ferret/*), supported by the NASA Planetary System. This research has made use of data and/or services provided by the International Astronomical Union's Minor Planet Center.

| Number | Name | 20yy/ mm/dd- yy/ mm/dd | Phase | $L_{PAB}$ | $B_{PAB}$ | Period(h) | P.E. | Amp | A.E. | Grp |
|---|---|---|---|---|---|---|---|---|---|---|
| 244 | Sita | 22/11/15-23/01/15 | *5.6,24.7 | 62 | -2 | 130.218 | 0.015 | 1.04 | 0.02 | MB-I |
| 329 | Svea | 22/10/03-22/12/27 | 2.0,22.8 | 10 | -7 | 22.778 | 0.010 | 0.11 | 0.01 | 416 |
| 421 | Zahringia | 22/12/30-23/02/11 | *15.0,9.1 | 125 | -10 | 24.983 | 0.015 | 0.19 | 0.02 | MB-I |
| 904 | Rockefellia | 22/12/28-23/01/15 | 9.5,14.2 | 82 | -18 | 6.823 | 0.018 | 0.11 | 0.03 | MB-O |
| 2479 | Sodankyla | 22/12/23-23/01/26 | 7.4,23.6 | 82 | 3 | 26.546 | 0.026 | 0.24 | 0.04 | MB-I |
| 4373 | Crespo | 22/11/11-22/12/18 | *5.5,20.3 | 52 | -7 | 16.185 | 0.022 | 0.14 | 0.03 | MB-I |
| 143947 | 2003 YQ117 | 22/11/26-22/12/06 | 67.5,50.2 | 70 | -40 | 36.477 | 0.026 | 0.85 | 0.04 | NEA |
| | 2015 RN35 | 22/12/16-22/12/16 | 44.1,38.9 | 83 | -20 | 0.478 | 0.079 | 0.74 | 0.11 | NEA |

Table I. Observing circumstances and results. The phase angle is given for the first and last date. If preceded by an asterisk, the phase angle reached an extremum during the period. $L_{PAB}$ and $B_{PAB}$ are the approximate phase angle bisector longitude/latitude at mid-date range (see Harris et al., 1984). Grp is the asteroid family/group (Warner et al., 2009). 416: 329 Svea, MB-I: main-belt inner, MB-O: main-belt outer.

| MPC | Observatory | Telescope | Camera |
|---|---|---|---|
| G05 | Obs.Astr.Giordano Bruno | SCT (D=203mm; f=6.3) | CCD Atik 420 m |
| I19 | Obs.Astr.El Gato Gris | SCT (D=355mm; f=10.6) | CCD SBIG STF-8300M |
| K14 | Obs.Astr.de Sencelles | Newtonian (D=250mm; f=4.0) | CCD SBIG ST-7XME |
| M24 | Oss.Astr.La Macchina del Tempo | RCT (D250mm; f=8.0) | CMOS ZWO ASI 1600MM |
| X12 | Obs.Astr.Los Cabezones | Newtonian (D=200mm; f=5.0) | CMOS QHY 174M |
| X31 | Obs.Astr.Galileo Galilei | RCT ap (D=405mm; f=8.0) | CCD SBIG STF-8300M |
| X39 | Obs.Astr.Antares | Newtonian (D=250mm; f=4.72) | CCD QHY9 Mono |
| Z03 | Obs.Astr.Río Cofio | SCT (D=254mm; f=6.3) | CCD SBIG ST-8XME |
| GC3 | Specola Giuseppe Pustorino 3 | RCT (D=400mm; f=5.7) | CCD Atik 383L+Mono |
| ODS | Obs.Astr.de Damián Scotta 1 | Newtonian (D=300mm; f=4.0) | CMOS QHY 174M |
| OD2 | Obs.Astr.de Damián Scotta 2 | Newtonian (D=250mm; f=4.0) | CCD SBIG STF-8300M |
| OMA | Obs.Astr.Vuelta por el Universo | Newtonian (D=150mm; f=5.0) | CMOS POA Neptune-M |
| RMC | Obs.Astr.de Raúl Melia Carlos Paz | Newtonian (D=254mm; f=4.7) | CMOS QHY 174M |

Table II. List of observatories and equipment.

References

Behrend, R. (2005web, 2014web). Observatoire de Geneve website. *https://obswww.unige.ch/~behrend/*

Collaborative Asteroid Lightcurve Link (CALL; 2011) *http://www.minorplanetobserver.com/DATA/submissions_results.htm*

Fauvaud, S.; Fauvaud, M. (2013). "Photometry of Minor Planets. I. Rotation Periods from Lightcurve Analysis for Seven Main-belt Asteroids." *Minor Planet Bulletin* **40(4)**, 224-229.

Harris, A.W.; Young, J.W.; Scaltriti, F.; Zappala, V. (1984). "Lightcurves and phase relations of the asteroids 82 Alkmene and 444 Gyptis." *Icarus* **57**, 251-258.

Marciniak, A.; Pilcher, F.; Oszkiewicz, D.; Santana-Ros, T.; Urakawa, S. and 19 colleagues (2015). "Against the biases in spins and shapes of asteroids." *Planetary and Space Science* **118**, 256-266.

Mazzone, F.D. (2012). Períodos software, version 1.0. *http://www.astrosurf.com/salvador/Programas.html*

Menke, J.; Cooney, W.; Gross, J.; Terrell, D.; Higgins, D. (2008). "Asteroid Lightcurve Analysis at Menke Observatory." *Minor Planet Bulletin* **35**, 155-160.

Petrov, N.A.; Vasil'ev, A.A.; Kuteeva, G.A.; Sokolov, L.L. (2018). "On the Trajectories of Asteroid Encounters with the Earth for 2015 RN35 and Apophis." *Solar System Research* **52**, 326-337.

Pray, D.P. (2006). "Lightcurve analysis of asteroids 326, 329, 426, 619, 1829, 1967, 2453, 10518 and 42267." *Minor Planet Bulletin* **33**, 4-5.

Robinson, L.E. (2002). "Photometry of Five Difficult Asteroids: 309 Fraternitas, 366 Vincentina 421 Zahringia, 578 Happelia, 959 Anne." *Minor Planet Bulletin* **29**, 30-31.

Sokolov, L.L.; Balyaev, I.A.; Kuteeva, G.A.; Petrov, N.A.; Eskin, B.B. (2020). "Possible Collisions and Approaches of Some Dangerous Asteroids with the Earth." *Solar System Research* **54**, 541-549.

Vander Haagen, G.A. (2010). "Lightcurve and HG Parameters for Slow Rotator 244 Sita." *Minor Planet Bulletin* **37**, 44-45.

Warner, B.D.; Harris, A.W.; Pravec, P. (2009). "The asteroid lightcurve database." *Icarus* **202**, 134-146.

Warner, B.D. (2010). "Upon Further Review: I. An Examination of Previous Lightcurve Analysis from the Palmer Divide Observatory." *Minor Planet Bulletin* **37**, 127-130.

Waszczak, A.; Chang, C.-K.; Ofek, E.O.; Laher, R.; Masci, F.; Levitan, D.; Surace, J.; Cheng, Y.-C.; Ip, W.-H.; Kinoshita, D.; Helou, G.; Prince, T.A.; Kulkarni, S. (2015). "Asteroid light curves from the Palomar Transient Factory survey: rotation periods and phase functions from sparse photometry." *Astronomical Journal* **150**, 75.

Weidenschilling, S.J.; Chapman, C.R.; Davis, D.R.; Greenberg, R.; Levy, D.H.; Binzel, R.P.; Vail, S.M.; Magee, M.; Spaute, D. (1990). "Photometric geodesy of main-belt asteroids: III. Additional lightcurves." *Icarus* **86**, 402-447.

## ROTATION PERIOD DETERMINATION FOR ASTEROID 2023 DZ2

Nick Sioulas
NOAK Observatory (L02)
Stavraki Ioannina, Greece
nsioulas@hotmail.com

(Received: 2023 April 12)

Photometry of near-Earth asteroid 2023 DZ2 were conducted from the NOAK Observatory, located in Greece, to determine its synodic rotation period. The results are: $P = 0.1046 \pm 0.0035$ h, $A = 0.64$ mag.

All observations were performed at the NOAK Observatory, Ioannina Greece (MPC-International Astronomical Union code L02), using a 0.25m Newtonian Skywatcher optical tube operating at f/4.7. The optical tube is mounted on an NEQ6 Skywatcher robotic mount and equipped with ATIK 460exm CCD camera. It is a high Quantum Efficiency CCD. No filters used for better signal-to-noise. Exposure time for all the images was 5 seconds. The camera was binned at 2×2. The image scale after 2×2 binning was 1.57 arcsec/pixel and the field of view 35.9′× 28.7′. In these fields, the asteroid and five comparison stars were measured for differential photometry.

All images were reduced in the standard manner using nightly flatfield files as well as dark-current and bias images. Photometric measurements and lightcurve analysis were performed using *MPO Canopus* (version 10.8.1.1; Warner, 2019). The *Cartes Du Ciel* was used as the planetarium software with the most recent ephemerides downloaded from MinorPlanetCenter and Artemis Capture was used for image capture.

2023 DZ2 was discovered by the Romanian-Spanish team Para-SOL (MPC 950). It is a near-Earth asteroid with a semi-major axis of 2.155AU, eccentricity 0.539, inclination 0.081deg, and an orbital period of 3.16 years. Its absolute magnitude is $H = 24.235$ (JPL, 2023). The period analysis shows a solution for the rotational period of $P = 0.1046 \pm 0.0035$ h with an amplitude $A = 0.64 \pm 0.03$ mag.

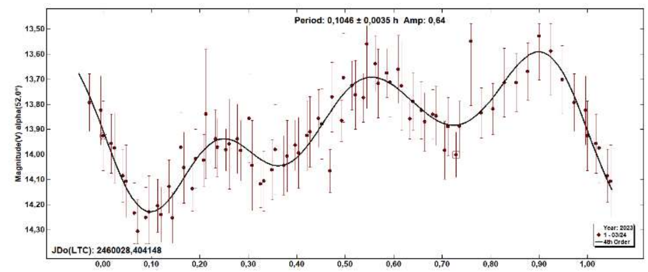


References

Harris, A.W., Young, J.W., Scaltriti, F., Zappala, V. (1984). "Lightcurves and phase relations of the asteroids 82 Alkmene and 444 Gyptis." *Icarus* **57**, 251-258.

JPL (2023). Small Body Database Browser. *https://ssd.jpl.nasa.gov*

Warner, B.D.; Harris, A.W.; Pravec, P. (2009). "The Asteroid Lightcurve Database." *Icarus* **202**, 134-146. Updated 2019 Aug. *http://www.minorplanet.info/lightcurvedatabase.html*

Warner, B.D. (2019). MPO Software, *MPO Canopus* v10.8.1.1. Bdw Publishing. *http://minorplanetobserver.com*

| Number | Name | yyyy mm/dd | Phase | $L_{PAB}$ | $B_{PAB}$ | Period(h) | P.E. | Amp | A.E. | Grp |
|---|---|---|---|---|---|---|---|---|---|---|
| 2023 | DZ2 | 2023 03/26 | 92.8 | 232.4 | -0.7 | 0.1046 | 0.004 | 0.64 | 0.03 | Apollo |

Table I. Observing circumstances and results. The phase angle is given for the first and last date. If preceded by an asterisk, the phase angle reached an extrema during the period. $L_{PAB}$ and $B_{PAB}$ are the approximate phase angle bisector longitude/latitude at mid-date range (see Harris et al., 1984). Grp is the asteroid family/group (Warner et al., 2009).

# GENERAL REPORT OF POSITION OBSERVATIONS BY THE ALPO MINOR PLANETS SECTION FOR THE YEAR 2022

Frederick Pilcher
4438 Organ Mesa Loop
Las Cruces, NM 88011 USA
fpilcher35@gmail.com

(Received: 2023 April 4)

Observations of positions of minor planets by members of the Minor Planets Section in calendar year 2022 are summarized.

During the year 2022 a total of 630 visual and 2 CCD observations of 170 different minor planets were reported by members of the Minor Planets Section.

The summary lists minor planets in numerical order, the observer and telescope aperture (in cm), UT dates of the observations, and the total number of observations in that interval. When a significant departure from the predicted magnitude was noted, it is stated in the next line below the number of positions. The year is 2022 in each case.

Positional observations were contributed by the following observers:

| Observer, Instrument | Location | Planets | Positions |
|---|---|---|---|
| Faure, Gérard | | 19 | 53 |
| 8 cm binoculars | Moliets (France) | | |
| 20 cm Celestron | Vaison la romaine (France) | | |
| 20 cm Celestron Fastar | Moliers | | |
| 35 cm Meade LX200 | Col de L'Arzelier (France) | | |
| 45 cm Dobsonian 450 | Col de L'Arzelier | | |
| 45 cm Stargate D450 | Observatoire des Baronnies Provencales | | |
| 82 cm Hyperion | Observatoire des Baronnies Provencales | | |
| 114 cm Dobsonian | Observatoire des Baronnies Provencales (France) | | |
| Harvey, G. Roger | Concord, North | 149 | 573 |
| 81 cm Newtonian | Carolina, USA | | |
| 35 cm Celestron | | | |
| Pryal, Jim | Ellensburg, WA USA | 1 | 4 |
| 20 cm f/10 SCT | | | |
| Rayon, Jean-Michel | | 2 | 9 (2CCD) |
| 45 cm Dobsonian 450 | Col de L'Arzelier (France) | | |
| 20 cm Vixen RS200SS | Meylan (France) | | |

| MINOR PLANET | OBSERVER & APERTURE (cm) | OBSERVING PERIOD (2022) | | NO. OBS. |
|---|---|---|---|---|
| 3 Juno | Faure, 8 | Sep 21 | | 2 |
| 61 Danae | Harvey, 35 | Jan 27 | | 6 |
| 1111 Reinmuthia | Faure, Rayon, 45 | Jul 26 | | 2 |
| 1184 Gaea | Faure, 45 | Oct 5 | | 2 |
| 1494 Savo | Faure, 35 | Jul 28 | | 3 |
| 1505 Koranna | Faure, 35 | Jul 2 | | 3 |
| 2019 van Albada | Faure, 35 | Jul 28 | | 3 |
| 2234 Schmadel | Harvey, 81 | Sep 22 | 0.4f@16.3 | 3 |
| 2357 Phereclos | Faure, 45 | Jul 26 | | 2 |
| 2552 Remek | Harvey, 81 | Sep 15 | | 3 |
| 2870 Haupt | Faure, 20 | Sep 20 | | 2 |
| 2924 Mitake-Mura | Harvey, 81 | Apr 25 | | 3 |
| 3076 Garber | Harvey, 81 | Aug 3 | | 3 |
| 3230 Vampilov | Harvey, 81 | May 29 | | 3 |
| 3317 Paris | Faure, 35 | Jul 28 | | 2 |
| 3403 Tammy | Faure, 35 | Jul 27 | | 2 |
| 3473 Sapporo | Harvey, 81 | Mar 2 | 0.4f@16.0 | 3 |
| 3596 Meriones | Harvey, 81 | Dec 29 | | 3 |
| 3661 Dolmatovskij | Harvey, 81 | Apr 4 | | 3 |
| 3676 Hahn | Harvey, 81 | Apr 25 | | 3 |
| 3701 Purkyne | Harvey, 81 | Jan 4 | | 3 |
| 3799 Novgorod | Harvey, 81 | Apr 25 | | 3 |
| 3827 Zdenekhorsky | Harvey, 81 | Sep 20 | | 3 |
| 3837 Carr | Harvey, 81 | Mar 1 | | 3 |
| 3920 Aubignan | Faure, 35 | Jul 3 | | 3 |
| 4256 Kagamigawa | Harvey, 81 | Oct 20 | | 3 |
| 4405 Otava | Harvey, 81 | Oct 20 | | 3 |
| 4411 Kochibunkyo | Harvey, 81 | Feb 10 | | 3 |
| 4433 Goldstone | Harvey, 81 | May 29 | | 3 |
| 4479 Charlieparker | Harvey, 81 | Apr 2 | | 6 |
| 4489 Dracius | Harvey, 81 | Oct 27-Nov 18 | | 4 |
| 4514 Vilen | Harvey, 81 | Mar 1 | | 3 |
| 4544 Xanthus | Harvey, 81 | Apr 10 | 0.5f@16.2 | 6 |
| 4672 Takuboku | Harvey, 81 | Apr 24 | | 6 |
| 4768 Hartley | Faure, 35 | Aug 24 | | 2 |
| 4796 Lewis | Harvey, 81 | Sep 22 | | 3 |
| 4841 Manjiro | Harvey, 81 | Jan 30 | | 3 |
| 4858 Vorobjov | Harvey, 81 | Feb 6 | | 3 |
| 5067 Occidental | Harvey, 81 | Apr 23 | | 3 |
| 5246 Migliorini | Faure, 35 | Jul 2 | | 2 |
| 5249 Giza | Harvey, 81 | Feb 20 | | 3 |
| 5261 Eureka | Faure, 35 | Jul 3 | | 4 |
| 5300 Sats | Harvey, 81 | Sep 16 | | 3 |
| 5408 The | Harvey, 81 | Mar 7 | | 3 |
| 5413 Smyslov | Harvey, 81 | Apr 1 | | 3 |
| 5554 Keesey | Harvey, 81 | Oct 19 | | 3 |
| 5693 1993 EA | Harvey, 81 | May 20 | | 6 |
| 5708 Melancholia | Harvey, 81 | Sep 22 | | 3 |
| 5861 Glynjones | Harvey, 81 | Oct 19 | | 3 |
| 5949 1985 RL3 | Harvey, 81 | May 29 | | 3 |
| 6026 Xenophanes | Harvey, 81 | Mar 7 | 0.5b@15.7 | 3 |
| 6036 Weinberg | Harvey, 81 | Sep 19 | | 6 |
| 6107 Osterbrock | Harvey, 81 | Mar 3-7 | | 9 |
| 6109 Balseiro | Harvey, 81 | Sep 15 | | 3 |
| 6183 Viscome | Faure, 35 | Aug 24 | | 3 |
| | Harvey, 81 | Sep 16 | | 3 |
| 6228 Yonezawa | Harvey, 81 | Mar 1 | | 3 |
| 6316 Mendez | Harvey, 81 | Sep 20 | | 3 |
| 6755 Solov'yanenko | Harvey, 81 | Dec 29 | | 3 |
| 6804 Maruseppu | Harvey, 81 | Dec 19 | | 3 |
| 6856 Bethsimmons | Harvey, 81 | Apr 23 | | 6 |
| 6872 1993 CN1 | Harvey, 81 | Mar 2 | | 3 |
| 6906 Johnmills | Harvey, 81 | Nov 29 | | 3 |
| 7004 Markthiemens | Harvey, 81 | Nov 4 | | 3 |
| 7172 Multatuli | Harvey, 81 | Feb 6 | | 3 |
| 7272 Darbydyar | Harvey, 81 | Apr 25 | | 3 |
| 7294 Barbaraakey | Harvey, 81 | Apr 10 | | 3 |
| 7335 1989 JA | Pryal, 20 | May 24 | | 4 |
| 7375 1980 PZ | Harvey, 81 | Aug 30 | | 3 |
| 7482 1994 PC1 | Faure, 20 | Jan 22 | | 5 |
| | Harvey, 81 | Jan 19 | | 6 |
| 7513 1985 RU2 | Harvey, 81 | Sep 22 | | 3 |
| 7727 Chepurova | Harvey, 81 | Mar 7 | | 3 |
| 8107 1995 BR4 | Harvey, 81 | Mar 1 | | 3 |
| 8260 Momcheva | Harvey, 81 | Sep 22 | | 3 |
| 8297 Gerardfaure | Faure, 114, 82 | Mar 25-Apr 4 | | 4 |
| 8417 Lancetaylor | Harvey, 81 | Sep 21 | | 3 |
| 8713 Azusa | Harvey, 81 | Jan 23 | | 3 |
| 8891 Irokawa | Harvey, 81 | Oct 4 | | 3 |
| 9346 Fernandel | Harvey, 81 | Dec 19 | | 3 |
| 9626 Stanley | Harvey, 81 | Jan 4 | | 3 |
| 9846 1990 OS1 | Harvey, 81 | Mar 26 | 0.5f@16.0 | 3 |
| 9853 l'Epee | Harvey, 81 | Aug 29 | | 3 |
| 9971 Ishihara | Harvey, 81 | Apr 22 | | 3 |
| 10288 Saville | Harvey, 81 | Oct 20 | | 3 |
| 10449 Takuma | Harvey, 81 | Aug 30 | | 3 |
| 10548 1992 PJ2 | Harvey, 81 | Aug 28 | | 3 |
| 10602 Masakazu | Harvey, 81 | Sep 22 | | 3 |
| 10640 1998 WU19 | Harvey, 81 | Jan 30 | | 3 |
| 10675 Kharlamov | Harvey, 81 | Oct 27 | | 3 |
| 10722 Monari | Harvey, 81 | Oct 27 | | 3 |
| 10765 1990 UZ | Harvey, 81 | Dec 28 | | 3 |
| 10939 1999 CJ19 | Harvey, 81 | Apr 24 | | 3 |
| 11001 Andrewulff | Harvey, 81 | Apr 1 | | 3 |
| 11023 1986 QZ | Harvey, 81 | Aug 28 | | 3 |
| 11043 Pepping | Harvey, 81 | Dec 19 | | 3 |
| 12127 Mamiya | Harvey, 81 | Sep 24 | | 3 |
| 12219 Grigor'ev | Harvey, 81 | Sep 24 | | 3 |
| 12499 1998 FR47 | Harvey, 81 | Aug 30 | | 3 |
| 12523 1998 HH100 | Harvey, 81 | Sep 21 | | 3 |
| 12787 Abetadashi | Harvey, 81 | Aug 30 | | 3 |
| 13138 1994 VA | Harvey, 81 | Aug 28 | | 3 |
| 14457 1993 FR23 | Harvey, 81 | Sep 24 | | 3 |
| 14859 1989 WU1 | Harvey, 81 | Sep 22 | | 3 |
| 15790 Keizan | Faure, 45 | Oct 4 | | 2 |
| | Harvey, 81 | Oct 15 | | 6 |

| MINOR PLANET | OBSERVER & APERTURE (cm) | OBSERVING PERIOD (2022) | NO. OBS. |
|---|---|---|---|
| 16171 2000 AD97 | Harvey, 81 | Feb 6 | 3 |
| 16432 1998 VL2 | Harvey, 81 | Nov 29 | 3 |
| 16827 1997 WD2 | Harvey, 81 | Nov 28 | 3 |
| 16835 1997 WT34 | Harvey, 81 | Oct 5 0.4f@16.2 | 3 |
| 17170 Vsevustinov | Harvey, 81 | Apr 10 | 3 |
| 17445 Avatcha | Harvey, 81 | Sep 16 0.4f@16.1 | 3 |
| 18153 2000 OC61 | Harvey, 81 | Sep 21 | 3 |
| 18882 1999 YN4 | Harvey, 81 | Jan 4 | 6 |
| 19230 Sugazi | Harvey, 81 | Aug 30 | 3 |
| 19364 Semafor | Harvey, 81 | Apr 1 | 3 |
| 19515 1998 QM76 | Harvey, 81 | Mar 3-7 | 5 |
| 19517 Robertocarlos | Harvey, 81 | Mar 27 | 3 |
| 20460 Robwhiteley | Harvey, 81 | Jan 6 | 6 |
| 20524 Bustersikes | Harvey, 81 | Oct 5 | 3 |
| 21055 1990 YR | Harvey, 81 | Oct 15 | 3 |
| 21609 Williamcaleb | Harvey, 81 | Oct 19 | 3 |
| 22176 2000 XG36 | Harvey, 81 | Nov 28 | 3 |
| 23448 1988 BG | Harvey, 81 | Jan 23 | 3 |
| 23606 1996 AS1 | Harvey, 35 | Jul 19 | 3 |
| | Faure, Rayon, 45 | Jul 26 | 5 |
| 23978 1999 JF21 | Harvey, 81 | Nov 4 | 3 |
| 24642 1984 SA | Harvey, 81 | Oct 5 | 3 |
| 25880 2000 QG196 | Harvey, 81 | Jan 30 | 3 |
| 25916 2001 CP44 | Rayon, 20 | Jul 1 | 2CCD |
| 26828 1989 WZ1 | Harvey, 81 | Oct 27 | 3 |
| 26967 1997 RZ7 | Harvey, 81 | Aug 28 | 3 |
| 27057 1998 SP33 | Harvey, 81 | Nov 28 | 3 |
| 30397 2000 KU39 | Harvey, 81 | Oct 19 | 3 |
| 31383 1998 XJ94 | Harvey, 81 | Mar 7 | 3 |
| 35143 1992 UF1 | Harvey, 81 | Oct 15-19 | 8 |
| 35368 1997 UB8 | Harvey, 81 | Oct 19 | 3 |
| 35369 1997 UJ11 | Harvey, 81 | Dec 17 | 6 |
| 39002 2000 UO33 | Harvey, 81 | Oct 21 | 6 |
| 39979 1998 HT12 | Harvey, 81 | Nov 28 | 3 |
| 51700 2001 KV23 | Harvey, 81 | Oct 4 | 3 |
| 53090 1998 YS7 | Harvey, 81 | Sep 15 | 3 |
| 53312 1999 JZ | Harvey, 81 | Jan 6 | 3 |
| 55401 2001 SX316 | Harvey, 81 | Feb 9 | 3 |
| 66875 1999 VY52 | Harvey, 81 | Nov 28 | 3 |
| 115916 2003 WB8 | Harvey, 81 | Jan 23 | 6 |
| 118303 1998 UG | Harvey, 81 | Dec 17 | 3 |
| 158091 2000 WH56 | Harvey, 81 | Aug 28 | 3 |
| 163692 2003 CY18 | Harvey, 81 | May 5 | 6 |
| 195208 2002 DZ3 | Harvey, 81 | Dec 17 | 6 |
| 217628 Lugh | Harvey, 81 | Nov 4 | 6 |
| 226554 2003 WR21 | Harvey, 81 | Dec 28 | 6 |
| 306399 1996 AX2 | Harvey, 81 | Nov 29 | 6 |
| 312942 1995 EK1 | Harvey, 81 | Oct 20 | 6 |
| 317255 2002 DJ5 | Harvey, 81 | Mar 26-27 | 12 |
| 422787 2001 WS1 | Harvey, 81 | Oct 19 | 6 |
| 455176 1999 VF22 | Harvey, 81 | Feb 20 | 6 |
| 506459 2002 AL14 | Harvey, 81 | Jan 23 | 6 |
| 523823 2015 BG311 | Harvey, 81 | Oct 15 | 6 |
| 2005 LW3 | Harvey, 81 | Nov 24 | 6 |
| 2008 TB27 | Harvey, 81 | Dec 17 | 6 |
| 2010 XC15 | Harvey, 81 | Dec 24 | 6 |
| 2013 YA14 | Harvey, 81 | Dec 24 | 6 |
| 2014 HK129 | Harvey, 81 | Dec 18 | 6 |
| 2015 RN35 | Harvey, 81 | Dec 17 | 6 |
| 2022 AC4 | Harvey, 81 | Jan 11 | 6 |
| 2022 BH7 | Harvey, 81 | Feb 16 | 6 |
| 2022 CO6 | Harvey, 81 | Feb 15 | 6 |
| 2022 FB2 | Harvey, 81 | Mar 28 | 6 |
| 2022 UC1 | Harvey, 81 | Oct 22 | 6 |

# LIGHTCURVE PHOTOMETRY OPPORTUNITIES: 2023 JULY-SEPTEMBER

Brian D. Warner
Center for Solar System Studies (CS3)
446 Sycamore Ave.
Eaton, CO 80615 USA
brian@MinPlanObs.org

Alan W. Harris
Center for Solar System Studies (CS3)
La Cañada, CA 91011-3364 USA

Josef Ďurech
Astronomical Institute
Charles University
18000 Prague, CZECH REPUBLIC
durech@sirrah.troja.mff.cuni.cz

Lance A.M. Benner
Jet Propulsion Laboratory
Pasadena, CA 91109-8099 USA
lance.benner@jpl.nasa.gov

We present lists of asteroid photometry opportunities for objects reaching a favorable apparition and have no or poorly-defined lightcurve parameters. Additional data on these objects will help with shape and spin axis modeling using lightcurve inversion. The "Radar-Optical Opportunities" section includes a list of potential radar targets as well as some that might be in critical need of astrometric data.

We present several lists of asteroids that are prime targets for photometry and/or astrometry during the period 2023 July through September. The "Radar-Optical Opportunities" section provides an expanded list of potential NEA targets, many of which are planned or good candidates for radar observations.

In the first three sets of tables, "Dec" is the declination and "U" is the quality code of the lightcurve. See the latest asteroid lightcurve data base (LCDB from here on; Warner et al., 2009) documentation for an explanation of the U code:

*http://www.minorplanet.info/lightcurvedatabase.html*

The ephemeris generator on the MinorPlanet.info web site allows creating custom lists for objects reaching V ≤ 18.0 during any month in the current year and up to five years in the future, e.g., limiting the results by magnitude and declination, family, and more.

*https://www.minorplanet.info/php/callopplcdbquery.php*

We refer you to past articles, e.g., Warner et al. (2021a; 2021b) for more detailed discussions about the individual lists and points of advice regarding observations for objects in each list.

Once you've obtained and analyzed your data, it's important to publish your results. Papers appearing in the *Minor Planet Bulletin* are indexed in the Astrophysical Data System (ADS) and so can be referenced by others in subsequent papers. It's also important to make the data available at least on a personal website or upon request. We urge you to consider submitting your raw data to the ALCDEF database. This can be accessed for uploading and downloading data at *http://www.alcdef.org*

The database contains more than 10.4 million observations for 24,202 objects (as of 2023 April 6), making it one of the more useful sources for raw data of dense time-series asteroid photometry.

Lightcurve/Photometry Opportunities

Objects with U = 3– or 3 are excluded from this list since they will likely appear in the list for shape and spin axis modeling. Those asteroids rated U = 1 or have only a lower limit on the period, should be given higher priority over those rated U = 2 or 2+. On the other hand, do not overlook asteroids with U = 2/2+ on the assumption that the period is sufficiently established. Regardless, do not let the existing period influence your analysis since even highly-rated result have been proven wrong at times. Note that the lightcurve amplitude in the tables could be more or less than what's given. Use the listing only as a guide.

All objects are reaching one of their five brightest apparitions from 1995-2050. Bold text indicates a near-Earth asteroid (NEA).

| | | Brightest | | | LCDB Data | | |
|---|---|---|---|---|---|---|---|
| Number | Name | Date | Mag | Dec | Period | Amp | U |
| 9328 | 1990 DL3 | 07 09.4 | 15.4 | -36 | 58.495 | 1.00 | 2 |
| 6400 | Georgealexander | 07 17.1 | 15.5 | -31 | 41.348 | 0.08-0.12 | 2 |
| 10546 | Nakanomakoto | 07 17.3 | 15.4 | -24 | 4.219 | | 2 |
| 5248 | Scardia | 07 19.7 | 15.1 | -21 | 6.046 | | 2 |
| 11466 | Katharinaotto | 07 19.9 | 15.2 | -20 | 166.093 | 0.55 | 2 |
| 3713 | Pieters | 07 21.8 | 15.2 | -23 | 6.9 | 0.07-0.10 | 2 |
| 1341 | Edmee | 07 22.8 | 13.9 | -25 | 23.745 | 0.22-0.60 | 2+ |
| 6405 | Komiyama | 07 24.1 | 15.1 | -20 | 19.855 | 0.13 | 2 |
| 9566 | Rykhlova | 07 26.5 | 15.4 | -13 | 8.8 | 0.56-0.95 | 2 |
| **154993** | **2005 EA94** | **07 28.4** | **15.1** | **-55** | **13.761** | **0.29** | **2** |
| 6790 | Pingouin | 07 30.3 | 15.5 | +4 | > 12 | 0.45 | 2- |
| 8778 | 1931 TD3 | 07 31.3 | 14.6 | -39 | 3.833 | 0.51 | 2 |
| 3257 | Hanzlik | 08 01.0 | 14.8 | -30 | 8.465 | 0.20 | 2 |
| 17939 | 1999 HH8 | 08 01.2 | 15.2 | -22 | 5.1 | 0.05-0.26 | 2 |
| 9053 | Hamamelis | 08 03.5 | 15.5 | -25 | 10.386 | 0.29-0.33 | 2 |
| 14815 | Rutberg | 08 03.6 | 15.2 | -11 | 150 | 1.0 | 2 |
| 16591 | 1992 SY17 | 08 03.6 | 15.4 | +2 | 2.737 | 0.17-0.18 | 2 |
| 4770 | Lane | 08 05.3 | 13.9 | -20 | 34.75 | 0.23 | 2 |
| 23268 | 2000 YD55 | 08 05.6 | 15.3 | -23 | 3.368 | 0.12 | 2 |
| 2683 | Brian | 08 10.3 | 15.5 | -17 | 22.528 | | 2 |
| 3130 | Hillary | 08 11.2 | 15.3 | -19 | 25.282 | 0.84 | 2 |
| 3739 | Rem | 08 15.0 | 14.9 | -18 | 68.906 | | 2- |
| 6108 | Glebov | 08 16.0 | 15.3 | -8 | 2.831 | 0.05-0.22 | 2 |
| 6205 | Menottigalli | 08 20.0 | 15.0 | -20 | 15.252 | 0.36-0.38 | 2+ |
| 3184 | Raab | 08 21.2 | 14.4 | -24 | 274.944 | 0.09 | 1 |
| 12867 | Joeloic | 08 22.9 | 15.1 | -8 | 813 | 0.71 | 2+ |
| 1329 | Eliane | 08 25.2 | 13.4 | -19 | 137.8 | 0.18-0.43 | 2 |
| 35085 | 1990 SL11 | 08 27.0 | 15.5 | -10 | 128 | 0.95 | 2- |
| 1557 | Roehla | 08 27.8 | 15.1 | -16 | 5.679 | | 2 |
| 12374 | Rakhat | 08 28.6 | 15.2 | -19 | 18.17 | 0.31 | 2 |
| 6982 | Cesarchavez | 08 28.7 | 15.5 | +7 | 16.08 | 0.10 | 2- |
| 3811 | Karma | 08 31.1 | 14.7 | -9 | 13.23 | 0.33-0.50 | 2+ |
| 903 | Nealley | 08 31.7 | 14.3 | -8 | 19.72 | 0.10-0.15 | 2 |
| 10152 | Ukichiro | 09 01.3 | 15.5 | -10 | 5.182 | | 2- |
| 14657 | 1998 YU27 | 09 02.1 | 15.3 | +9 | 33.58 | 0.30-0.46 | 2 |
| 7422 | 1992 LP | 09 02.2 | 15.2 | -13 | 81.493 | 0.51 | 2 |
| 3855 | Pasasymphonia | 09 03.0 | 14.5 | -19 | 6.513 | 0.18 | 2 |
| 2461 | Clavel | 09 03.9 | 15.2 | -10 | 3.5 | 0.33 | 2 |
| 1051 | Merope | 09 06.9 | 14.2 | +4 | 27.2 | 0.11-0.20 | 2 |
| 4226 | Damiaan | 09 07.3 | 14.1 | +1 | 24 | 0.05 | 1 |
| 4121 | Carlin | 09 08.9 | 15.0 | -47 | 97.295 | 0.77 | 2 |
| 2090 | Mizuho | 09 09.0 | 14.3 | -4 | 5.47 | 0.25-0.30 | 2+ |
| 3127 | Bagration | 09 10.5 | 14.8 | +2 | > 16 | 0.1 | 1 |
| 2029 | Binomi | 09 10.7 | 15.3 | +5 | 3.756 | 0.51-0.52 | 2 |
| 6427 | 1995 FY | 09 11.0 | 15.5 | -3 | 6.195 | 0.59-0.84 | 2 |
| 11065 | 1991 XE2 | 09 13.3 | 15.4 | -20 | > 8 | 0.1 | 1+ |
| 1525 | Savonlinna | 09 16.3 | 14.9 | +8 | 14.634 | 0.50-0.52 | 2 |
| 2630 | Hermod | 09 17.9 | 15.5 | -3 | 19.428 | | 2 |
| 4729 | Mikhailmil' | 09 21.5 | 14.1 | +3 | 38.31 | 0.36-0.37 | 2+ |
| 2096 | Vaino | 09 24.2 | 15.1 | +2 | 5.55 | 0.06-0.10 | 2 |
| 2687 | Tortali | 09 24.2 | 14.9 | -12 | 21.75 | 0.19 | 2 |
| 3055 | Annapavlova | 09 24.2 | 15.5 | -1 | 44.626 | 0.41 | 2 |
| 4190 | Kvasnica | 09 25.7 | 15.4 | +7 | 13.42 | 0.09 | 2- |
| 4278 | Harvey | 09 27.0 | 15.3 | -5 | 9.647 | | 2 |
| 4288 | Tokyotech | 09 27.3 | 14.4 | -15 | 3.18 | 0.11-0.19 | 2+ |
| 2374 | Vladvysotskij | 09 28.1 | 14.8 | +9 | 5.398 | 0.48 | 2 |
| 2831 | Stevin | 09 30.7 | 13.9 | -6 | 3213 | 0.3-0.50 | 2 |

Low Phase Angle Opportunities

The Low Phase Angle list includes asteroids that reach very low phase angles ($\alpha < 1°$). The "$\alpha$" column is the minimum solar phase angle for the asteroid. Getting accurate, calibrated measurements (usually V band) at or very near the day of opposition can provide important information for those studying the "opposition effect." Use the on-line query form for the LCDB to get more details about a specific asteroid.

*https://www.minorplanet.info/php/callopplcdbquery.php*

The best chance of success comes with covering at least half a cycle a night, meaning periods generally < 16 h, when working objects with low amplitude. Objects with large amplitudes and/or long periods are much more difficult for phase angle studies since, for proper analysis, the data must be reduced to the average magnitude of the asteroid for each night. Refer to Harris et al. (1989) for the details of the analysis procedure.

As an aside, it is arguably better for physical interpretation (e.g., *G* value versus albedo) to use the maximum light rather than mean level to find the phase slope parameter (*G*), which better models the behavior of a spherical object of the same albedo, but it can produce significantly different values for both *H* and *G* versus using average light, which is the method used for values listed by the Minor Planet Center. Using and reporting the results of both methods can provide additional insights into the physical properties of an asteroid.

The International Astronomical Union (IAU) has adopted a new system, H-$G_{12}$, introduced by Muinonen et al. (2010). It will be some years before H-$G_{12}$ becomes widely used, and hopefully not until a discontinuity flaw in the $G_{12}$ function has been fixed. This discontinuity results in false "clusters" or "holes" in the solution density and makes it impossible to draw accurate conclusions.

We strongly encourage obtaining data as close to 0° as possible, then every 1-2° out to 7°, below which the curve tends to be non-linear due to the opposition effect. From 7° out to about 30°, observations at 3-6° intervals should be sufficient. Coverage beyond 50° or so is not generally helpful since the H-G system is best defined with data from 0-30°.

It's important to emphasize that all observations should (must) be made using high-quality catalogs to set the comparison star magnitudes. These include ATLAS, Pan-STARRS, SkyMapper, and Gaia2/3. Catalogs such as CMC-15, APASS, or the MPOSC from *MPO Canopus* have too high systematic errors.

Also important is that that there are sufficient data from each observing run such that their location can be found on a combined, phased lightcurve derived from two or more nights obtained *near the same phase angle.* If necessary, the magnitudes for a given run should be adjusted so that they correspond to mid-light of the combined lightcurve. This goes back to the H-G system being based on average, not maximum or minimum light.

The asteroid magnitudes are brighter than in others lists because higher precision is required and the asteroid may be a full magnitude or fainter when it reaches phase angles out to 20-30°. Even so, starting now, the list will include objects that reach V ≤ 15.0 at opposition. The list of objects using the previous limit of V ≤ 14.0 was becoming very short.

| Num | Name | Date | α | V | Dec | Period | Amp | | U |
|---|---|---|---|---|---|---|---|---|---|
| 9945 | Karinaxavier | 07 02.4 | 0.56 | 15.0 | -22 | | | | |
| 1461 | Jean-Jacques | 07 03.6 | 0.44 | 14.6 | -22 | 16.56 | 0.08 | 0.09 | 2 |
| 364 | Isara | 07 04.6 | 0.30 | 12.6 | -22 | 9.156 | 0.30 | 0.40 | 3 |
| 710 | Gertrud | 07 04.9 | 0.61 | 14.8 | -21 | 8.288 | 0.26 | 0.30 | 3- |
| 1154 | Astronomia | 07 07.1 | 0.81 | 14.8 | -25 | 18.115 | | 0.39 | 3- |
| 15 | Eunomia | 07 08.0 | 0.98 | 8.8 | -25 | 6.083 | 0.40 | 0.53 | 3 |
| 1456 | Saldanha | 07 08.7 | 0.39 | 14.6 | -21 | 19.035 | 0.09 | 0.26 | 3- |
| 380 | Fiducia | 07 09.7 | 0.90 | 12.5 | -25 | 13.69 | 0.04 | 0.32 | 3 |
| 1939 | Loretta | 07 10.1 | 0.46 | 15.0 | -24 | 23.88 | | 0.20 | 2 |
| 851 | Zeissia | 07 11.4 | 0.97 | 14.2 | -20 | 9.341 | 0.38 | 0.53 | 3 |
| 811 | Nauheima | 07 12.3 | 0.69 | 14.2 | -20 | 4.001 | 0.11 | 0.20 | 3 |
| 1442 | Corvina | 07 14.8 | 0.70 | 15.0 | -20 | 77.920 | | 0.19 | 2 |
| 1074 | Beljawskya | 07 15.0 | 0.32 | 15.0 | -23 | 6.284 | 0.31 | 0.37 | 3 |
| 1284 | Latvia | 07 18.5 | 0.81 | 14.0 | -23 | 9.55 | 0.10 | 0.23 | 3- |
| 1699 | Honkasalo | 07 19.6 | 0.91 | 13.7 | -19 | 11.115 | 0.15 | 0.32 | 3- |
| 3520 | Klopsteg | 07 22.8 | 0.34 | 14.7 | -20 | | | | |
| 3002 | Delasalle | 07 22.9 | 0.45 | 14.4 | -21 | 6.534 | 0.31 | 0.47 | 3 |
| 507 | Laodica | 07 23.5 | 0.54 | 13.5 | -18 | 4.706 | 0.18 | 0.47 | 3 |
| 7234 | 1986 QV3 | 07 23.9 | 0.21 | 15.0 | -20 | 2.848 | 0.29 | 0.30 | 3 |
| 1262 | Sniadeckia | 07 29.6 | 0.23 | 14.3 | -19 | 17.57 | 0.06 | 0.16 | 3 |
| 296 | Phaetusa | 07 31.9 | 0.22 | 14.3 | -19 | 4.539 | 0.38 | 0.70 | 3 |
| 889 | Erynia | 08 01.1 | 0.42 | 14.0 | -17 | 9.89 | 0.47 | 0.67 | 3 |
| 402 | Chloe | 08 03.2 | 0.17 | 12.7 | -18 | 10.664 | 0.19 | 0.37 | 3 |
| 888 | Parysatis | 08 03.4 | 0.94 | 13.1 | -20 | 5.931 | 0.22 | 0.26 | 3 |
| 240 | Vanadis | 08 05.0 | 0.37 | 12.6 | -18 | 10.64 | 0.13 | 0.34 | 3 |
| 275 | Sapientia | 08 09.0 | 0.07 | 13.1 | -16 | 14.931 | 0.05 | 0.12 | 3- |
| 773 | Irmintraud | 08 16.2 | 0.16 | 12.4 | -14 | 6.751 | 0.05 | 0.25 | 3 |
| 2043 | Ortutay | 08 19.5 | 0.20 | 14.7 | -13 | 7.747 | 0.44 | 0.56 | 3- |
| 1156 | Kira | 08 21.9 | 0.94 | 14.9 | -14 | 2.971 | 0.19 | 0.26 | 3 |
| 1085 | Amaryllis | 08 23.2 | 0.54 | 14.1 | -13 | 18.111 | 0.14 | 0.20 | 3- |
| 5144 | Achates | 08 23.9 | 0.40 | 14.6 | -10 | 5.958 | 0.18 | 0.35 | 3 |
| 318 | Magdalena | 08 28.6 | 0.56 | 14.1 | -8 | 42.65 | 0.06 | 0.16 | 3 |
| 3811 | Karma | 08 31.1 | 0.22 | 14.8 | -9 | 13.23 | 0.33 | 0.50 | 2+ |
| 2326 | Tololo | 08 31.4 | 0.30 | 14.4 | -9 | 9.488 | 0.14 | 0.33 | 3- |
| 903 | Nealley | 08 31.7 | 0.20 | 14.3 | -8 | 19.72 | 0.10 | 0.15 | 2 |
| 163 | Erigone | 09 01.7 | 0.17 | 12.8 | -8 | 16.136 | 0.32 | 0.37 | 3 |
| 232 | Russia | 09 02.3 | 0.42 | 14.1 | -9 | 21.905 | 0.14 | 0.31 | 3 |
| 1004 | Belopolskya | 09 06.3 | 0.26 | 14.0 | -7 | 9.038 | 0.09 | 0.14 | 3- |
| 366 | Vincentina | 09 06.7 | 0.32 | 12.7 | -7 | 12.736 | 0.05 | 0.09 | 3- |
| 684 | Hildburg | 09 06.8 | 0.51 | 13.7 | -5 | 11.91 | 0.07 | 0.23 | 3- |
| 656 | Beagle | 09 08.4 | 0.13 | 15.0 | -6 | 7.035 | 0.57 | 1.20 | 3 |
| 2090 | Mizuho | 09 09.1 | 0.76 | 14.3 | -4 | 5.47 | 0.25 | 0.30 | 2+ |
| 1269 | Rollandia | 09 12.0 | 0.48 | 14.7 | -6 | 65. | 0.02 | 0.13 | 2 |
| 51 | Nemausa | 09 12.8 | 0.77 | 10.7 | -2 | 7.783 | 0.10 | 0.25 | 3 |
| 834 | Burnhamia | 09 15.4 | 0.40 | 13.4 | -2 | 13.875 | 0.15 | 0.22 | 3 |
| 327 | Columbia | 09 18.1 | 0.08 | 13.4 | -2 | 5.932 | 0.16 | 0.42 | 3 |
| 1142 | Aetolia | 09 20.6 | 0.57 | 14.9 | -3 | 10.730 | 0.15 | 0.22 | 3- |
| 1622 | Chacornac | 09 21.2 | 0.63 | 14.5 | -2 | 12.206 | 0.21 | 0.25 | 2 |
| 238 | Hypatia | 09 21.4 | 0.80 | 11.6 | +1 | 8.875 | 0.10 | 0.21 | 3 |
| 321 | Florentina | 09 21.7 | 0.95 | 13.9 | -3 | 2.871 | 0.31 | 0.52 | 3 |
| 263 | Dresda | 09 22.2 | 0.49 | 13.7 | +1 | 16.809 | 0.37 | 0.55 | 3 |
| 60 | Echo | 09 22.4 | 0.58 | 11.4 | +1 | 25.208 | 0.10 | 0.22 | 3 |
| 1305 | Pongola | 09 23.8 | 0.94 | 15.0 | -3 | 8.335 | 0.14 | 0.19 | 3- |
| 313 | Chaldaea | 09 24.6 | 0.58 | 12.4 | -1 | 8.392 | 0.08 | 0.24 | 3 |
| 1227 | Geranium | 09 25.8 | 0.26 | 14.4 | +1 | 12.363 | | 0.08 | 3 |
| 256 | Walpurga | 09 26.9 | 0.07 | 14.1 | +1 | 16.664 | 0.34 | 0.58 | 3 |
| 3451 | Mentor | 09 27.5 | 0.51 | 15.0 | -1 | 7.702 | 0.11 | 0.63 | 3 |
| 1369 | Ostanina | 09 30.1 | 0.92 | 14.2 | +0 | 8.400 | 0.73 | 1.11 | 3 |

## Shape/Spin Modeling Opportunities

Those doing work for modeling should contact Josef Ďurech at the email address above. If looking to add lightcurves for objects with existing models, visit the Database of Asteroid Models from Inversion Techniques (DAMIT) web site

*https://astro.troja.mff.cuni.cz/projects/damit/*

Additional lightcurves could lead to the asteroid being added to or improving one in DAMIT, thus increasing the total number of asteroids with spin axis and shape models.

Included in the list below are objects that:

1. Are rated U = 3– or 3 in the LCDB
2. Do not have reported pole in the LCDB Summary table
3. Have at least three entries in the Details table of the LCDB where the lightcurve is rated U ≥ 2.

The caveat for condition #3 is that no check was made to see if the lightcurves are from the same apparition or if the phase angle bisector longitudes differ significantly from the upcoming apparition. The last check is often not possible because the LCDB does not list the approximate date of observations for all details records. Including that information is an on-going project.

*With the wide use of sparse data from the surveys for modeling that produces hundreds of statistically valid poles and shapes, the need for data for main-belt objects is not what it used to be. The best use of observing time might be to concentrate on near-Earth asteroids, or on asteroids where the only period was derived from sparse data, which can help eliminate alias periods.*

The latter targets are usually flagged with an 'S' on the LCDB summary line. Regardless, it's a good idea to visit the DAMIT site and see what it has, if anything, on the target(s) you've picked for observations.

Objects in **bold** text are at a favorable apparition. Those in italic text are near-Earth objects.

| | | Brightest | | | LCDB Data | | |
|---|---|---|---|---|---|---|---|
| Num | Name | Date | Mag | Dec | Period | Amp | U |
| 1344 | Caubeta | 07 02.0 | 15.2 | -30 | 3.122 | 0.16-0.55 | 3 |
| 1644 | Rafita | 07 02.3 | 15.4 | -21 | 3.344 | 0.13-0.38 | 3 |
| **19516** | **1998 QF80** | **07 03.7** | **15.0** | **-29** | **5.438** | **0.32-0.35** | **3** |
| 143 | Adria | 07 05.0 | 12.8 | -37 | 22.005 | 0.07-0.10 | 3 |
| 3447 | Burckhalter | 07 05.1 | 15.1 | -61 | 59.8 | 0.30-0.39 | 3 |
| 4440 | Tchantches | 07 06.8 | 15.5 | -22 | 2.788 | 0.21-0.34 | 3 |
| 1416 | Renauxa | 07 08.2 | 15.4 | -36 | 8.7 | 0.09-0.40 | 3 |
| 1456 | Saldanha | 07 08.8 | 14.6 | -21 | 19.035 | 0.09-0.26 | 3- |
| 1765 | Wrubel | 07 08.9 | 14.0 | -41 | 5.26 | 0.11-0.33 | 3 |
| 2409 | Chapman | 07 09.0 | 14.6 | -19 | 3.153 | 0.14 | 3 |
| 326 | Tamara | 07 11.0 | 11.9 | -65 | 14.445 | 0.10-0.27 | 3 |
| 3782 | Celle | 07 11.2 | 15.2 | -19 | 3.84 | 0.11-0.17 | 3 |
| 811 | Nauheima | 07 12.3 | 14.2 | -20 | 4.001 | 0.11-0.20 | 3 |
| 3001 | Michelangelo | 07 14.3 | 15.3 | -26 | 8.345 | 0.12-0.28 | 3 |
| **49385** | **1998 XA12** | **07 15.8** | **15.4** | **-9** | **2.523** | **0.15-0.30** | **3** |
| **2873** | **Binzel** | **07 17.2** | **14.3** | **-24** | **2.704** | **0.06-0.14** | **3** |
| 971 | Alsatia | 07 21.8 | 14.4 | -32 | 9.614 | 0.17-0.29 | 3 |
| 1539 | Borrelly | 07 23.0 | 15.4 | -19 | 15.922 | 0.54-0.76 | 3 |
| 894 | Erda | 07 26.4 | 13.7 | -2 | 4.69 | 0.05-0.27 | 3 |
| **11386** | **1998 TA18** | **07 26.9** | **15.3** | **-10** | **15.959** | **0.49-0.84** | **3** |
| 914 | Palisana | 07 27.5 | 11.7 | +22 | 8.681 | 0.03-0.24 | 3- |
| **1262** | **Sniadeckia** | **07 29.6** | **14.2** | **-19** | **17.57** | **0.06-0.16** | **3** |
| 633 | Zelima | 07 30.0 | 13.8 | -13 | 11.73 | 0.14-0.49 | 3 |
| 1567 | Alikoski | 08 03.9 | 14.9 | -40 | 16.374 | 0.08-0.16 | 3 |
| 240 | Vanadis | 08 05.0 | 12.5 | -18 | 10.64 | 0.13-0.34 | 3 |
| **6265** | **1985 TW3** | **08 08.2** | **14.7** | **-26** | **2.709** | **0.26-0.36** | **3** |
| 275 | Sapientia | 08 09.0 | 13.0 | -16 | 14.931 | 0.05-0.12 | 3- |
| 612 | Veronika | 08 12.1 | 14.3 | +15 | 8.243 | 0.09-0.14 | 3 |
| 677 | Aaltje | 08 14.1 | 13.9 | -5 | 16.608 | 0.10-0.37 | 3 |
| **3833** | **Calingasta** | **08 14.9** | **15.5** | **+2** | **199** | **0.70-1.20** | **3** |
| **773** | **Irmintraud** | **08 16.2** | **12.4** | **-14** | **6.751** | **0.05-0.25** | **3** |
| **2763** | **Jeans** | **08 21.2** | **13.7** | **-10** | **7.8** | **0.13-0.18** | **3** |
| **5144** | **Achates** | **08 23.8** | **14.5** | **-10** | **5.958** | **0.18-0.35** | **3** |
| 973 | Aralia | 08 24.6 | 14.7 | -18 | 7.366 | 0.20-0.25 | 3 |
| 213 | Lilaea | 08 25.3 | 12.0 | -16 | 12.042 | 0.07-0.20 | 3 |
| 1319 | Disa | 08 25.3 | 15.1 | -7 | 7.08 | 0.24-0.27 | 3 |
| **9873** | **1992 GH** | **08 27.9** | **15.0** | **-26** | **2.926** | **0.15-0.39** | **3** |
| 318 | Magdalena | 08 28.7 | 14.0 | -8 | 42.65 | 0.06-0.16 | 3 |
| 142 | Polana | 08 30.3 | 13.4 | -7 | 9.764 | 0.11-0.24 | 3 |
| 7288 | 1991 FE1 | 08 30.8 | 15.5 | -6 | 4.889 | 0.47-0.53 | 3 |
| 1867 | Deiphobus | 09 02.3 | 15.5 | +19 | 58.66 | 0.10-0.27 | 3- |
| 3317 | Paris | 09 07.4 | 15.2 | -22 | 7.081 | 0.08-0.14 | 3 |
| **3606** | **Pohjola** | **09 08.8** | **14.8** | **+16** | **5.847** | **0.11-0.21** | **3** |
| 81 | Terpsichore | 09 09.2 | 11.7 | -9 | 10.943 | 0.02-0.15 | 3 |
| 863 | Benkoela | 09 14.6 | 14.2 | -30 | 7.032 | 0.05-0.27 | 3 |
| **8356** | **Wadhwa** | **09 14.6** | **14.4** | **-8** | **3.043** | **0.11-0.15** | **3** |
| 834 | Burnhamia | 09 15.3 | 13.3 | -2 | 13.875 | 0.15-0.22 | 3 |
| 1149 | Volga | 09 15.7 | 14.3 | +14 | 27.262 | 0.14-0.26 | 3- |
| 1302 | Werra | 09 15.7 | 15.1 | -7 | 8.183 | 0.09-0.26 | 3- |
| 766 | Moguntia | 09 16.1 | 14.0 | -7 | 4.816 | 0.06-0.23 | 3 |
| 786 | Bredichina | 09 17.4 | 14.1 | -20 | 29.434 | 0.04-0.60 | 3- |
| 1305 | Pongola | 09 23.7 | 15.1 | -3 | 8.335 | 0.14-0.19 | 3- |
| 862 | Franzia | 09 24.5 | 13.6 | +18 | 7.523 | 0.07-0.13 | 3 |
| 2729 | Urumqi | 09 26.4 | 15.2 | -3 | 3.127 | 0.19-0.35 | 3 |
| 465 | Alekto | 09 26.7 | 14.8 | +7 | 10.936 | 0.12-0.18 | 3 |
| 5806 | Archieroy | 09 27.2 | 15.5 | +37 | 12.163 | 0.34-0.55 | 3 |
| 429 | Lotis | 09 28.2 | 12.8 | +11 | 13.577 | 0.09-0.24 | 3 |
| 542 | Susanna | 09 28.7 | 12.7 | -8 | 10.069 | 0.11-0.30 | 3 |

| Num | Name | H | Diam | BDate | BMag | BDec | Period | AMn | AMx | U | A | G | Notes |
|---|---|---|---|---|---|---|---|---|---|---|---|---|---|
| 68548 | 2001 XR31 | 16.71 | 1.350 | 07 28.6 | 15.7 | -22 | | | | | 55 | 15 | |
| **154244** | **2002 KL6** | **17.66** | **0.873** | **08 06.3** | **14.0** | **47** | **4.6063** | **0.39** | **1.15** | **3** | **370** | **405** | **Galad et al. (2010)** |
| 4769 | Castalia | 17.53 | 0.927 | 08 16.4 | 15.6 | 19 | 4.095 | | 1.00 | 3 | 45 | 15 | Hudson et al. (1997) |
| **6037** | **1988 EG** | **19.0** | **0.471** | **08 19.7** | **14.6** | **28** | **2.7602** | **0.19** | **0.20** | **3-** | **690** | **240** | **PHA Pravec et al. (2021web)** |
| 358744 | 2008 CR118 | 18.95 | 0.482 | 08 29.1 | 15.1 | -56 | | | | | 220 | 65 | |
| 523950 | 1998 SZ27 | 20.30 | 0.259 | 09 11.2 | 16.5 | -10 | | | | | 45 | 15 | |
| 458732 | 2011 MD5 | 17.93 | 0.771 | 09 14.5 | 13.9 | -4 | | | | | 155 | 45 | |
| 518640 | 2008 KZ5 | 20.08 | 0.286 | 09 19.2 | 17.6 | -81 | 5.789 | | 0.31 | 3- | 25 | 8 | Pravec et al. (2019web) |
| | 2009 UG | 23.3 | 0.065 | 10 02.3 | 15.8 | -19 | 5.88 | | 0.38 | 2+ | 1795 | 515 | Warner (2017) See text |

Table I. A list of near-Earth asteroids reaching brightest in 2023 January-March. PHA: potentially hazardous asteroid. NHATS: Near-Earth Object Human Space Flight Accessible Targets Study. Diameters are based on $p_V$ = 0.20. The Date, V, and Dec columns are the mm/dd.d, approximate magnitude, and declination when at brightest. Amp is the single or range of amplitudes. The A and G columns are the approximate SNRs for an assumed full-power Arecibo (not operational) and Goldstone radars. The references in the Notes column are those for the adopted period.

Radar-Optical Opportunities

Table I below gives a list of near-Earth asteroids reaching maximum brightness for the current quarter-year based on calculations by Warner. We switched to this presentation in lieu of ephemerides for reasons outlined in the 2021 October-December opportunities paper (Warner et al., 2021b), which centered on the potential problems with ephemerides generated several months before publication.

The initial list of targets started using the planning tool at

*https://www.minorplanet.info/php/callopplcdbquery.php*

where the search was limited to near-Earth asteroids only that were V ≤ 18 for at least part of the quarter.

The list was then filtered to include objects that might be targets for the Goldstone radar facility or, if it were still operational, the Arecibo radar. This was based on the calculated radar SNR using

*http://www.naic.edu/~eriverav/scripts/index.php*

and assuming a rotation period of 4 hours (2 hours if $D \leq 200$ m) if a period was not given in the asteroid lightcurve database (LCDB; Warner et al., 2009). The SNR values are estimates only and assume that the radar is fully functional.

If an asteroid was on the list but failed the SNR test, we checked if it might be a suitable target for radar and/or photometry sometime through 2050. If so, it was kept on the list to encourage physical and astrometric observations during the current apparition. In most of those cases, the SNR values in the "A" and "G" columns are not for the current quarter but the year given in the Notes column. If a better apparition is forthcoming through 2050, the Notes column in Table I contains SNR values for that time.

The final step was to cross-reference our list with that found on the Goldstone planned targets schedule at

*http://echo.jpl.nasa.gov/asteroids/goldstone_asteroid_schedule.html*

In Table I, objects in bold text are on the Goldstone proposed observing list as of early 2023 April.

It's important to note that the final list in Table I is based on *known* targets and orbital elements when it was prepared. It is common for newly discovered objects to move in or out of the list. We recommend that you keep up with the latest discoveries by using the Minor Planet Center observing tools.

In particular, monitor NEAs and be flexible with your observing program. In some cases, you may have only 1-3 days when the asteroid is within reach of your equipment. Be sure to keep in touch with the radar team (through Benner's email or their Facebook or Twitter accounts) if you get data. The team may not always be observing the target but your initial results may change their plans. In all cases, your efforts are greatly appreciated.

For observation planning, use these two sites

MPC: *http://www.minorplanetcenter.net/iau/MPEph/MPEph.html*
JPL: *http://ssd.jpl.nasa.gov/?horizons*

Cross-check the ephemerides from the two sites just in case there is discrepancy that might have you imaging an empty sky.

## About YORP Acceleration

Near-Earth asteroids are particularly sensitive to YORP acceleration. YORP (Yarkovsky–O'Keefe–Radzievskii–Paddack; Rubincam, 2000) is the asymmetric thermal re-radiation of sunlight that can cause an asteroid's rotation period to increase or decrease. High precision lightcurves at multiple apparitions can be used to model the asteroid's *sidereal* rotation period and see if it's changing.

It usually takes four apparitions to have sufficient data to determine if the asteroid rotation rate is changing under the influence of YORP. This is why observing an asteroid that already has a well-known period remains a valuable use of telescope time. It is even more so when considering the BYORP (binary-YORP) effect among binary asteroids that has stabilized the spin so that acceleration of the primary body is not the same as if it would be if there were no satellite.

## 2009 UG

2009 UG has been included, even though it doesn't reach brightest until early October, because it will never be as bright through 2050. About every seven years, a "favorable" apparition occurs but each one after 2023 will be increasingly worse. For example, at the next possibility, 2030 October, the asteroid will be V~16.7 at brightest and in 2037 October, V~18.8 will be all it can muster. All non-favorable apparitions are at V < 23.5.

## The Quarterly Target List Table

The Table I columns are

| | |
|---|---|
| Num | Asteroid number, if any. |
| Name | Name assigned by the MPC. |
| H | Absolute magnitude from MPCOrb. |
| Dkm | Diameter (km) assuming $p_V = 0.2$. |
| Date | Date (mm dd.d) of brightest magnitude. |
| V | Approximate V magnitude at brightest. |
| Dec | Approximate declination at brightest. |
| Period | Synodic rotation period from summary line in the LCDB summary table. |
| Amp | Amplitude range (or single value) of reported lightcurves. |
| U | LCDB U (solution quality) from 1 (probably wrong) to 3 (secure). |
| A | Approximate SNR for Arecibo (if operational and at full power). |
| G | Approximate SNR for Goldstone radar at full power. |
| Notes | Comments about the object. |

"PHA" is a potentially hazardous asteroid. NHATS is for "Near-Earth Object Human Space Flight Accessible Targets Study." Presume that that astrometry and photometry have been requested to support Goldstone observations. The sources for the rotation period are given in the Notes column. If none are qualified with a specific period, then the periods from multiple sources were in general agreement. Higher priority should be given to those where the current apparition is the last one V ≤ 18 through 2050 or several years to come.

## References


Galad, A.; Kornos, L.; Vilagi, J. (2010). "An Ensemble of Lightcurves from Modra." *Minor Planet Bull*. **37**, 9-15.

Harris, A.W.; Young, J.W.; Bowell, E.; Martin, L.J.; Millis, R.L.; Poutanen, M.; Scaltriti, F.; Zappala, V.; Schober, H.J.; Debehogne, H.; Zeigler, K.W. (1989). "Photoelectric Observations of Asteroids 3, 24, 60, 261, and 863." *Icarus* **77**, 171-186.

Hudson, R.S.; Ostro, S.J.; Harris, A.W. (1997). "Constraints on Spin State and Hapke Parameters of Asteroid 4769 Castalia Using Lightcurves and a Radar-Derived Shape Model." *Icarus* **130**, 165-176.

Muinonen, K.; Belskaya, I.N.; Cellino, A.; Delbò, M.; Levasseur-Regourd, A.-C.; Penttilä, A.; Tedesco, E.F. (2010). "A three-parameter magnitude phase function for asteroids." *Icarus* **209**, 542-555.

Pravec, P.; Wolf, M.; Sarounova, L. (2019web; 2021web). *http://www.asu.cas.cz/~ppravec/neo.htm*

Rubincam, D.P. (2000). "Radiative Spin-up and Spin-down of Small Asteroids." *Icarus* **148**, 2-11.

Warner, B.D.; Harris, A.W.; Pravec, P. (2009). "The Asteroid Lightcurve Database." *Icarus* **202**, 134-146. Updated 2021 Dec. *http://www.minorplanet.info/lightcurvedatabase.html*

Warner, B.D. (2017). "Near-Earth Asteroid Lightcurve Analysis at CS3-Palmer Divide Station: 2016 October-December." *Minor Planet Bul*. **44**, 98-107.

Warner, B.D.; Harris, A.W.; Durech, J.; Benner, L.A.M. (2021a). "Lightcurve Photometry Opportunities" 2021 January-March." *Minor Planet Bull.* **48**, 89-97.

Warner, B.D.; Harris, A.W.; Durech, J.; Benner, L.A.M. (2021b). "Lightcurve Photometry Opportunities" 2021 October-December." *Minor Planet Bull.* **48**, 406-410.

## IN THIS ISSUE

This list gives those asteroids in this issue for which physical observations (excluding astrometric only) were made. This includes lightcurves, color index, and H-G determinations, etc. In some cases, no specific results are reported due to a lack of or poor-quality data. The page number is for the first page of the paper mentioning the asteroid. EP is the "go to page" value in the electronic version.



***THE MINOR PLANET BULLETIN*** (ISSN 1052-8091) is the quarterly journal of the Minor Planets Section of the Association of Lunar and Planetary Observers (ALPO, http://www.alpo-astronomy.org). Current and most recent issues of the *MPB* are available on line, free of charge from:

*https://mpbulletin.org/*

The Minor Planets Section is directed by its Coordinator, Prof. Frederick Pilcher, 4438 Organ Mesa Loop, Las Cruces, NM 88011 USA (fpilcher35@gmail.com). Robert Stephens (rstephens@foxandstephens.com) serves as Associate Coordinator. Dr. Alan W. Harris (MoreData! Inc.; harrisaw@colorado.edu), and Dr. Petr Pravec (Ondrejov Observatory; ppravec@asu.cas.cz) serve as Scientific Advisors. The Asteroid Photometry Coordinator is Brian D. Warner (Center for Solar System Studies), Palmer Divide Observatory, 446 Sycamore Ave., Eaton, CO 80615 USA (brian@MinorPlanetObserver.com).

*The Minor Planet Bulletin* is edited by Professor Richard P. Binzel, MIT 54-410, 77 Massachusetts Ave, Cambridge, MA 02139 USA (rpb@mit.edu). Brian D. Warner (address above) is Associate Editor. Assistant Editors are Dr. David Polishook, Department of Earth and Planetary Sciences, Weizmann Institute of Science (david.polishook@weizmann.ac.il) and Dr. Melissa Hayes-Gehrke, Department of Astronomy, University of Maryland (mhayesge@umd.edu). The *MPB* is produced by Dr. Pedro A. Valdés Sada (psada2@ix.netcom.com).

Effective with Volume 50, the *Minor Planet Bulletin* is an electronic-only journal; print subscriptions are no longer available. In addition to the free electronic download of the *MPB* as noted above, electronic retrieval of all *Minor Planet Bulletin* articles (back to Volume 1, Issue Number 1) is available through the Astrophysical Data System:

*http://www.adsabs.harvard.edu/*

Authors should submit their manuscripts by electronic mail (rpb@mit.edu). Author instructions and a Microsoft Word template document are available at the web page given above. All materials must arrive by the deadline for each issue. Visual photometry observations, positional observations, any type of observation not covered above, and general information requests should be sent to the Coordinator.

* * * * *

The deadline for the next issue (50-4) is July 15, 2023. The deadline for issue 51-1 is October 15, 2023.

**THIS PAGE INTENTIONALLY LEFT BLANK**